EU-CIRCLE

A pan-European framework for strengthening Critical Infrastructure resilience to climate change

D3.2 Report on climate related critical event parameters

Contractual Delivery Date: 31/12/2017	Actual Delivery Date: 30/09/2018
Type: Document	Version: V1.0

Dissemination Level [Public] Deliverable

Statement

This deliverable introduces the first linkage between climate parameters and hazrads and critical infrastructures. Initially the deliverable defines how climate paraeters and hazards can be defined in terms of the dynamical properties that characterise. Also, using CI related design thresholds, proposes a coherent approach to define the exposure of CI to climate risks.

EU-CIRCLE is a project that has received funding from the European Union's Horizon 2020 research and innovation programme under grant agreement No 653824. Please see http://www.eu-circle.eu/http://www.eu-circle.eu/for more information.

Preparation Slip			
	Name	Partner	Date
From	Nadine Habermann, Ralf Hedel, Thanasis Sfetsos, Albert Chen	UNEXE, Fraunhofer IVI, NCSRD	17/09/2018
Reviewer	Ivan Güttler	DHMZ	19/09/2018
Reviewer	Ksenija Cindrić Kalin	DHMZ	20/09/2018
For delivery	A. Sfetsos	NCSRD	30/09/2018

Document Log			
Issue	Date	Comment	Author / Organization
V0.0	25/07/17	Initial ToC prepared by UNEXE and sent to Ralf Hedel	L. Vamvakeridou-Lyroudia, A. Chen UNEXE
V0.1	21/09/2017	ToC modified after teleconference with the other WP3 partners	UNEXE
V0.2	08/05/2018	Revision of ToC	N. Habermann, R. Hedel (IVI)
V0.5	19/06/2018	First consolidated version provided to partners	N. Habermann (Fraunhofer IVI)
V0.7	04/08/18	Revision	T. Katopodis, A. Eleftheriadou, T. Sfetsos (NCSRD)
V0.9	17/09/18	Version for final review	N. Habermann (Fraunhofer IVI)
V1.0	01/10/18	Minor corrections after review	N. Habermann, R. Hedel (Fraunhofer IVI), T. Sfetsos (NCSRD)

Executive Summary

The modelling of climate hazards warrants the quantification of their severity and characterictics. Various hazard-specific parameters are applicable for the description of hazards. The objective of this deliverable is to homogeneously characterise different hazards in order to ensure their comparability and understanding by modellers and CI stakeholders. The main characteristics identified for the description of different hazard types are the speed of event, the hazard intensity or magnitude and the affected area. Forest fires are characterised by the Fire Weather Index, fireline intensity and the rate of spread. The consequence of flooding is often described as a combination of depth, discharge, extent, duration and water quality. Floods are distinguished in fluvial and pluvial flooding. The speed of both events are described by the inundation or precipitation rate. Flood depth, discharge and flow velocity are the most commonly applied parameters that characterise fluvial flooding. For pluvial flooding, these are the rainfall intensity and total rainfall. The convective available potential energy is a measure to characterise lightning risk during thunderstorms. For snow risk assessment in the scope of EU-CIRCLE the snow hight is applied. During droughts, the regional water exploitation and the regional water exploitation index plus enable the measurement of water scarcity. Cold snaps are described by low ambient temperatures and the ice accumulation index. Wind hazards can be characterised by the wind speed.

At current state of research, different methods for hazard specific modelling exist. The simulation of wildfires can be achieved by the use of the Behave fire behaviour model, the Fire Tactic and the Geographic Fire Management Information System. Many physical-based modelling approaches enable flood simulations. Recently, data-driven models using data analytic algorithm received attention in flood modelling. For the simulation of pluvial or coastal flooding exceeding the capacities of drainage systems, overland flow models are applicable.

Infrastructure assets are subject to regulations that determine thresholds for specific hazard events. On European level, the Eurocodes determine design requirements and measurement methods for different hazards and structures. Further, other design thresholds are introduced in various publications as well as in national regulations.

The processing of climate outputs defines risk parameters as return periods of extreme events. The probability of occurrence can be estimated using the peaks-over-threshold method or the block maximum method. The analysis of asset exposure can follow either single-hazard or multi-hazard analyses.

Content

List of Figures

List of Tables

List of domain specific abbreviations

AAWR	Actual Available Water Resources
ARI	Average Recurrence Interval
BTU	British thermal unit
CAPE	Convective available potential energy
CDI	Combined Drought Index
CI	Critical infrastructure
DHS	District heating substation
DMC	Index of moisture content of the organic layer
EDC	Drought Index
ETa	Actual Evapotranspiration
EU	European Union
EVT	Extreme Value Theory
FEPS	Fire Emission Production Simulator
FWI	Fire Weather Index
GEV	Generalised Extreme Value
G-FMIS	Geographic Fire Management Information System
GIS	Geographic Information System
HYSPLIT	Hybrid Single Particle Lagrangian Integrated Trajectory Model
LTAA	Long Term Annual Average
P	Precipitation
POI	Point of interest
Qsub	Natural subsurface discharge
RBD	River Basin District
RCM	Reliability centered maintenance
RCP	Representative Concentration Pathways
Run	Unrecoverable surface runoff
RWR	Renewable Water Resources
SPI-n	Standard Precipitation Index
WEI	Water Exploitation Index
WEI+	Water Exploitation Index plus
ΔfP	Soil moisture anomaly
ΔfAPAR anomaly	Anomaly of Fraction of Absorbed Photosynthetically

1 Introduction

1.1 Deliverable subject matter

CI assets and networks are vulnerable to severe climate events. The main objective of the EU-CIRCLE project is the development of a compound approach for the modelling of CI behaviour in case of hazardous events. Natural hazards are phenomenons that are likely to cause damages and losses to CI assets. The natural hazards examined and estimated within the EU-CIRCLE project are the following:

- Extreme temperature,
- Wind,
- Snow,
- Ice, frost and cold spells,
- Sea level rise,
- Storm surge,
- Forest fire and
- Flood.

In order to model climate hazards, it is necessary to quantify their severity and characterictics. Therefor various hazard-specific parameters are applicable for the description of hazards. The objective is to homogeneously characterise different hazards in order to ensure their comparability. Natural hazards are often classified by parameters, such as:

- *Magnitude*: the severity of the event in terms of e.g. produced energy (wildfire), volume (flood), wind speed (storms), or displaced material (landslides, coastal erosion)
- *Duration*: the time that the event will last
- *Extent*: the potentially affected geographical area
- *Onset speed:* the onset can last from a few seconds to a few hours (e.g. meteotsunamis, flash floods), from a few hours to a few days (e.g. storm winds, storm surges, frosts, river floods) or from weeks to months and years (e.g. droughts)

By means of physical units the modeller is enabled to map the hazard. The parameters vary concerning their degree of abstraction and the quantity of considered variables. The appropriate selection of parameters applied in the modelling allows CI operators and stakeholders to understand the characteristics of natural hazardous events despite their complexity and provides the modelling of the behaviour of their CI assets most realistically for them. Besides, the modelling of natural phenomena requires the estimation of return periods for hazardous events. For each hazard the probability of occurrence needs to be calculated in order to take their frequency into account.

When considering parameters associated with hazardous climatic events, existing design standards for CI assets should also be considered. Infrastructure assets are often subject to regulations that determine thresholds for specific natural or man-made hazards. Simply put, many CI assets are resilient to hazards below a certain magnitude, provided that their construction and maintenance happened according to established standards. These requirements can be abstracted from national and international guidelines. Critical thresholds are distinguished in structural and operational thresholds. Structural thresholds set a limit for a hazard intensity (e.g. inundation depth), that an asset must be able to withstand without developing structural damage or changes in its structural integrity. Further, the operational thresholds determine up to which hazard magnitude the CI service must be maintained without disruptions. There can be several thresholds marking staged reduced service levels, since CI assets do not necessarily need to be shut down immediately when they cannot provide their service faultlessly. This deliverable is intended to provide an overview of diverse parameters relevant for the assessment of impacts and damages from natural hazards to CI assets and networks.

1.2 Link to other deliverables

Recent deliverables already addressed the topic of climate related critical event parameters with varying profundity. Deliverable D 1.1 includes definitions of some parameters introduced in this deliverable. The deliverable D 1.3 briefly addresses the role of climate parameters within the strategic EU-CIRCLE risk assessment framework. Deliverable D 1.5 describes the required data for the damage assessment in specific case studies (e.g. duration of heat waves, wind speed and direction for forest fires or land use, precipitation, rainfall intensity etc. for flood events). For each case study, the deliverable states, which parameters need to be regarded for the description of hazard impacts. However, the D 1.5 does not include further specifications of the parameters. Deliverable D 2.1 provides an overview of weather and climate based models and datasets, which are relevant for the EU-CIRCLE damage assessment. The deliverable introduces different climate data providers and weather prediction models. It includes links to different databases for different types of climate data. The D 2.1 investigates hydrological, landslide, flood and wildfire parameters and addresses the quantification of these parameters. Further, it presents existing approaches for hazard modelling, regarding the data required as input. Finally, the deliverable D 2.2 lists and introduces different climate databases with regard to types and accessibility of data and the data content. The deliverable includes for each database a register of regarded variables or parameters for different hazards (e.g. air temperature, air humidity, wind speed and direction, precipitation volume, snow depth, water equivalent to snow etc.)

1.3 Structure of the deliverable

Following the introduction, chapter 2 contains explanations on the use of parameters that are applied in order to describe the extent of hazards in the modelling. Further the chapter provides a collection of parameters for different hazards that are regarded in the scope of the EU-CIRCLE project. In chapter 2.8 the deliverable provides an overview of existing approaches for the modelling of specific climate hazards. Chapter 4 compiles different design thresholds for CI assets that predefine the CI resilience to diverse hazardous events. Chapter 5 addresses the probability of occurrence for extreme events. It introduces existing approaches for the estimation of said probabilities and examines their limitations. The penultimate chapter 6 introduces models for the assessment of CI exposure to climate hazards. Finally, chapter 7 summarises the content of this deliverable.

2 Critical event parameters

2.1 Overview

This chapter lists and shortly describes the types of natural hazards and related critical event parameters for CI (pertaining to the strength, duration, spatial scale, magnitude, physical/chemical parameters and evolution of the climate hazard).

Identifying the climate vulnerabilities of assets and operations requires a detailed knowledge of projected climate change hazards and the factors affecting the likelihood of each potential impact (e.g. region, geography, and hydrology, among others). These potential impacts should then be evaluated in terms of the utility's own assets and operations, considering specific locations and other relevant attributes[1]. A basic understanding of the various types of climate hazards can be gained by consulting existing resources that provide an inventory of the potential impacts and the relevant vulnerabilities of electric utilities. Several reports detail climate change vulnerabilities relevant to the energy sector[2].

A screening analysis may be completed for separate climate hazards, but the approach is best used for cases in which there are regional variations either in the projected climate hazards (e.g. monthly precipitation or high temperature) or in the attributes of a utility's assets and operations (e.g. height above sea level or safe operating temperature). Regional variations could affect their vulnerability to potential impacts.

The proper identification of a critical threshold for a specific climate screening parameter is highly important for the screening analysis. These thresholds are simply values above or below which the likelihood of a climate impact is considered sufficient to render the asset or operation vulnerable[3]. The following existing design thresholds were found during the literature review process and transformed into a unique design with the aim to safeguard harmony and homogeneity. Critical thresholds are mainly linked on the asset and operational attributes and concern:

- Historical operating parameters associated with damage, accelerated wear, increased costs, or service interruption/disruption.
- Design parameters or structured operating parameters
- Measureable physical characteristics of assets or infrastructures

For some climate hazards, a threshold indicates a clear point at which damage or disruption could occur (e.g. intake water temperatures above which a nuclear power plant cannot operate). For other climate hazards or potentially vulnerable assets or operations, a threshold can be set as a point along an increasing slope of likelihood that the asset will suffer a significant cost or impact.

[1] DOE, "Climate Change and the Electricity Sector Guide for Climate Change Resilience Planning," Sep. 2016

[2] DOE, "U.S. energy sector vulnerabilities to climate change and extreme weather," U.S. Department of Energy, DOE/PI-0013., Jul. 2013; DOE, "Climate Change and the U.S. Energy Sector: Regional Vulnerabilities and Resilience Solutions," US Department of Energy, 2015.; DOE, "Effect of Sea Level Rise on Energy Infrastructure in Four Major Metropolitan Areas," Sep. 2014., Melillo, J. M., Richmond, Terese (T. C.), and Yohe, G. W., "Climate Change Impacts in the United States: The Third National Climate Assessment," 2014.

[3] DOE, "Climate Change and the Electricity Sector Guide for Climate Change Resilience Planning," Sep. 2016

In setting thresholds, a planner tries to identify the point above which the risk of impact is great enough to qualify as a vulnerability.

In order to describe the different hazard types, three main characteristics can be defined:

- Speed of event
- Intensity /Magnitude
- Affected area

Each of these characteristics will be introduced and briefly described. The aim is to homogeneously characterise the different hazards in order to compare them among each other's (see Table 1).

Speed of event

The speed of event characterises the lapse of time from the occurrence of the first precursor to the intensity peak of the hazardous event. It is referred to rapid-onset and slower-acting (slow onset) natural hazards. The speed of onset of a hazard is an important variable since it conditions warning time. Some events (e.g. flash floods) allow no or insufficient time for warning. Events such as hurricanes or floods typically have warning periods of minutes or hours and the likelihood of occurrence is known for several hours or days in advance. Other hazards such as drought, desertification, and subsidence act slowly over a period of months or years.

Intensity/ Magnitude

The intensity and the magnitude of an extreme event represent an exceptional and harmful condition. Several types of hazards like rainfalls and storms are common atmospheric events but if those phenomena exceed certain thresholds of intensity they become hazardous. Magnitude is related to the amount of energy released during the hazardous event, or refers to the size of the hazard. Magnitude is indicated using a scale, consisting of classes, related to an increase of energy.

Affected Area

The affected area designates the region that has been struck with a natural hazard and identifies the size and the impact of the hazard risk area.

Table 1: Characterisation of hazards

Hazard	Category[4]	Speed of event	intensity	Affected area
Temperature	M	Temperature change with time [°C/y]	Temperature [°C; °F] T_{max} above threshold T_{min} below threshold	Area over/below parameter threshold
Precipitation	M	Precipitation rate change with time [mm/y]	Rainfall intensity [mm/h]; Total rainfall [mm] Light, moderate, heavy, extreme threshold exceedance	Flooded area [ha]

[4] Based on (IRDR, 2014) classification, H:Hydrological, M: Meteorological and C: Climatological

Wind	M	Wind speed change with time [m/s]	Wind and gusts speed [m/s]	Area over/below parameter threshold
Snow/Ice	M	Snow gauge change with time [cm/y]	Ice accumulation index Snow gauge [mm; cm; m]	Covered area [ha]
Solar radiation	M	Change of solar power with time [W/y]	Irradiance [W/m²]	Area over/below parameter threshold
Sea level rise	M	Rise rate [mm/y; mm/10 y]	Rise rate [mm/y; mm/10 y] Accumulated increasing of sea level [m] Threshold esceedance [m]	Area below sea level [ha]
Lightning activity	M	Seconds / Minutes	CAPE values	Area ovr threshold
Storm surge	M	Velocity [m/s]	Storm surge height [m]	Inundated area [ha]
Waves	M	Velocity [m/s]	Wave height [m]	Inundated area [ha]
Forest fire	C	Rate of spread [m/min]	Fire line intensity [kW/m]	Burned area [ha]
Flood	H	Rise rate [m/s]	Flood depth [m] Discharge [m³/s] Flow velocity [m/s]	Inundated area [ha]
Heat wave	M	Change of T_{Max} with time [K/y] Temperature change with time [K/y]	Consecutive days with T_{max} above threshold	Area above parameter threshold
Cold snap	M	Change of T_{Min} with time [K/y] Temperature change with time [K/y]	Consecutive days with T_{min} below threshold	Area below parameter threshold
Drought	C	Precipitation rate change with time [mm/y] Temperature change with time [K/y]	Water Exploitation Index [hm³] Drought indices	Area over parameter threshold

2.2 Forest fires

2.2.1 Risk indicators - Fire Weather Index (FWI)

Fire weather indices have become reliable tools for the assessment of the potential risk of regional fires[5]. The estimation of these indices is based on a number of meteorological variables (wind, precipitation, air temperature and relative air humidity) that play a part in forest fire initiation and propagation[6]. The calculation of the FWI system indices of the Canadian Forest Fire Hazard Indexing System is based on the following meteorological data: noon air temperature [°C], relative air humidity [%], wind speed at 10 m height [m/s] and 24 hour precipitation amount [mm]. The FWI system is comprised of the following indices:

- FFMC - Index of the moisture content of the fine fuels
- DMC - Index of moisture content of the organic layer
- EDC - Drought Index, indicating the soil water deficit.

At the intermediate level there are two indices linked with fire behavior or propagation:

- ISI - Initial propagation index that combines the FFMC and the wind speed values to provide the propagation velocity of the fire on flat ground, as should be the case during the initial phase of a fire and
- BUI - which integrates the two subindices DMC and EDC to give an estimate of the proportion of vegetation available (medium and coarse particles) that will effectively assist in the propagation.

The final result of this system is the FWI as an expression of the possibility of the occurrence of fires and their respective hazards[7]. FWI values range from 0 to above 100 and are categorised, for operational purposes, in four to six classes, depending on the application area, corresponding to the different fire danger levels[8,9,10,11]. Given the high physical diversity of European area, it is obvious that appropriate and non-uniform classification of FWI is necessary in order to obtain a reasonable FWI value interpretation into fire Risk indicator, for the various sub-regions within Europe. Nevertheless, a five class classification is considered as appropriate for the purposes of EU - CIRCLE.

[5] Holsten A, Dominic AR, Costa L, Kropp JP. (2013) Evaluation of the performance of meteorological forest fire indices for German federal states. Forest Ecology and Management. 2013;287:123-31

[6] Huesca M, Litago J, Palacios-Orueta A, Montes F, Sebastián-López A, Escribano P. (2009) Assessment of forest fire seasonality using MODIS fire potential: A time series approach. Agricultural and Forest Meteorology.;149:1946-55

[7] Viegas DX, Reis RM, Cruz MG, Viegas MT (2004). Calibração do Sistema Canadiano de Perigo de Incêndio para Aplicação em Portugal. Silva Lusitana.;12:77-93

[8] Alexander ME (1994) Proposed revision of fire danger class criteria for forest and rural areas in New Zealand. NRFA / NZFRI, Circular 1994/2, Wellington.

[9] Dimitrakopoulos AP, Bemmerzouk AM, Mitsopoulos ID (2011) Evaluation of the Canadian fire weather index system in an eastern Mediterranean environment. Meteorological Applications. 18, Issue 1, 83–93

[10] Camia A. and Bovio G, 2000, Description of the indices implemented in EUDIC software for the European meteorological forest fire risk mapping. Joint Research Centre, Institute for Environment and sustainability Land Management Unit

[11] Palheiro PM, Fernandes P, Cruz MG (2006) A fire behaviour-based fire danger classification for maritime pine stands: Comparison of two approaches. Forest Ecology and Management 234,S54

2.2.2 Critical fire parameters

Fireline intensity and rate of spread parameters are main descriptors of wildland fire behaviour. Fireline Intensity, also called Byram's intensity, is the rate of energy release per unit length of the fire front expressed as British termal unit (BTU) per foot of fireline per second or as kilowatts per meter of fireline[12]. This is a physical parameter that is related to flame length. Frontal fire intensity is a major determinant of certain fire effects and difficulty of control. Numerically, it is equal to the product of the net heat of combustion, quantity of fuel consumed in the flaming front, and linear rate of spread.

Fire intensity classes are conceptually introduced in Hirsch (1996)[13], where general fire behaviour descriptions are based on head fire intensity are associated with a range of fire intensity values [kW/m]. The concept of fire intensity class is formally adopted in Taylor (1998)[14] as one of the key outputs for each rate of spread/fire intensity class table of the Field guide to the Canadian Forest Fire Behaviour Prediction System. Each fire intensity class 1 to 6 is assigned with a range of fire intensity values [kW/m].

For the purposes of EU - CIRCLE, the thresholds of fireline intensity and rate of spread classes (1-5) where defined based on previous research results and operational experience in European countries largely affected by forest fires. The threshold values of the forest fire parameters for the determination of the likelihood categories that are used in the frame of EU–CIRCLE are shown in Table 2. Within EU-CIRCLE, the fire simulation model, has been linked as described in section 3.5 with a chemical dispersion model to estimate the air concentrations of smoke and other particulate matter on the ground level (0 - 20 m). These have been derived in accordance with limits on air pollution concentrations and World Health Organization recommendations for average 24h values (Table 3).

Additionally, the burned areas produce smoke, which for the purposes of EU-CIRCLE has been considered to be particulate matter of 10μm diameter. The PM10 concentration can be integrated on a daily basis (24h) to match with existing EU air quality regulations (Directive 2008/50/EU). Furthermore, for modeling purposes a vertical integration for a height of up to 20 m is recommended which is the area where the vast majority of population resides.

[12] Paysen, Timothy, R.J. Ansley, J. Brown, G. Gottfried, S. Haase, M. Harrington, M. Narog, S. Sackett, R. Wilson. 2000. Fire in Western Shrubland, Woodland, and Grassland Ecosystems. Chapter 6. USDA Forest Service Gen. Tech. Rep. RMRS-GTR-42-vol. 2.

[13] Hirsch, K.G. 1996. Canadian forest Fire Behavior Prediction (FBP) System: user's guide. Nat. Resour. Can., Can. For. Serv., North. For. Cent., Edmonton, Alberta. Spec. Rep.7

[14] Alan H. Taylor, Carl N. Skinner: Fire history and landscape dynamics in a late-successional reserve, Klamath Mountains, California, USA, Forest Ecology and Management, Volume 111, Issues 2–3, 1998, Pages 285-301, ISSN 0378-1127, https://doi.org/10.1016/S0378-1127(98)00342-9.

Table 2: Theshold values and likelyhood categories of forest fire parameters

	EU – CIRCLE likelihood categories					
Parameters	**Very Low**	**Low**	**Medium**	**High**	**Very High**	**Exceptional**
FWI	<30	30-50	50-60	60-80	80-100	>100
FFMC	<84	84-89	90-93	94-94	>95	
EDC	<80	80-200	200-300	300-700	700-1000	>1000
Rate of Spread [m/min]	<3	3-8.5	8.5-20	20-50	>50	
Fireline Intensity [kW/m]	<750	750-3500	3500-10000	10000-30000	>30000	

Table 3: Likelihood categories for 24h average PM10 concentration / smoke at ground level (0-20 m) from forest fires

	EU – CIRCLE likelihood categories					
Parameters	**Very Low**	**Low**	**Medium**	**High**	**Very High**	**Exceptional**
SMOKE [µg/m^3] (as PM2.5)	0-35	35-50	50-100	100-200	200-300	>300

2.3 Flood

The consequence of flooding is often described as a comination of depth [m], velocity [m/s], discharge [cms], extent [ha], duration [hr;day;week], and quality [-]. These characteristerics are associated with different vulnerablity, fragility, and socio-economic factors to determine the damage or impact of flood events. For pluvial events, the intensity or accumulation of precipitation are utilised to describe the main driver that leads to flooding, which are also used for the standards for designing drainage networks. The combined sewer overflows often pollute the environment such that the concentration of contamination is also considered. The occurrence of fluvial events depends on the conveyance capacity of river channels and the protection level of embankments. Therefore, the discharge and water level of flow are the critical parameters to describe such events. Coastal flooding may occur due to sea level rise or storm surge. For the former, it is a long term process and the water level is the major factor leading to flooding. For the latter, the moving speed and height of waves are the main drivers.

For determining these parameters in flood modelling, either historical observations or statistical analyses can be used as the inputs of initial and/or boundary conditions. The modelling results normally include the above-mentioned critical parameters that can be used to determine the impact to critical infrastructures. For simulations using historical records, these information can be used to calibrate and validate the flood models, while the results using statistical analyses can be used to estimate the likelihood of hazard impacts.

2.4 Thunderstoms - A Lightning Risk Index

Thunderstorms and lightning are considered as potentially hazardous events for CI (especially chemical industry) and for the purposes of EU-CIRCLE. The convective available potential energy (CAPE) is a measure of the energy that can be realised if there is enough heating to give convection. For CAPE values up to about 1000, the probability of heavy showers increases. Table 4 gives a rough guide on the likelihood of lightning:

Table 4: Likelihood categories of lightning

	EU – CIRCLE likelihood categories					
Parameters	**Very Low**	**Low**	**Medium**	**High**	**Very High**	**Exceptional**
CAPE [J/kg]		< 1 000	1 000 - 2 500	2 500 - 3 500	> 3 500	
Daily number of events nearby CI	0	1	2 - 10	10 - 30	30 – 50	> 50

2.5 Snow

Risk indices are based on meteorological data, and usually involve the quantitative estimation of a natural hazard and more rarely qualitative approaches. In the case of snow risk assessment, several critical climatic parameters are taken into account, either during the design of new CI or during the assessment of the existing assets. Depending on the local conditions, snow on the ground will have different qualities in relevance with the temperature changes, winds blow, or on the time that it remains on the ground. The variables that are usually applicable for the snow risk assessment are the weight of snow or the weight density, in possible combination with the local wind. Within EU-CIRCLE we propose the use of the height of snow (in mm) / 6h, which is a common output of all Regional Climate Models (see Table 5).

Table 5: Likelihood categories for snow

	EU – CIRCLE likelihood categories				
Parameters	**Very Low**	**Low**	**Medium**	**High**	**Very High - Exceptional**
Snowfall [mm/6h]	< 0.1	0.1 - 3	3 - 8	8 - 15	> 15

2.6 Extreme temperature

2.6.1 Drought

As average global temperatures continue to rise, droughts and water scarcity are likely to pressurise CI sectors dependable on water resources availability such as energy, water, wastewater and river-based transportation[15]. There are several distinct hazards that may decrease the availability of water resources and affect CI as well. Their categorisation is based on their duration and their cause. The main causes are natural occurrence due to climate and manmade causes with regard to differences in supply and demand. In Table 6 the hazards that affect water availability are categorised by means of their timescale and causes.

Table 6: Timescale and causes of hazards affecting water availability[16]

Hazards	Timescale	Causes
Dry spell	Short-term (days, weeks)	Natural
Water shortage	Short-term (days, weeks)	Manmade
Drought	Mid-term (months, seasons, years)	Natural
Water scarcity	Mid-term (months, seasons, years)	Manmade
Aridity	Long-term (decades)	Natural
Desertification	Long-term (decades)	Natural or Manmade

The term drought defines a temporary decrease in water availability for instance due to rainfall deficiency. Drought is an indistinct event of water deficiency that results from the combination of many complex factors and neither the beginning nor the end can be precisely defined[17]. The World

[15] M. Davis and S. Clemmer, "How Climate Change Puts Our Electricity at Risk," Power Failure, 2014
[16] Strosser et al., 2012, Gap Analysis of the Water Scarcity and Droughts Policy in the EU, Pierre Strosser, Thomas Dworak, Pedro Andrés Garzon Delvaux, Maria Berglund, Guido Schmidt, Jaroslav Mysiak, Maggie Kossida, IacovosIacovides, Victoria Ashton, European Commission, Tender ENV.D.1/SER/2010/0049
[17] Addressing the challenge of water scarcity and droughts in the European Union, COMMUNICATION FROM THE COMMISSION TO THE EUROPEAN PARLIAMENT AND THE COUNCIL, COM(2007) 414 final, Brussels, 18.7.2007.

Meteorological Organization defines drought as: "a marked unusual period of abnormally dry weather characterised by prolonged deficiency below a certain threshold of precipitation over a large area and persisting for timescale longer than a month"[18]. Water scarcity is a long-term condition identified by the occurrence of differences between demanded and offered water resources. In order to classify a water shortage situation, spatial and temporal parameters are needed to define reference points for the comparison of current or projected supply and demand of water resources[19]. Phenomena that affect the availability of water, such as water scarcity and drought are in general slow in their onset and have a long duration that may be measured in weeks, months and even years. Their slow onset creates difficulties in the identification of the phenomenon since events of dry spells could be both normal to the regional climate and abnormal if they, for instance, last longer than usual. To define the impacts of water scarcity, it is necessary to draft the water balance of the relevant river basin district (RBD) in order to assess the quantitative status of freshwater resources. The required components of the hydrological cycle are presented in Table 7, together with an example of Malta's RBD.

Table 7. Water balance of Malta's river basin district[20] (* LTAA: Long Term Annual Average)

Parameter	LTAA* [hm^3]	2010 [hm^3]	Comments
Precipitation (P)	174	162	
Actual Evapotranspiration (ETa)	105	97	Assumed at 60% of total precipitation in both cases
Renewable Water Resources (RWR = P – ETa)	69	65	
Natural subsurface discharge (Qsub)	23	23	
Unrecoverable surface runoff (Run)	6	6	Estimated at 25% of total surface runoff generated (initial estimate)
Actual Available Water Resources (AAWR = RWR – Qsub – Run)	40	36	
Total Abstraction	37.5	43.7	
Returned water	10	8	Return from leakages - value is reducing due to leakage program

[18] WMO, 2012, Standardized Precipitation Index. User Guide, World Meteorological Organization, Geneva, Switzerland (2012) WMO-No. 01090. ISBN 978-92-63-11091-6

[19] Mediterranean Water Scarcity and Drought Report, Technical Report - 009 – 2007, produced by the MEDITERRANEAN WATER SCARCITY & DROUGHT WORKING GROUP (MED WS&D WG), April 2007

[20] Data provided by the EIONET NFP of Malta (Malta Resources Authority, Regulation Unit) during the EEA Consultation of the WEI+ in August 2012, in Kossida et. al., 2012

The European Environment Agency uses the Water Exploitation Index (WEI) for countries and the regional WEI plus (WEI+) for river RBD to assess water scarcity[21]. A WEI value above 20% indicates water scarcity whereas a value higher than 40% indicates severe water scarcity[22]. From Table 7 it is possible to calculate the WEI+ which is defined as the ratio of total abstraction minus returned water over the actual available water resources (WEI+ = (Abstraction-Returned water) / AAWR). Calculating the WEI+ for the RBD of Malta, it is possible to draw two conclusions. First, the RBD of Malta is already severely water stressed with a LTAA of WEI+ of 69 % and the climatic conditions of 2010 increased this water stress even more to a WEI+ of 99 %[23]. Therefore, in order to model the impacts of water scarcity, it is required to firstly model the water balance of the RBD and then assess the effects of the climatic conditions using the WEI+.

To identify drought events, it is necessary to initially define the normal conditions and then choose relevant threshold values. Drought indicators are used for the identification of the onset, the severity, and the end of a drought. These indicators need to be objective measures of the system status[24]. Common indicators are based on meteorological and hydrological variables such as rainfall, stream flow, soil moisture, reservoir storage and ground water levels. The European Drought Observatory of the Joint Research Centre uses the Combined Drought Index (CDI) which is a complex index that uses in combination three different indices to define Watch, Warning and Alert levels of drought. The indices used by the Combined Drought Index are:

- Standard Precipitation Index (SPI-n)[25] which is a statistical indicator which compares the total precipitation received at a particular location during a period of ***n*** months with associated long-term rainfall distribution. It is expressed as deviation from a median value.
- Soil moisture anomaly (ΔfP), comparing the daily soil moisture with the long term average to assess the effects of the hydrological drought to plants providing information on spatial distribution of the soil water content and its time evolution.
- Anomaly of Fraction of Absorbed Photosynthetically (ΔfAPAR anomaly): Active Radiation focusing on the fraction of solar energy which is absorbed by the vegetation.

The classification characteristics for identifying the different drought levels based on the Combined Drought Index factsheet of EDO[26] are as shown in Table 8:

Table 8: drought levels classification

Drought levels	**Indices boundaries**
Watch	SPI-3 < -1 or SPI-1 < -2
Warning	ΔpF> 1 and (SPI-3 < -1 or SPI-1 < -2)

[21] https://www.eea.europa.eu/data-and-maps/indicators/use-of-freshwater-resources-2/assessment-2
[22] Stockholm Environmental Institute, Sweden – Raskin et al. 1997: Comprehensive assessment of the freshwater resources of the world (Document prepared for UN Commission for Sustainable Development 5th Session 1997)
[23] Data provided by the EIONET NFP of Malta (Malta Resources Authority, Regulation Unit) during the EEA Consultation of the WEI+ in August 2012, in Kossida et. al., 2012
[24] "Waterscarcity management in the context of the WFD", Water Scarcity Drafting Group, MED Joint Process WFD /EUWI, June 2006.
[25] McKee et al., 1993, The relationship of drought frequency and duration to time scales, T.B. McKee, N.J. Doeskin, J. Kleist, Proceedings of the 8th Conference on Applied Climatology, American Meteorological Society, Boston, MA (1993), pp. 179-184
[26] http://edo.jrc.ec.europa.eu/documents/factsheets/factsheet_combinedDroughtIndicator.pdf

Alert	ΔfAPAR< -1 and (SP-3< -1 or SPI-1< -2)
Partial recovery	ΔfAPAR< -1 and ($SP\text{-}3_{m-1}$ < -1 and SPI-3 >-1) or ΔfAPAR< -1 and ($SP\text{-}1_{m-1}$ < -2 and SPI-1 >-2))
Full recovery	$SPI\text{-}3_{m-1}$ < -1 and SPI-3 >-1 or $SP\text{-}1_{m-1}$ < -2 and SPI-1 >-2

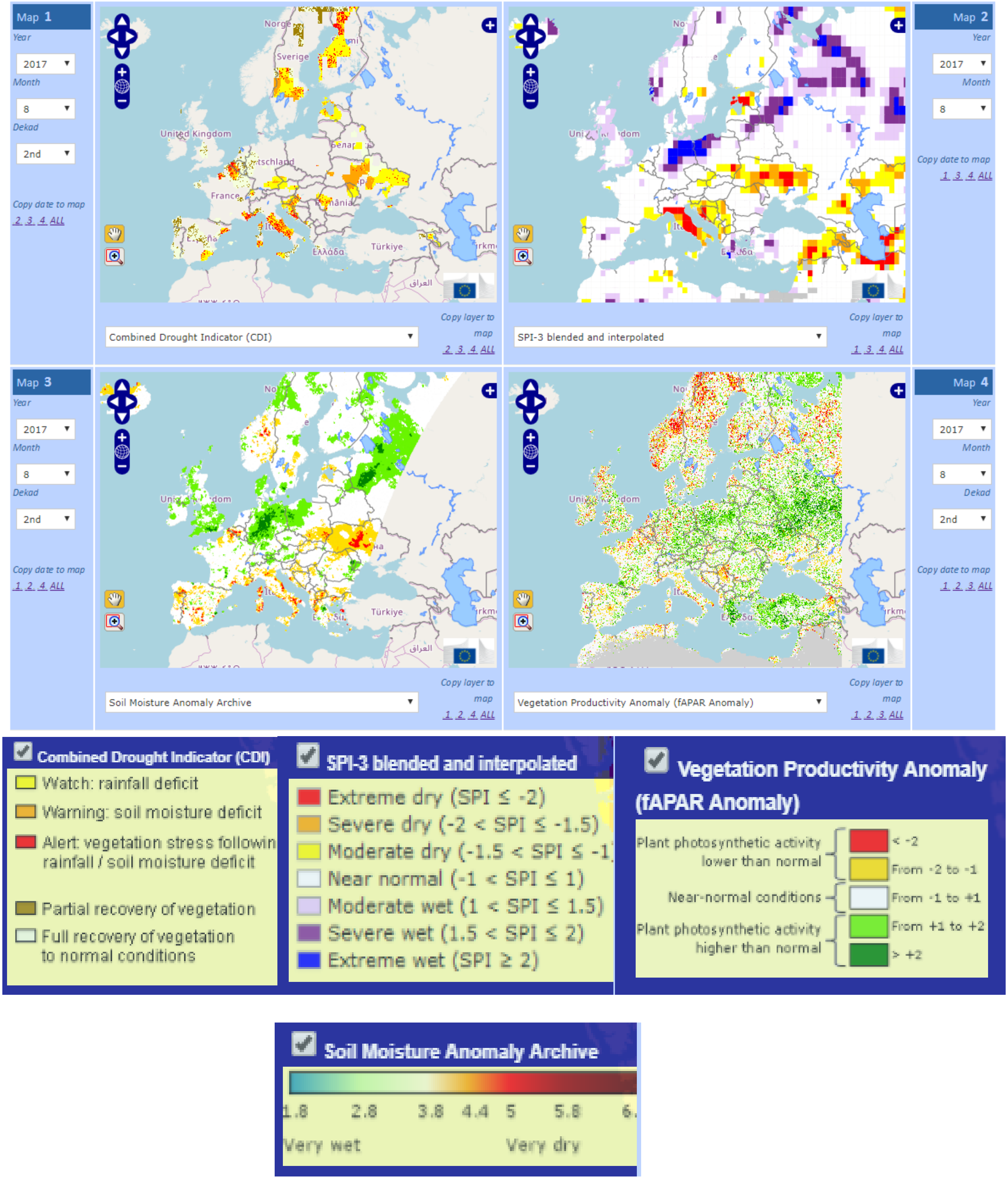

Figure 1: CDI, SPI-3, ΔfP, ΔfAPAR for August 2017[27]

[27] JRC http://edo.jrc.ec.europa.eu

Figure 1 presents a map visualisation of all four indicators for August 2017 extracted from the European Drought Observatory of the Joint Research Centre. From the results of the three indices SPI-3, ΔfP and ΔfAPAR the CDI was estimated identifying areas like Italy, South and North-East France, West Balkans, Ukraine, West Bulgaria, Finland and parts of Sweden were either at alert or at a warning level due to the CDI index. Even though the CDI is used by the EDO JRC it is somewhat a complex index to use it in modelling. The indicator used more often to assess and model drought conditions is the SPI-3 for meteorological drought and SPI-12 for hydrological drought[28]. A drought event starts when the SPI falls below −1 and ends when it turns positive[29]. Figure 2 presents the application of SPI-12 in historical rainfall data for Southern Europe from 1950 to 2012 identifying several drought occurrences in the 1990s.

Table 9 presents how the United States Drought Monitor classifies areas in different categories of drought severity. The classification uses 5 different indicators and since their ranges usually do not coincide, the drought category is selected based on the majority of the indicators and on local impact observations. The indicators are used to show in the Drought Monitor map the areas under drought and label their intensity. While D1 is the least intense level and D4 the most intense, D0 shows areas that have abnormally dry conditions that may lead to drought. Drought is defined as a moisture deficit that is so severe that may have social, environmental or economic effects. These effects are classified based on short-term, typically less than 6 months i.e. effects on agriculture, grasslands etc. and long-term, typically more than 6 months, i.e. effects on hydrology, ecology etc.

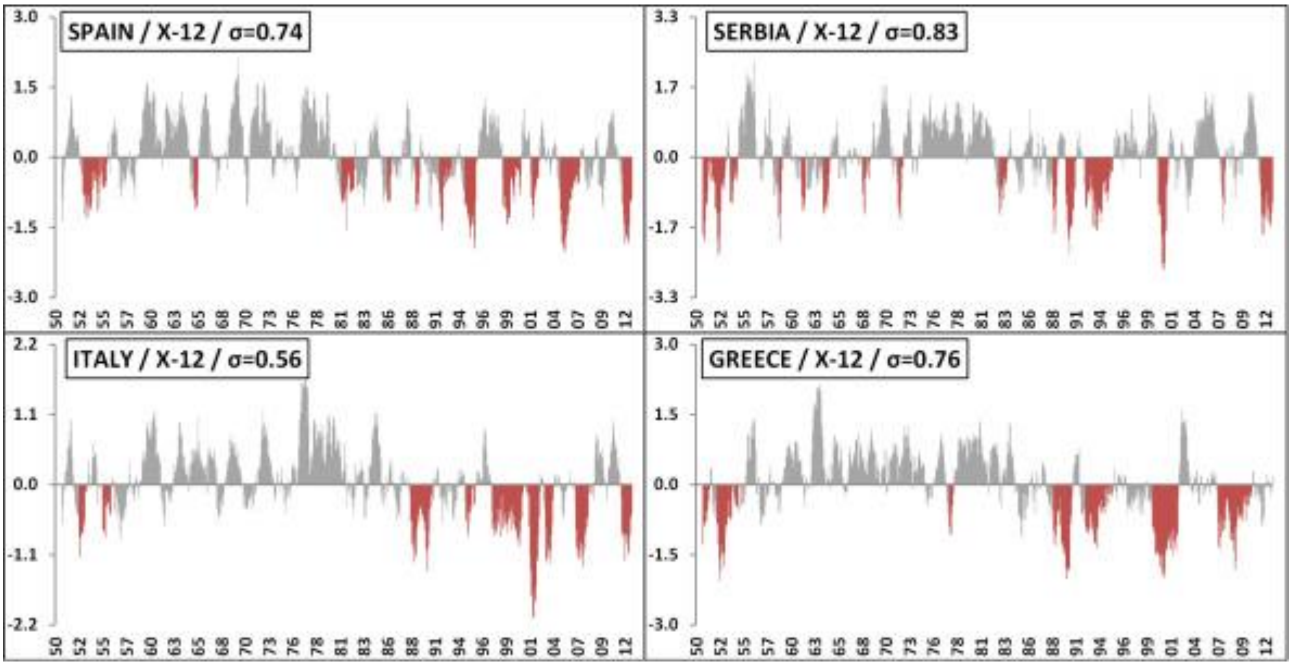

Figure 2. Southern Europe country drought events (marked in red) series for the period 1950–2012[30]

[28] WMO, 2012, Standardized Precipitation Index. User Guide, World Meteorological Organization, Geneva, Switzerland (2012) WMO-No. 01090. ISBN 978-92-63-11091-6

[29] McKee et al., 1993, The relationship of drought frequency and duration to time scales, T.B. McKee, N.J. Doeskin, J. Kleist, Proceedings of the 8th Conference on Applied Climatology, American Meteorological Society, Boston, MA (1993), pp. 179-184

[30]Spironi et al., 2015, The biggest drought events in Europe from 1950 to 2012, Jonathan Spinoni,GustavoNaumann,Jürgen V. Vogt,Paulo Barbosa, Journal of Hydrology: Regional Studies

Table 9: U.S. drought monitor severity classification[31]

Category	Description	Impacts	Palmer Drought Index	CPC Soil Moisture Model [percentiles]	USGS Weekly Streamflow [percentiles]	Standardised Precipitation Index	Objective Short and long-term Indicator on Blends
D0	Abnormally dry	Slow planting and growth of crops and pastures, water deficit	-1.0 to -1.9	21 – 30	21 – 30	-0.5 to -0.7	21 – 30
D1	Moderate drought	damage to crops, pastures, streams, reservoirs, or wells low, water shortages, voluntary water-use restrictions	-2.0 to -2.9	11 - 20	11 – 20	-0.8 to -1.2	11 – 20
D2	Severe drought	Crop or pasture losses, water shortages, water restrictions imposed	-3.0 to -3.9	6 – 10	6 – 10	-1.3 to -1.5	6 – 10
D3	Extreme drought	Major crop and pasture losses, widespread water shortages or restrictions	-4.0 to -4.9	3 – 5	3 – 5	-1.6 to -1.9	3 – 5
D4	Exceptional drought	Exceptional crop and pasture losses, water shortages in reservoirs, streams and wells cause water emergencies.	≤ -5	0 – 2	0 – 2	≤ - 0.2	0 – 2

2.6.2 Cold snaps

The precise criterion for a cold wave is determined by the rate at which the temperature falls, and the minimum to which it falls, associated with hazardous weather, like frost and icing. A cold wave is a rapid fall in temperature within a 24-hour period requiring substantially increased protection to agriculture, infrastructure, commerce, and social activities. Table 10 presents a recommended set of limits which is valid for South Europe. However, when cold snaps are coinsiding with ice conditions, the Ice accumulation index can also be used (see Table 11).

[31] http://www.al.com/news/index.ssf/2014/12/mobile_goes_from_rainiest_city.html

Table 10: Likelihood categories for low air temperature (South Europe)

	EU – CIRCLE likelihood categories					
Parameters	**Very Low**	**Low**	**Medium**	**High**	**Very High**	**Exceptional**
Low Air Temperature [˚C]	> 0	0 - (-2)	(-2) - (-5)	(-5) - (-10)	(-10) - (-15)	< (-15)

Table 11: Ice accumulation index[32]

Average ice amount [m]	Wind [m/s]	Damage and impact	Ice damage index
< 0.00635	< 6.7056	Minimal risk of damage to exposed utility systems; no alerts or advisories needed for crews, for outages.	**1**
0.00254 - 0.00635	6.7056 - 11.176	Some isolated or localised utility interruptions are possible, typically lasting only a few hours. Roads and bridges may become slick and hazardous.	
0.00635 - 0.0127	>6.7056		
0.00254 - 0.00635	11.176 – 15.6464	Scattered utility interactions expected, typically lasting 12 to 24 hours. Roads and travel conditions may be extremely hazardous due to ice accumulation.	**2**
0.00635 - 0.0127	6.7056 - 11.176		
0.0127 - 0.01905	<6.7056		
0.00254 - 0.00635	≥ 15.6464	Numerous utility interruptions with some damage to main feeder lines and equipment expected. Tree limb damage is excessive. Outages lasting 1 – 5 days.	**3**
0.00635 - 0.0127	11.176 – 15.6464		
0.0127 - 0.01905	6.7056 - 11.176		
0.01905 - 0.0254	<6.7056		
0.00635 - 0.0127	≥ 15.6464	Prolonged and widespread utility interruptions with extensive damage to main distribution feeder lines & some high voltage transmission lines/structures. Outages lasting 5 – 10 days.	**4**
0.0127 - 0.01905	11.176 – 15.6464		
0.01905 - 0.0254	6.7056 - 11.176		
0.0254 - 0.0381	<6.7056		
0.0127 - 0.01905	≥ 15.6464	Catastrophic damage to entire exposed utility systems, including both distribution and transmission networks. Outages could last several weeks in some areas. Shelters needed.	**5**
0.01905 - 0.0254	≥ 11.176		
0.254 - 0.0381	≥ 6.7056		
>0.0381	Any		

[32] http://www.spia-index.com/index

2.6.3 Heat Waves

Heat waves, determined by a persistent period of abnormal warm weather, can cause expensive livestock and crop losses, and damage CI such as roads, railways and bridges. Table 12 presents an example of high air temperatures over South Europe. In future, the broad trends in extreme heat are expected to continue – heat waves are expected to become more intense and more frequent.

Table 12: Likelihood categories for high air temperature – South Europe

	EU – CIRCLE likelihood categories					
Parameters	Very Low	Low	Medium	High	Very High	Exceptional
High Air Temperature [˚C]	< 30	30 - 33	33 – 35	35 - 39	39 – 42	> 42

2.7 Wind

For wind risk assessment, several parameters are taken into account both during the design of new CI or the assessment of existing ones. The most common paramter is the wind velocity or pressure, which is used for the assessment of the wind load along with additional parameters, such as turbulence intensity, terrain category, reference height, orography, upstream slope, neighbouring buildings and building characteristics (shape, dynamic characteristics, natural frequencies, modal shapes, equivalent masses, logarithmic decrements of damping, slenderness, roughness, structural factors, solidity, reference area, etc.). National specifications provide maps comprising local wind loads based on metereological measurements[33]. For different regions, critical design thresholds for the wind load are applied. With exceedance of the design load, damage develops on the structure depending on the local situations. The severity will either result in minor damages (serviceability limit state) or major/severe damages (ultimate limit state).

Table 13 presents the EU - CIRCLE selected limits describing a wind event.

Table 13: Likelihood categories for wind

	EU – CIRCLE likelihood categories					
Parameters	Very Low	Low	Medium	High	Very High	Exceptional
Average value	0 - 3	3 - 12	12 - 15	15 - 20	20 – 30	> 30

[33] https://www.apsei.org.pt/media/recursos/documentos-de-outras-entidades/CFPA-guideline-riscos naturais/cfpa_e_guideline_no_3_2013_n_1389624941.pdf

Gust [m/s]	< 10	10 - 15	15 - 20	20 - 25	25 – 35	> 35

2.8 Human Comfort Index

One of the most common issues faced by workers of CI is related to the heat stress during outdoor work. This is already regulated in almost all European countries and could potentially bring operations to a temporary halt or a change of working shifts. Such indices include the Wet Bulb Globe Temperature, the Thermal Work Limit, the Discomfort Index, the Environmental Stress Index, the Personal Stress Index and the HUMINDEX. All these regard the air temperature and relative humidity and could also include parameters related to the clothing and type of work. The Association Advancing Occupational and Environmental Health established a set of thresholds for different types of outdoor working activity that relate Wet Bulb Globe Temperature to the amount of pause that each worker should take each hour [34] (Table 14). Additionally the HUMIDEX provides a set of indicators relating the value of the index to the degree of comfort as:

1) Comfortable – Range 20-29,

2) Some discomfort – Range 30-39,

3) Great discomfort – Range 40-45,

4) Dangerous – Range > 45,

5) Imminent stroke – Range > 54. [35]

Table 14: Threshold values of Wet Bulb Globe Temperature [° C]

Work%	Pause %	Type of Activity		
Hourly schedule		Light	Moderate	Heavy
Continue	-	30.0	26.7	25.0
75%	25%	30.6	28.0	25.9
50%	50%	31.4	29.4	27.9
25%	75%	32.2	31.1	30.0

[34] https://www.acgih.org/docs/default-source/presentations/2006/04_tlv-pa-update_aihce06.pdf?sfvrsn=c9fbdf0d_2
[35] https://www.ccohs.ca/oshanswers/phys_agents/humidex.html

3 Climate hazard modelling approaches

3.1 Climate modelling

Climate models are extensively analysed and described in deliverables D2.1[36] and D2.2[37] of WP2. Specifically, these deliverables provided a joined overview of both numerical weather prediction (NWP) and climate models (PRUDENCE[38], ENSEMBLES[39], EURO-CORDEX[40] and MED-CORDEX[41]), their datasets, and EU - CIRCLE relevant impact models and datasets. Furthermore, an extended investigation was required according to data availability, access policy of the data, terms of use and their limitations in being utilised. This work has provided starting reference for the subsequent analysis of climate drivers for specific EU-CIRCLE case studies.

For the purpose of the EU-CIRCLE project, the use of the latest generation of the reliability centered maintenance (RCM) simulations over Europe was suggested from EURO - CORDEX framework. EURO - CORDEX is the European branch of the CORDEX initiative and will produce ensemble climate simulations based on multiple dynamical and empirical-statistical downscaling models forced by multiple global climate models from the Coupled Model Intercomparison Project Phase 5. The results of large number of RCM simulations on the 50-km and 12.5-km horizontal resolutions are available through the Earth System Grid Federation system and WCRP CORDEX project which consists of several data nodes. In addition, future projections cover periods up to the end of the 21st century based on greenhouse gas emission scenarios (Representative Concentration Pathways (RCPs)) corresponding to stabilization of radiative forcing after the 21st century at 4,5 W/m² (RCP4.5), rising radiative forcing crossing 8,5 W/m² at the end of 21st century (RCP8.5), and peaking radiative forcing within the 21st century at 3,0 W/m² and declining afterwards (RCP2.6).

Climate data (drivers) results of ICHEC-EC-EARTH/SMHI-RCA4, global and regional models respectively, were downscaled on 12.5-km spatial/horizontal resolution for the time period from 2006 to 2050 and for the three RCPs. Climate variables were selected based on the necessary data according to each EU – CIRCLE case study and analysed by the processing tools for the production of the climate hazard information.

3.2 Empirical Statistical and Dynamical Downscaling

The selection and processing of climate drivers has also involved the applied techniques of empirical statistical downscaling through R-markdown scripts (ESD tool) and dynamical downscaling bases on numerical weather prediction/climate models (e.g. Weather Research and Forecast model (WRF-ARW)[42]) for the production of localised climate projections. These

[36] The EU-CIRCLE consortium (2017): D2.1 Report on Typology of Climate Related Hazards, http://www.eu-circle.eu/research/deliverables/

[37] The EU-CIRCLE consortium (2017): D2.2 Report on Climate Related Hazards Information Collection Mechanisms, http://www.eu-circle.eu/research/deliverables/

[38] Prediction of Regional scenarios and Uncertainties for Defining EuropeaN Climate change and Effects

[39] ENSEMBLE-based Predictions of Climate Changes and their Impacts

[40] European COordinated Regional climate Downscaling Experiment

[41] Mediterranean COordinated Regional climate Downscaling Experiment

[42] Skamarock, W. C., J. B. Klemp, J. Dudhia, D. O. Gill, D. M. Barker, M. G. Duda, X.-Y. Huang, W. Wang, and J. G.Powers (2008), A description of the Advanced Research WRF version 3, NCAR Tech. Note, NCAR/TN- 475 +STR, 125pp., Natl. Cent. for Atmos. Res.,

techniques are further analysed in D2.3 which is related to the tools for processing climate information hazards. For the next steps, these techniques regard the findings within D2.1 and D2.2[43] by providing a starting reference for the subsequent analysis in specific EU - CIRCLE case studies. The previous deliverable findings list relevant climate related databases, meteorological services, weather forecasting models over Europe (with focus on the case study locations) according to both their potential suitability and limitations.

3.3 Forest fires

3.3.1 Behave / Rothermel's fire behaviour model

Rothermel's fire behaviour model is a deterministic model which rely on physical interpretation of fire behaviour, whose mechanisms can be described by mathematical equations. This model constitutes the basis of the Behave system and of the North-American National Forest Fire Danger Rating System. The Behave system is used to predict the main behaviour characteristics of a fire occurring at a site where the fire propagation conditions are known. This system has been operational for many years in the United States and is widely used by the forestry services and firefighting units. Rothermel's fire behaviour model has been enhanced during the period that Behave was developed and came into use. The basic equations have remained the same as in the original, but the various factors have been adjusted to improve the model's pertinence. Wilson (1980)[44] translated the model's equations into the metric system, which made Behave applicable outside of United States. Since then, Rothermel (1983, 1991)[45] and Rothermel et al. (1991) wrote several technical papers indicating the path to be followed.

The model is based on the translation into energy terms of the propagation mechanism, which is considered as a series of fire initiation events. It relies on the application of the conservation of energy within a unit volume of fuel. It takes the equation proposed by Frandsen (1971)[46] in which the rate of fire propagation is defined as the ratio between the heat flux absorbed per unit volume of fuel and the heat needed to ignite this unit volume of fuel. The Behave system is structured into two sub-systems, the Fuel subsystem and the Burn subsystem, which are further subdivided into programs and modules. Burgan and Rothermel (1984)[47] described the Fuel sub-system as a tool for modelling forest fuels. This sub-system is composed of two programs: the Newmdl program

Boulder

[42] https://www.entsoe.eu/about-entso-e/Pages/default.aspx

[42] https://ses.jrc.ec.europa.eu/we-nutshell

[43] The EU-CIRCLE consortium (2017): D2.1 Report on Typology of Climate Related Hazards, http://www.eu-circle.eu/research/deliverables/;
The EU-CIRCLE consortium (2017): D2.2 Report on Climate Related Hazards Information Collection Mechanisms, http://www.eu-circle.eu/research/deliverables/

[44] Wilson, Ralph (1980): Reformulation of forest fire spread equations in SI units, USDA Forest Service, ttps://www.fs.fed.us/rm/pubs_int/int_rn292.pdf

[45] Rothermel, Richard C. (1980): How to Predict the Spread and Intensity of Forest and Range Fires. Gen. Tech. Rep. INT-143. Ogden, UT: U.S. Department of Agriculture, Forest Service, Intermountain Forest and Range Experiment Station; 1983. 1 61 p;
Rothermel, Richard C. 1991. Predicting behavior and size of crown fires in the Northern Rocky Mountains. Res. Pap. INT-438. Ogden, UT: U.S. Department of Agriculture, Forest Service, Intermountain Research Station. 46 p.

[46] William H. Frandsen (1971): Fire spread through porous fuels from the conservation of energy, Combustion and Flame, Volume 16, Issue 1, 1971, https://doi.org/10.1016/S0010-2180(71)80005-6.

[47] Burgan, Robert E.; Rothermel, Richard C. BEHAVE: fire behavior prediction and fuel modeling system--FUEL subsystem. General Technical Report I NT-167. Ogden, UT: U. S. Department of Agriculture, Forest Service, Intermountain Forest and Range Experiment Station; 1984. 126 p.

intended to develop fuel models and the Tstmdl program intended to test the reliability of fuel models developed by the former program and if need be, adjust the parameters. This subsystem allows the user to record fuel characteristics. A library of thirteen basic models covers all the North American forest communities. If the community is not correctly described by one of these, the user builds a new fuel model (Newmdl) that is then tested (Tstmdl) in order to check that the predictions are plausible. The Burn subsystem has been described in detail by Andrews (1986)[48] and by Andrews and Chase (1989)[49] and is composed of modules designed to predict fire behaviour in the fuel model(s) produced by the Fuel sub-system. Three modules use equations from Rothermel's model. The Direct module allows direct input of parameters into the model, whereas the Site module, which functions like the Direct module, determines the moisture content of particulate fuel, according to predictions. The Size module determines the area and perimeter length of the burnt area as a function of time, from a point fire source. The Burn subsystem also contains more specialised modules for determining the moisture content of particulate fuel from topographic and meteorological data for the area in the question (Moisture module), the maximum distance that flying sparks may travel (Spot module) and the probability that they will ignite a new fire (Ignition module), the height of crown scorching (Scorch module) and the probability of tree death (Mortality module). The Contain module evaluates the work needed to contain the fire. Finally, the Burn subsystem contains technical modules (RH, Map and Slope).

3.3.2 Fire Tactic

FireTactic® was developed by Intergraph Public Safety France in close cooperation with the French Fire Brigades in order to support the Civil Protection Services to optimise forest fire fighting operations. This is done through a simple and efficient forest fire propagation modelling tool that helps managers to make quick and documented decisions concerning the fire fighting plans. The I/MFFS module runs in a Personal Desktop Computer or portable that was tested by the French Civil Protection authorities (CIRCOSC, CODIS) but also in the firefront as well as for training purposes in the Fire Academy in South France. The user makes measurement of distances, areas, perimeters, water requirements etc. This product uses as background a standard map (1/25000 of scale for instance) or aerial photos and provides optimal information concerning the topographic and other forest fire related information for the user. FireTactic® has been tested under operational conditions by the French Fire Brigades since 1998.

3.3.3 Geographic Fire Management Information System (G-FMIS)

G-FMIS is a decision support system for the organization and refinement of forest fire management by exploiting the capabilities of the Geographic Information Systems (GIS) and the scientific knowledge on fire behavior. G-FMIS simulates fire behaviour using Rothermel's model and fire propagation using cellular automata techniques based on Dijskra algorithms. G-FMIS is a proprietary product, including a core software which has been developed in C++ and is availabe in

[48] Andrews, Patricia L. BEHAVE: fire behavior prediction and fuel modeling system-BURN Subsystem, part 1. General Technical Report INT-194. Ogden, UT: U.S. Department of Agriculture, Forest Service, Intermountain Research Station; 1986

[49] Andrews, Patricia L.; Chase, Carolyn H. 1989. BEHAVE: fire behavior prediction and fuel modeling system-BURN subsystem, Part 2. Gen. Tech. Rep. INT-260. Ogden, UT: U.S. Department of Agriculture, Forest Service, Intermountain Research Station.

both desktop and web version. The desktop version runs under ARCGIS-ArcMap[50] environment. The web version includes interfaces for the connection with other web plattforms and is also equipped with a user-friendly web-based interface which allows the users to set up the simulation parameters. G-FMIS-Web provide a number of services for wind-field calculation, fire behaviour and propagation simulation and transformation of output data for the presentation in web-mapping environments (e.g. Google Earth, Google Maps, etc.).

Models for the simulation and mapping of smoke from forest fires are described in chapter 3.5.

3.4 Flooding

In principle, flood modelling can be categroised as geographical analysis, hydrological, hydraulic, computational fluid dynamic, and data-driven approaches. Without considering actual flow dynamic, topography analyses can identify possible flow paths and depressions that flood will accumulate. Such functions are available in many GIS software modules, such as QGIS[51] and ArcMap[52]. The identified flow paths via terrain analyses often end up local depressions, where in reality the flow will continue moving toward downstream when the depressions are filled. Therefore, terrain filling or bouncing ball algorithm[53] are introduced to allow such analyses better delinearate flow paths and ponds. To simulate the rainfall-runoff process, hydrological models (e.g. HEC-HMS[54], GloFAS[55], LISFLOOD[56], Grid-to-Grid[57], and WMS[58]) that describe catchments as lumped parameters are widely used. However, hydrological models ignore the detailed variations (i.e. terrain changes) of environment that they are limited to provide accurate results when those details are dominating the flood propagations. Hence, more complicated hydraulic modelling are required to fulfil the purpose. For fluvial flooding that inundation concentrates to river channels and their adjacent floodplains, river models such as HEC-RAS[59]and MIKE 11[60], are useful tool for such conditions. For urban areas where drainage networks are widely built to reduce surface runoff, sewer network models (e.g. SWMM[61] and SIPSON[62]) are therefore developed to simulate the flow in drainage system. The sewer models can be extended to simulate flow movement

[50] An overview of the Hydrology toolset—Help | ArcGIS Desktop. http://desktop.arcgis.com/en/arcmap/10.5/tools/spatial-analyst-toolbox/an-overview-of-the-hydrology-tools.htm. Accessed 20 Jul 2018

[51] Raster Terrain Analysis Plugin. In: QGIS User Guide. https://docs.qgis.org/2.18/en/docs/user_manual/plugins/plugins_raster_terrain.html. Accessed 20 Jul 2018

[52] An overview of the Hydrology toolset—Help | ArcGIS Desktop. http://desktop.arcgis.com/en/arcmap/10.5/tools/spatial-analyst-toolbox/an-overview-of-the-hydrology-tools.htm. Accessed 20 Jul 2018

[53] Maksimović C, Prodanović D, Boonya-Aroonnet S, et al (2009) Overland flow and pathway analysis for modelling of urban pluvial flooding. J Hydraul Res 47:512–523 . doi: 10.3826/jhr.2009.3361

[54] Scharffenberg W (2016) HYdrologic Modeling System HEC-HMS User's Manual, Version 4.2

[55] Alfieri L, Burek P, Dutra E, et al (2013) GloFAS - global ensemble streamflow forecasting and flood early warning. Hydrol Earth Syst Sci 17:1161–1175 . doi: 10.5194/hess-17-1161-2013

[56] De Roo APJ (1999) LISFLOOD: a rainfall-runoff model for large river basins to assess the influence of land use changes on flood risk. Ribamod River Basin Model Manag Flood Mitig Concert Action Eur Comm EUR 18287:349–357

[57] Cole S, Robson A, Moore B (2010) The Grid-to-Grid Model for nationwide flood forecasting and its use of weather radar

[58] Aquaveo (2018) WMS 10.1 - The All-in-one Watershed Solution. https://www.aquaveo.com/software/wms-watershed-modeling-system-introduction. Accessed 20 Jul 2018

[59] Brunner GW (2016) HEC-RAS River Analysis System Users Manual Version 5.0. http://www.hec.usace.army.mil/software/hec-ras/documentation/HEC-RAS%205.0%20Users%20Manual.pdf. Accessed 20 Jul 2018

[60] DHI (2017) MIKE 11. A modelling system for rivers and channels, Reference Manual. DHI Water & Environment

[61] Rossman LA (2010) Storm Water Management Model User's Manual Version 5.0. National Risk Management Research Laboratory, Office of Research and Development, U.S. Environmental Protection Agency

[62] Djordjević S, Prodanović D, Maksimović Č, et al (2005) SIPSON–Simulation of Interaction between Pipe flow and Surface Overland flow in Networks. Water Sci Technol 52:275–283

confined by road kerbs as so called dual drainage approach[63,64]. Apart from the above-mentioned physical-based modelling approaches, data-driven models using data analytic algorithm such as artificial neuron networks[65] or support vector machine[66] are also receiving great intrests in flood modelling. This type of approach depends on a great amount of data for model training to determine the relationship between input and output varibles. Once the models are properly trained, they can provide efficient forecasting with a fraction of computing time that the physical-based modelling requires. Nevertheless, to simulate pluvial or coastal flooding that are beyond the conveyance capacity of drainage systems and road netowks, overland flow modelling are proven a better approach to simulate such scenarios. A wide varity of overland models have been developed to simulate flood scenarios for different applications, such as CADDIES[67], Citycat[68], FLO-2D[69] , HiPIMS[70], JFLOW[71], LISFLOOD-FP[72], PDWAVE[73] and UIM[74]. Some of the overland models are integrated with the sewer network models to better describe the flow interaction between surface and sewer networks [75,76,77,78]. Many commercial software (e.g. Flood Modeller, Infoworks ICM, MIKE Urban, XP Drainage) include multiple modules such that those models are capable of dealing the combinations of above modelling approaches.

Pender (2006)[79] classified various academic and commercial flood models into 0D, 1D, 1D+, 2D-, 2D, 2D+, and 3D approaches according to the dimensionality of modelling. The Environment Agency[80] further reviewed a number of 2D hydraulic models and tested their performance with eight benchmarking cases. Most of the models can be applied to simulate coastal, fluvial, and pluvial flooding, however, due to the assumption of methodologies, some are struggling to deliver accurate results for specific types of flooding that the models are not designed for.

---

[63] Djordjević S, Prodanović D, Maksimović C (1999) An approach to stimulation of dual drainage. Wat Sci Tech 39:95–103
[64] Leandro J, Djordjević S, Chen AS, Savić DA (2009) Flood inundation maps using an improved 1D/1D model. Tokyo, Japan
[65] Duncan AP, Chen AS, Keedwell EC, et al (2012) Urban flood prediction in real-time from weather radar and rainfall data using artificial neural networks. Weather Radar Hydrol - IAHS Red Proc 351:568–573
[66] Lin G-F, Chen G-R, Wu M-C, Chou Y-C (2009) Effective forecasting of hourly typhoon rainfall using support vector machines: EFFECTIVE FORECASTING OF HOURLY TYPHOON RAINFALL. Water Resour Res 45:n/a-n/a . doi: 10.1029/2009WR007911
[67] Guidolin M, Chen AS, Ghimire B, et al (2016) A weighted cellular automata 2D inundation model for rapid flood analysis. Environ Model Softw 84:378–394 . doi: 10.1016/j.envsoft.2016.07.008
[68] Glenis V, McGough AS, Kutija V, et al (2013) Flood modelling for cities using Cloud computing. J Cloud Comput Adv Syst Appl 2:1
[69] O'Brien JS, Julien PY, Fullerton WT (1993) Two-Dimensional Water Flood and Mudflow Simulation. J Hydraul Eng 119:244–261 . doi: 10.1061/(ASCE)0733-9429(1993)119:2(244)
[70] Smith LS, Liang Q (2013) Towards a generalised GPU/CPU shallow-flow modelling tool. Comput Fluids 88:334–343 . doi: 10.1016/j.compfluid.2013.09.018
[71] Lamb R, Crossley M, Waller S (2009) A fast two-dimensional floodplain inundation model. Proc Inst Civ Eng-Water Manag 162:363–370 . doi: 10.1680/wama.2009.162.6.363
[72] Bates PD, De Roo APJ (2000) A simple raster-based model for flood inundation simulation. J Hydrol 236:54–77 . doi: 10.1016/S0022-1694(00)00278-X
[73] Leandro J, Chen AS, Schumann A (2014) A 2D parallel diffusive wave model for floodplain inundation with variable time step (P-DWave). J Hydrol 517:250–259 . doi: 10.1016/j.jhydrol.2014.05.020
[74] Hsu MH, Chen SH, Chang TJ (2000) Inundation simulation for urban drainage basin with storm sewer system. J Hydrol 234:21–37 . doi: 10.1016/S0022-1694(00)00237-7
[75] Hsu MH, Chen SH (2002) Urban inundation model with dynamic interactions between overland and storm sewer flows. Chongli, Taiwan
[76] Chen AS, Djordjević S, Leandro J, Savic D (2007) The urban inundation model with bidirectional flow interaction between 2D overland surface and 1D sewer networks. Lyon, France, pp 465–472
[77] Chen A, Leandro J, Djordjevic S (2016) Modelling sewer discharge via displacement of manhole covers during flood events using 1D/2D SIPSON/P-DWave dual drainage simulations. Urban Water J 13:830–840 . doi: 10.1080/1573062X.2015.1041991
[78] Martins Ricardo Daniel Oliveira Mendes (2016) Development of a Fully Coupled 1D/2D Urban Flood Model. University of Coimbra
[79] Pender G (2006) Briefing: Introducing the flood risk management research consortium. Proc Inst Civ Eng Water Manag 159:3–8 . doi: 10.1680/wama.2006.159.1.3
[80] Néelz S, Pender G (2013) Benchmarking 2D hydraulic models Summary. Environment Agency

3.5 Chemical sector

3.5.1 Fire Emission Production Simulator (FEPS)

The FEPS[81] is a user-friendly computer program designed for scientists and resource managers with some working knowledge of Microsoft Windows® applications. The software manages data concerning consumption, emissions and heat release characteristics of prescribed burns and wildland fires. Total burn consumption values are distributed over the life of the burn to generate hourly emission and release information. Data managed includes the amount and fuel moisture of various fuel strata, hourly weather, and a number of other factors. FEPS can be used for most forest, shrub and grassland types in North America and the world. The program allows users to produce reasonable results with very little information by providing default values and calculations; advanced users can customise the data they provide to produce very refined results. FEPS incorporates a flexible user interface that allows the user to customise a burning event. The user may adjust fuel loadings, fuel moistures, fuel consumption algorithms, fuelbed proportions and fire growth rates to fit specific events or situation, and can specify diurnal changes in meteorological conditions that will modify plume rise. Furthermore, many intermediate results are exposed to the user. The user may accept these results, or insert values of their own. FEPS produces hourly emission and heat release data for prescribed and wildland fires.

3.5.2 Hybrid Single Particle Lagrangian Integrated Trajectory Model (HYSPLIT)

The HYSPLIT is a computer model that is used to compute air parcel trajectories and dispersion or deposition of atmospheric pollutants. The main features of HYSPLIT are:

- **Trajectories**
  - Single or multiple (space or time) simultaneous trajectories
  - Optional grid of initial starting locations
  - Computations forward or backward in time
  - Default vertical motion using omega field
  - Other motion options: isentropic, isosigma, isobaric, isopycnic
  - Trajectory ensemble option using meteorological variations
  - Output of meteorological variables along a trajectory
  - Integrated trajectory clustering option
- **Air Concentrations**
  - 3D particle dispersion or splitting puffs (top-hat or Gaussian)
  - Instantaneous or continuous emissions, point or area sources
  - Multiple resolution concentration output grids
  - Fixed concentration grid or dynamic sampling

[81] https://www.fs.fed.us/pnw/fera/feps/FEPS_users_guide.pdf

- Wet and dry deposition, radioactive decay, and resuspension
- Emission of multiple simultaneous pollutant species
- Automated source-receptor matrix computation
- Ensemble dispersion based on variations in meteorology, turbulence, or physics
- Concentration probability output for multiple simulations
- Integrated dust-storm emission algrorithm
- Define rate constants to convert one species to another
- Mass can be transferred to a Eulerian module for global-scale simulations

Further detailed descriptions of the HYSPLIT model can be found in Draxler and Hess (1997, 1998)[82]. Smoke estimations are produced by HYSPLIT where advection and diffusion calculations are made in a Lagrangian framework following the transport, while concentrations are calculated on a fixed grid. The transport and dispersion of smoke can be calculated by assuming the release of puffs with either a pre-defined Gaussian or top-hat (zero outside, one inside) horizontal distribution that increases with time, or from the turbulent dispersal of an initial fixed number of particles, or by combining both puff and particle methods by assuming a puff distribution in the horizontal and particle dispersion in the vertical direction. In this way, the greater accuracy of the vertical dispersion parameterization of the particle model is combined with the advantage of having fewer pollutant puffs to represent the horizontal distribution.

3.5.3 Cameo

"The CAMEO software is a system of software applications used widely to plan for and respond to chemical emergencies. It is one of the tools developed by the United States Environment Agency (EPA) and the National Oceanic and Atmospheric Administration (NOAA) to assist front-line chemical emergency planners and responders."[83] The CAMEO system integrates a database application that includes four core modules to assist with data management requirements under the Emergency Planning and Community Right-to-Know Act (CAMEOfm), an extensive chemical database with critical response information for thousands of chemicals (CAMEO Chemicals), a mapping capability (MARPLOT) and an atmospheric dispersion model (ALOHA). All modules work interactively to share and display critical information in a timely fashion.

3.5.4 ALOHA

ALOHA is an atmospheric dispersion model used for evaluating releases of hazardous chemical vapors, smoke fire etc. ALOHA allows the user to estimate the downwind dispersion of a cloud based on the physical characteristics of the puff, atmospheric conditions, and specific circumstances of the release. In case of fire, ALOHA cannot model all the complex processes that happen (like the generation and distribution of byproducts), but it can predict the area where the

82 Draxler, R.R. and G.D. Hess (1998), An overview of the HYSPLIT_4 modelling system for trajectories, dispersion, and deposition. Aust. Meteor. Mag. 47, 295-308.
Draxler, R.R. and G.D. Hess (1997), Description of the HYSPLIT_4 modeling system. NOAA Technical Memo ERL ARL-224, December, 24 p.
[83] https://www.epa.gov/cameo/what-cameo-software-suite

heat radiated by the fire called thermal radiation and could be harmful, or it can predict the area covered by smoke and ash. Threat zones can be displayed on MARPLOT maps to help users assess geospatial information, such as whether vulnerable locations (such as hospitals and schools) might be impacted by the release or whether other nearby factors (such as construction zones) might complicate the response. The key program features are:

- *Generation* of a variety of scenario-specific output, including threat zone pictures, threats at specific locations and source strength graphs.
- *Calculation* on how quickly chemicals are escaping from tanks, puddles, and gas pipelines and prediction on how those release rates change over time.
- *Modelling* many release scenarios: toxic gas clouds, BLEVEs (Boiling Liquid Expanding Vapor Explosions), jet fires, vapor cloud explosions, and pool fires.
- *Evaluation* of different types of hazard (depending on the release scenario): toxicity, flammability, thermal radiation, and overpressure.
- *Modelling* the atmospheric dispersion of chemical spills on water.

3.5.5 FLEXPART

FLEXPART[84] "is a Lagrangian transport and dispersion model suitable for the simulation of a large range of atmospheric transport processes. Applications range from the dispersion of radionuclides or air pollutants, over the establishment of flow climatologies, to the analysis of Earth's water cycle. FLEXPART also produces output suitable for inverse determination of emission sources, e.g., of greenhouse gases, smoke dispersion or volcanic ash."[85]

[84] Stohl, A., M. Hittenberger, and G. Wotawa (1998): Validation of the Lagrangian particle dispersion model FLEXPART against large scale tracer experiments. Atmos. Environ. 32, 4245-4264.
Stohl, A., and D. J. Thomson (1999): A density correction for Lagrangian particle dispersion models. Bound.-Layer Met. 90, 155-167.
Stohl, A., C. Forster, A. Frank, P. Seibert, and G. Wotawa (2005): Technical Note : The Lagrangian particle dispersion model FLEXPART version 6.2. Atmos. Chem. Phys. 5, 2461-2474.

[85] https://www.flexpart.eu/

4 CI design thresholds and requirements

4.1 Infrastructure Standards – The Structural Eurocodes

At European level, Eurocodes have been proposed addressing climate resilience in different infrastructure sectors. The Structural Eurocodes are a harmonised set of structural design standards of buildings and civil engineering works constructed in the European Union (EU), developed by European Committee for Standardisation over the last 30 years in order to cover the design of all types of structures in steel, concrete, timber, masonry and aluminium. There are ten Eurocodes, each published in a number of separate Parts; 58 Parts in total. Some Parts give general rules and other give rules applicable to one form of construction. When the 58 Eurocodes parts were published in 2007, the implementation of the Eurocodes was extended to all European countries and there were firm steps towards their international adoption. Eurocodes embody national experience and research output together with the expertise of international technical and scientific organisations. From March 2010, the Eurocodes were intended to be the only standards for the design of structures in the countries of the EU and the European Free Trade Association. Although the Eurocodes are harmonised documents that are applicable throughout Europe, certain provisions such as the setting of partial factors for safety are chosen by the national standards bodies. The Eurocodes are thus accompanied by national annexes that set out those national choices. The ten Eurocodes are[86]:

- EN 1990 Eurocode: Basis of Structural Design
- EN 1991 Eurocode 1: Actions on structures
- EN 1992 Eurocode 2: Design of concrete structures
- EN 1993 Eurocode 3: Design of steel structures
- EN 1994 Eurocode 4: Design of composite steel and concrete structures
- EN 1995 Eurocode 5: Design of timber structures
- EN 1996 Eurocode 6: Design of masonry structures
- EN 1997 Eurocode 7: Geotechnical design
- EN 1998 Eurocode 8: Design of structures for earthquake resistance
- EN 1999 Eurocode 9: Design of aluminium structures

4.2 Forest fires

4.2.1 Thresholds for forest fires

Climate change affects multiple factors that increase wildfire risk. Wildfires can shut down the lines and produce power outages whilst electricity transmission and distribution network are highly vulnerable to this event. Hence wildfires have important consequences for the power sector. They can directly damage transmission poles and other electricity infrastructure. Fires in

[86] http://eurocodes.jrc.ec.europa.eu/showpage.php?id=13

and around distribution lines can burn down the lines and damage distribution poles. According to Davis and Clammer (2014)[87], the strength of steel is reduced to 0.5 at a temperature range from 500 – 600 °C and this is the point where steel transmission towers are not able to bear the design load. At 420°C the galvanising increases with consequences for the corrosion prevention after the fire[88]. This temperature is supposed to be reached after 10 minutes of fire exposure. However, the greatest risk comes from smoke and particulate matter. Smoke and ash from fires can ionise the air, creating an electrical path away from transmission lines[89]. Higher air temperatures have led to drier forests and earlier snowmelts, both of which contribute to wildfire risk[90]. Droughts and higher air temperatures also help make wildfires more intense and longer-lasting. Moreover, when aircrafts drop near an electric line, this action can lead to the fouling of power lines or can drop them on the floor. Then the heavy actions as repairing the lines or cleaning them have to start immediately to avoid functional problems.

Table 15: Forest fires - critical structural and operational thresholds of the energy sector

Asset	Design threshold	Impacts on asset
Distribution lines EHV transmission lines Step up_down substations	Structural & operational threshold: Temperature > 500 – 600 °C Temperature > 420 °C	According to Davis and Clammer (2014) [91], the strength of steel is reduced to 0.5 at a temperature range from 500 – 600 °C. At 420°C the galvanising increases with consequences for the corrosion prevention after the fire after 10 minutes of fire exposure[92].
Distribution substations Transformer	Operational threshold: PM2.5 concentration >350 µg/m3	Smoke (fine particulate matter) can ionise the air and shut down the lines producing power outages[93].

[87] M. Davis and S. Clemmer, "How Climate Change Puts Our Electricity at Risk," Power Failure, 2014
[88] Jeannette Sieber née Schulz, "Adaptation Options and Decision-Support for Electricity Infrastructure Operators under Influence of Extreme Hydro-Meteorological Events," Journal of Integrated Disaster Risk Management, Special IDRiM2010 Conference Paper, ISSN: 2185-8322, 2011a
[89] T. J. Feeley et al., "Water: A critical resource in the thermoelectric power industry," Energy, vol. 33, no. 1, pp. 1–11, Jan. 2008
[90] D. M. Ward, "The effect of weather on grid systems and the reliability of electricity supply," Clim. Change, vol. 121, no. 1, pp. 103–113, Nov. 2013.
[91] M. Davis and S. Clemmer, "How Climate Change Puts Our Electricity at Risk," Power Failure, 2014
[92] Jeannette Sieber née Schulz, "Adaptation Options and Decision-Support for Electricity Infrastructure Operators under Influence of Extreme Hydro-Meteorological Events," Journal of Integrated Disaster Risk Management, Special IDRiM2010 Conference Paper, ISSN: 2185-8322, 2011a;
European Commission, "Investment needs for future adaptation measures in EU nuclear power plants and other electricity generation technologies due to effects of climate change. Final report.", 2011
[93] T. J. Feeley et al., "Water: A critical resource in the thermoelectric power industry," Energy, vol. 33, no. 1, pp. 1–11, Jan. 2008;
T. Brandt, A. Varma, R. Brent, S. Marcu, R. Connor, and K. Harries, "Effects of Fire Damage on the Structural Properties of Steel Bridge Elements. Final Report," 2011.

Wooden pylon	Flame temperature (> 650°C)	Wooden pylon are submitted to fire front leading to their destruction

Table 16: Design thresholds for forest fires and smoke

CI sector	Asset	Design threshold	Impacts
Energy Electricity	Distribution lines EHV transmission lines Step up_down substations	Structural threshold: Temperature > 500 – 600 °C Operational threshold: Temperature > 420 °C	According to Davis and Clammer (2014) [94], the strength of steel is reduced to 0.5 at a temperature range from 500 – 600 °C. At 420°C the galvanising increases with consequences for the corrosion prevention after the fire after 10 minutes of fire exposure[95].
	Distribution substations Transformer	Operational threshold: PM2.5 concentration 350 µg/m3	Smoke (fine particulate matter) can ionise the air and shut down the lines producing power outages[96].
	Wooden pylon	Flame temperature > 650°C)	Wooden pylons are submitted to fire front leading to their destruction
Transportation	Roads Highway	PM_{moyen}>30 mg/m^3 10 <PM_{moyen}>30 mg/m^3 PM_{moyen}<10 mg/m^3	• No visibility • Medium visibility • Good visibility

4.2.2 PM2.5 thresholds for smoke

These three particle types are the most toxic due to their deep penetration capacity and ability to adsorb other contaminants and free them into the blood system. Fine particles cause an inflammatory response in the lungs which can aggravate existing chronic breathing illnesses such as bronchitis. They also increase lung cancer occurrences. Short term effects caused by fine particles are well known and cause increased hospitalizations due to breathing diseases and asthma. A higher mortality rate is observed in cases of cardio respiratory diseases. Long term

[94] M. Davis and S. Clemmer, "How Climate Change Puts Our Electricity at Risk," Power Failure, 2014
[95] Jeannette Sieber née Schulz, "Adaptation Options and Decision-Support for Electricity Infrastructure Operators under Influence of Extreme Hydro-Meteorological Events," Journal of Integrated Disaster Risk Management, Special IDRiM2010 Conference Paper, ISSN: 2185-8322, 2011a;
European Commission, "Investment needs for future adaptation measures in EU nuclear power plants and other electricity generation technologies due to effects of climate change. Final report.", 2011
[96] T. J. Feeley et al., "Water: A critical resource in the thermoelectric power industry," Energy, vol. 33, no. 1, pp. 1–11, Jan. 2008; T. Brandt, A. Varma, R. Brent, S. Marcu, R. Connor, and K. Harries, "Effects of Fire Damage on the Structural Properties of Steel Bridge Elements. Final Report," 2011

exposure to these particles also causes a shorter life expectancy. Particles are contaminating the electric line when a forest fire propagates towards them. When they are deposited on the electrical conductors, this phenomenon reduces the capacity of the insolator and causes a short circuit leading to a thermal heating of the lines. Thus, an automatic control of electric lines has to be done after each forest fire event by helicopter, which is a very expensive action.

An experimental approach led by CEREN in 2015 on prescribed burnings estimated firefighter exposure levels to smoke for forest fire team members, by measuring fine particle concentrations in their immediate environment. Three exposure levels were defined (high, moderate and low). Strong exposures imply fine particle concentration peaks higher or equal to 100mg/m^3 along with an average concentration above 30 mg/m^3. In this situation, breathing difficulties are important. Furthermore, when concentrations reach 200 mg/m^3, visibility becomes very limited and interveners evolve in an almost opaque environment.

Figure 3: Strong, moderate and low exposure during prescribed burnings (CEREN experiments 2015)

Moderate exposure faces particle concentration peaks ranging from 25 to 100 mg/m^3 and an average concentration between 10 and 30 mg/m^3. Smoke is less dense but breathing discomfort and irritations are present. A low exposure has concentration peaks lower than 25 mg/m^3 and an average concentration lower than 10 mg/m^3. Smoke odor is noticeable but not unaccommodating and visibility is good. The thresholds obtained (see Table 17) during those experimentations have been applied for determining visibility classes on transport network.

Table 17: Results of CEREN study concerning visibility

No visibility	Medium visibility	Good visibility
$[PM_{moyen}] > 30$ mg/m³	10 mg/m³ $< [PM_{moyen}] <$ 30 mg/m³	$[PM_{moyen}] < 10$ mg/m³
Road should be closed	Road should be closed	No closure of road

4.3 Flood

Table 18 presents an overview of design values for various CI assets according to Eurocodes. Each type of CI has been designed to withstand inundation levels specific for each installation site.

Table 18: Flooding – critical structural and operational thresholds

Asset	Design thresholds	Impacts
Electricity[97]		
Power plant	Structural threshold: 1.2 m inundation	electrical switch gear located 1 m above ground
Control room	Structural threshold: 2.0 m inundation 0.3 m inundation	Maximum damage at 2.0 m inundation, 40 % damage at 0.3 m inundation
Distribution substation	Structural threshold: 3.0 m inundation 1.0 m inundation	Basement level: 15 % damage at 3.0 m inundation Mounted on wood/concrete pylons with overhead lines: damage to foundations of the towers resulting in their collapse
Step up/down subsations	Structural threshold: 3.0 m inundation	15 % damage at 3.0 m inundation
Transformer	Structural and operational threshold: 2.0 m inundation	Basement level: total damage at 2.0 m inundation
District Heating Substation (DHS)	Floods might affect the operation of DHS substations in the same manner as "Conveyance or Treatment" critical services of **Water Infrastructure.**	Link to Conveyance or Treatment assets.
District Heating Underground Thermal Water Pipes	Floods might affect the structural behavior of DHS Underground thermal water pipelines in a like manner as water pipelines might be affected in water sector, as possible landslides might occur.	Link to water sectors' Distribution assets.
Water		
Boreholes / source and intake pumping stations	0.3 m above the entrance	Flood water infiltration: risk for drinking water quality

[97] Chakraborti SK, "American electric power's coal pile management program," in Bulk Solids Handling, vol. 15, 1995, pp. 421–428

		Storm water volumes: increased asset usage/deterioration due to greater storm water volumes Intense rainfall: increased surface runoff, reduction of aquifer recharge, reduction of supply security
Storage reservoirs and aqueducts	Assets above ground: 1.5 m above the entrance	Intense rainfall: changed soil conditions, slippage of soil dams, capacity exceedance (service failure, flooding, asset loss) Soil erosion: siltation of dams (asset deterioration and loss)
Treatment works	0.3 m above the entrance	Increased runoff: greater sediment levels, uncreased risk to drinking water quality Intense rainfalls: risk to drinking water quality from biological consequences of discolouration and odour problems
Service reservoirs, distribution storage	Assets above ground: 1.5 m above the entrance	Risk to drinking water quality due to contamination of underground storage tanks
SCADA & telemetry	0.3 m above the entrance	Failure of electrical equipment
Dams, reservoirs[98]	0.6 m freeboard to top of dam (rural and urban) Water surface at or below emergency spillway Dam/reservoir must drain in	Loss of structural integrity, overtopping, breach

[98] New Mexico Department of Transportation 2007: Drainage Design Criteria – Revision of 06/07

	< 96 h	
Transport		
Roads	floods with Annual Exceedance Probability of 2% (≈ Average Recurrence Interval (ARI) of 50 years)[99]	Insufficient drainage, slippery surfaces, aquaplaning, damage to superstructure
Bridges[100]	minimum hydraulic force on bridge pier = 75 kN/pier minimum stream velocity = 2.0 m/s. *force on superstructure*: depth of debris mat: the greater of 3.0 m or structural depth of superstructure in elevation + 1.5 m *force on substructure*: minimum depth of debris mat = 3.0 m resilient to 0.6 m inundation[101]	Loss of stability of bridge piers, bridge collapse
Tunnels[102]	probable maximum precipitation event + 300 mm 100 year ARI flood 100 year ARI storm tide	Insufficient drainage, aquaplaning, structural damage

The main risk that flooding poses to the energy sector concerns power stations, electricity transmission and major distribution substations, as overhead lines, underground cables[103]. Major fluvial and pluvial flooding events have occurred in the UK in recent years, with electricity supplies being affected. According to Tebaldi et al. (2012)[104], the drainage system of a coal stockpile is designed for a 1-in-10-year, 24-hour rainfall event. If this threshold is exceeded, the stockpile drenches. Moreover, wet coal has a reduced heating value, as moisture contained in the coal is converted to steam using additional energy for this process[105]. On the other hand coastal flooding

---

[99] State of Queensland (Department of Transport and Main Roads) 2015: Road Drainage Manual
[100] State of Queensland (Department of Transport and Main Roads) 2018: Design Criteria for Bridges and Other Structures, http://creativecommons.org/licenses/by/3.0/au/
[101] New Mexico Department of Transportation 2007: Drainage Design Criteria – Revision of 06/07
[102] State of Queensland (Department of Transport and Main Roads) 2018: Design Criteria for Bridges and Other Structures, http://creativecommons.org/licenses/by/3.0/au/
[103] S. Smith, "The Performance of Distribution Utility Poles in Wildland Fire Hazard Areas. What We Know and Don't Know." 2014
[104] C. Tebaldi, D. Adams-Smith, and N. Heller, "The heat is on: U.S. temperature trends," Climate Central. Online at www.climatecentral.org/news/the-heat-is-on/., Princeton, NJ, 2012.

[105] Sunrise Powerlink Project, "Attachment 1A: Effect of Wildfires on Transmission Line Reliability Collocation of Transmission Alternatives with the Southwest Powerlink," Jan. 2008;

J. Sathaye et al., "Estimating risk to California energy infrastructure from projected climate change," CEC-500-2012-057, Sacramento, CA, California Energy Commission., 2012.

impacts possess a high risk to energy infrastructure located in coastal areas[106]. According to Hazus approach[107], control room damages start to occur at 0 m, and maximised instantly at the flooding depth of two meters. Also additional damage to cabling and incidental damage to transformers and switchgear might arise.

On the other hand, Chakraborti (1995)[108] refers to 40% damage after 0.3m regarding natural gas classifications, functionality thresholds and damage functions. Additionally high/medium voltage substations are more vulnerable to floods because they are mostly installed outdoors. In such a case the substation goes out of order[109]. Such situation is less severe due to fewer customers affected, but more probable is the flooding of MV/LV underground or ground floor substations that can be found especially in urban areas[110]. Percent damage by depth of flooding up to 15%, assuming electrical switch gear is located 1m above grade according to Hazus approach. An indirect impact of extreme precipitation could be the high humidity of the substations resulting in water leaks into the substation and water in cable trenches[111].

4.4 Snow

4.4.1 Electricity sector infrastructure

Critical design thresholds for the snow load are applied for group regions in Europe with similar latitudes and dependent on their altitude. For this purpose measured data of hundreds of meteorological stations in Europe were analysed and the characteristic values of the ground snow load were determined by means of extreme value statistics.

Increased frequency and intensity of extreme precipitation might increase the functional or structural damages to infrastructure distribution and transmission networks. Events of snow and extreme precipitation may also affect renewables. Hence changing annual or seasonal patterns can affect river flows and water levels behind dams, either reducing or increasing power output[112]. In that event hydropower may be affected which makes up to 20 % of the total installed capacity for electricity generation in Europe[113]. Therefore, snow, hailstone and extreme precipitation are considered as major threats to electricity infrastructure. In that event, Jurgemeyer and Miller (2012)[114] describe hail as a special threat to overhead lines, while on the other hand there are

[106] L. McColl, T. Angelini, and R. Betts, "Climate Change Risk Assessment for the Energy Sector," Defra Project Code GA0204, Cimate change risk assessment UK, 2012

[107] Chakraborti SK, "American electric power's coal pile management program," in Bulk Solids Handling, vol. 15, 1995, pp. 421–428.

[108] Chakraborti SK, "American electric power's coal pile management program," in Bulk Solids Handling, vol. 15, 1995, pp. 421–428.

[109] Hatt R, "Handling coal: Sticky when wet. PowerOnline. http://www.poweronline.com/doc/Handling- Coal-sticky-when-wet-0001. Accessed 19 April 2013," 2001.

[110] Hatt R, "Handling coal: Sticky when wet. PowerOnline. http://www.poweronline.com/doc/Handling- Coal-sticky-when-wet-0001. Accessed 19 April 2013," 2001.

[111] Hatt R, "Coal quality and combustion workshop. Coal Combustion, Inc. http://www.coalcombustion.com/PDF%20Files/webcqcclassoutline.pdf." 2004

[112] European Commission, "Energy in Europe 1999 - Annual Energy Review," Jan. 2000

[113] W. Yu, T. Jamasb, and M. Pollitt, "Does weather explain cost and quality performance? An analysis of UK electricity distribution companies," Energy Policy, vol. 37, no. 11, pp. 4177–4188, Nov. 2009.

[114] M. Jurgemeyer and B. Miller, "NESC Wind and Ice load effects on wood distribution pole design," in Rural Electric Power Conference (REPC), 2012 IEEE, 2012, pp. B1–1.

three loading conditions concerning snow loads, defined as light, medium, and heavy loading, according to ANSI/IEEE (2007)[115] and Ducloux and Nygaard (2014)[116], for structures below 18 m in height.

Since 1971, French accretion design rules have been described according to a thickness of accretion (snow, rime or glaze), i.e. 2, 4 or 6 cm, associated with a unique density of 600 kg/m^3, which are the equivalent of 2, 5 and 10 kg/m, respectively, onto the ISO reference collector. It is important to underline the fact that all the lines designed according to 5 kg/m (4 cm of an accreted snow of density 600 kg/m^3) have never been damaged by any wet snow events in specific plains in France since their construction[117]. According to Chakraborti (1995)[118] and Abi-Samra et al. (2010)[119], foundations of towers might be damaged resulting in their collapse.

With respect now to the underground lines, the threshold for cable breakage varies with local conditions. Analysis of the data in DOE (2015)[120] showed that in almost all cases, the thermal resistance was reduced to less than 0.5 °C-m/W when the accumulated rain over consecutive days exceeded 15 mm. Conversely the data showed increase in the thermal resistivity during dry periods (periods where the rainfall during the week was less than 2.5 mm). Structural thresholds are considered due to a landslide event as a secondary impact of flooding. On the contrary underground wires may also be vulnerable to damage due to saltwater intrusion associated with sea level rise[121]. Moreover, taking into consideration the District Heating assets there is a risk that water will freeze within these pipelines[122], in case of long enough extreme cold temperature and heat supply are not restored.

Table 19: Snow/extreme precipitation critical functional and structural thresholds of the electricity sector

Asset	Design threshold	Impacts on asset
Distribution lines Distribution	Structural thresholds: • Hailstones Threshold: 15 mm diameter • Intense rainfall: 50 mm/d (EU-CIRCLE approach) or 5 days of cumulative rainfall >	Jurgemeyer and Miller (2012)[124] describe hail as a special threat to overhead lines. Intense rainfall is also a special threat[125].

[115] ANSI/IEEE, “National Electrical Safety Code.” 2007
[116] H. Ducloux and B. E. Nygaard, “50-year return-period wet-snow load estimation based on weather station data for overhead line design in France,” Nat. Hazards Earth Syst. Sci., vol. 14, no. 11, pp. 3031–3041, Nov. 2014.
[117] Roger A and Pielke Sr, Climate Vulnerability, Understanding and Addressing Threats to Essential Resources, vol. 1. 2013
[118] Chakraborti SK, “American electric power’s coal pile management program,” in Bulk Solids Handling, vol. 15, 1995, pp. 421–428.
[119] N. Abi-Samra, K. Forsten and R. Entriken, “Sample Effects of Extreme Weather on Power Systems and Components, Part I: Sample Effects on Distribution Systems,” 2010.
[120] DOE, “Climate Change and the Electricity Sector: Guide for Assessing Vulnerabilities and Developing Resilience Solutions to Sea Level Rise,” Jul. 2015
[121] M. Feofilovs and F. Romagnoli, “Resilience of critical infrastructures: probabilistic case study of a district heating pipeline network in municipality of Latvia,” Energy Procedia, vol. 128, pp. 17–23, Sep. 2017
[122] AECOM, “Torondo Hydro-Electric System Public Infrastructure Engineering Vulnerability Assessment Pilot Case study,” 60263582, Sep. 2012

substations	70 mm of rain. 1. Heavy Combined Threshold = 1.27 cm and 0.191 kN/m^2 & T = - 20 °C 2. Medium Combined Threshold = 0.63 cm and 0.191 kN/m^2 & T = - 10 °C 3. Light Combined Threshold= 0.43 kN/m^2 and T = - 1 °C • Snowfall > 10 cm (2 - 3 days/year) Snow on ground with depths > 30 cm for 5 days or more[123]	Three are the snow loading conditions according to ANSI/IEEE (2007)[126] and Ducloux and Nygaard (2014)[127], for structures below 18 m in height. All the lines designed according to 5 kg m−1 (4 cm of an accreted snow of density 600 kg m−3) have never been damaged by any wet snow[128].
EHV transmission lines	Structural thresholds: • Hailstones Threshold= 15 mm • Intense rainfall= 150 mm/3h • Prolonged rainfall =350 mm/10h • 1 kg per 1 m of a line (Central EU) • 5 kg/m (4 cm of an accreted snow of density 600 kg/m³) • Snowfall > 10 cm (2 - 3 days/year)[129]	Floods by intense (3 h) or prolonged (10 h) accumulated rainfall described detailed by Hashmi et al., (2013)[130]. High voltage lines are designed in such a way to hold loads over 1 kg per 1 m of a line[131].

[124] M. Jurgemeyer and B. Miller, “NESC Wind and Ice load effects on wood distribution pole design,” in Rural Electric Power Conference (REPC), 2012 IEEE, 2012, pp. B1–1.
[125] Chakraborti SK, “American electric power’s coal pile management program,” in Bulk Solids Handling, vol. 15, 1995, pp. 421–428;
N. . Abi-Samra, K. . Forsten, and R. Entriken, “Sample Effects of Extreme Weather on Power Systems and Components, Part I: Sample Effects on Distribution Systems,” 2010

[123] E. Simonson, “Transformer ratings and transformer life,” 1998, vol. 1998, pp. 7–7.

[126] ANSI/IEEE, “National Electrical Safety Code.” 2007.

[127] H. Ducloux and B. E. Nygaard, “50-year return-period wet-snow load estimation based on weather station data for overhead line design in France,” Nat. Hazards Earth Syst. Sci., vol. 14, no. 11, pp. 3031–3041, Nov. 2014.
[128] Roger A and Pielke Sr, Climate Vulnerability, Understanding and Addressing Threats to Essential Resources, 2013.
[129] E. Simonson, “Transformer ratings and transformer life,” 1998, vol. 1998, pp. 7–7.
[130] M. Hashmi, M. Lehtonen, and S. Hänninen, “Effect of Climate Change on Transformers Loading Conditions in the Future Smart Grid Environment,” Open J. Appl. Sci., vol. 03, no. 02, pp. 24–29, 2013.

[131] J. F. C. Flores, B. Lacarrière, J. N. W. Chiu, and V. Martin, “Assessing the techno-economic impact of low-temperature subnets in conventional district heating networks,” Energy Procedia, vol. 116, pp. 260–272, Jun. 2017.; EUROHEAT & POWER, “Guidelines for District Heating Substations,” Oct. 2008.

	Snow on ground with depths>30cm for 5 days or more	
Distribution underground lines	Both functional and operational thresholds: • Thermal resistance < 0.5 [(K*m)/W] when 15mm of accumulated rainfall. Accumulated rainfall < 2.5 mm (during the week)	DOE (2015)[132] showed that in almost all cases, the thermal resistance was reduced to less than 0.5 °[(K*m)/W] when the accumulated rain over consecutive days exceeded 15 mm. increased thermal resistivity during dry periods (periods where the rainfall during the week was less than 2.5 mm)).

4.4.2 Buildings, Civil engineering structures and Bridges

The EN 1991-1-3[133] gives guidance to determine the values of loads due to snow for the structural design of buildings and civil engineering works for sites at altitudes above 1500 m. For bridges, which are specific engineering works, along with Eurocodes, the German DIN standards were applied. The design thresholds for snow on bridges is defined in DIN 1055[134], discriminating two cases: when a bridge is open or when it is under construction. Once the design load is exceeded, damage will start to be developed on structure depending on the local situations (material, structural system, magnitude of snow load, environment). The severity of damage will belong either in Serviceability Limit State with minor damages or in Ultimate Limit State with major and most severe damages. Structural failure from snow load is influenced by the characteristics of the building[135]. The snow loads affect mainly the roof of structures. The variables in roof snow load are roof geometry and roofing material, exposure to wind, and insulation.

The Eurocode prEN 1991-1-3 maps give the characteristic values of the snow loads on sea level for the relevant European countries. Several snow loadmaps are available for different climatic regions. The snow load on the roof is derived from the snow load on the ground, multiplying by appropriate conversion factors (shape, thermal and exposure coefficients). Properties of a roof or other factors causing different patterns can include: a) the shape of the roof; b) its thermal properties; c) the roughness of its surface; d) the amount of heat generated under the roof; e) the proximity of nearby buildings; f) the surrounding terrain; g) the local meteorological climate, in particular its windiness, temperature variations, and likelihood of precipitation (either as rain or as snow). The maps for the several climatic regions are subdivided into snow load zones *Z*. In addition to the values of the altitude the numbers *Z* of these zones are the basic input parameters for the determination of the characteristic value of the ground snow load s_k. The characteristic value of

[132] DOE, "Climate Change and the Electricity Sector: Guide for Assessing Vulnerabilities and Developing Resilience Solutions to Sea Level Rise," Jul. 2015.

[133] EN 1991-1-3. Eurocode 1 - Actions on structures - Part 1-3: General actions - Snow loads

[134] https://www.din.de/en

[135] https://www.fema.gov/media-library-data/7d8c55d1c4f815edf3d7e7d1c120383f/FEMA957_Snowload_508.pdf

snow load on the ground s_k [kN/m^2] (annual probability of exceedence of 0.02 with return period of 50 years, excluding exceptional snow loads) is given in EN 1991-1-3 discrimanting Europe in specific regions.

The snow load on the roof ***s*** [kN/m^2] is evaluated based on the equation:

a) for the persistent/ transient design situations

$s = \mu_i C_e C_t\ s_k$

μ_i is the snow load shape (roof shape) coefficient

s_k is the characteristic value of snow load on the ground for the relevant altitude

s_{Ad} is the design value of exceptional snow load on the ground for a given location

C_e is the exposure coefficient

C_t is the thermal coefficient

b) for the accidental design situations where exceptional snow load is the accidental action

$s = \mu_i C_e C_t\ s_{Ad}$

c) for the accidental design situations where exceptional snow drift is the accidental action and where Annex B applies

$s = \mu_i\ s_k$

Table 20: Critical climatic parameters and thresholds of snow in Eurocode EN 1991-1-3

Design threshold			**Impact on asset**
Weight (kg)			
Alpine region	Zone 1, Altitude A = 0 m	71,38kg/m^2	Structural failure from snow load is influenced by the characteristics of the building[136]
	Zone 2, Altitude A = 0 m	132,56 kg/m^2	
	Zone 3, Altitude A = 0 m	193,74 kg/m^2	
	Zone 4, Altitude A = 0 m	295,72 kg/m^2	
Central East	Zone 1, Altitude A = 0 m	30,59kg/m^2	
	Zone 2, Altitude A = 0 m	50,99kg/m^2	
	Zone 3, Altitude A = 0 m	81,58 kg/m^2	
	Zone 4/5, Altitude A = 0 m	122,37 kg/m^2	

[136] Risk Management Series Snow Load Safety Guide FEMA P-957 / January 2013

Greece	Zone 1, Altitude A = 0 m	40,79kg/m^2	
	Zone 2, Altitude A = 0 m	81,58kg/m^2	
	Zone 4, Altitude A = 0 m	173,35 kg/m^2	
Iberian Peninsula	Zone 1, Altitude A = 0 m	10,20kg/m^2	
	Zone 2, Altitude A = 0 m	30,59kg/m^2	
	Zone 4, Altitude A = 0 m	71,38 kg/m^2	
Mediterranian region	Zone 1, Altitude A = 0 m	30,59kg/m^2	
	Zone 2, Altitude A = 0 m	81,58kg/m^2	
	Zone 3, Altitude A = 0 m	132,56 kg/m^2	
	Zone 4/5, Altitude A = 0 m	203,94 kg/m^2	
Central West	Zone 1, Altitude A = 0 m	10,20kg/m^2	
	Zone 2, Altitude A = 0 m	20,39kg/m^2	
	Zone 3, Altitude A = 0 m	40,79 kg/m^2	
	Zone 4/5, Altitude A = 0 m	71,38 kg/m^2	
Sweden, Finland	Zone 1, Altitude A = 0 m	122,37kg/m^2	
	Zone 2, Altitude A = 0 m	203,94kg/m^2	
	Zone 3, Altitude A = 0 m	275,32 kg/m^2	
	Zone 4/5, Altitude A = 0 m	397,69 kg/m^2	
UK, Ireland	Zone 1, Altitude A = 0 m	4,08 kg/m^2	
	Zone 2, Altitude A = 0 m	20,39 kg/m^2	
	Zone 3, Altitude A = 0 m	30,59 kg/m^2	
	Zone 4/5, Altitude A = 0 m	50,99 kg/m^2	
Czech Republic	Region I	76,48 kg/m^2	
	Region II	107,07 kg/m^2	
	Region III	152,96 kg/m^2	
	Region IV	229,44 kg/m^2	
	Region V	> 229,44 kg/m^2	
Iceland	Region 1	214,14 kg/m^2	
	Region 2	224,34 - 387,49 kg/m^2	
	Region 3	397,70 - 622,03 kg/m^2	
	Region 4	> 622,03 kg/m^2	
	Zone 1, Altitude 0.007 A – 1.4	≥71,38 kg/m^2	

Poland	Zone 2	91,77 kg/m^2	
	Zone 3, Altitude 0.006 A – 0.6	≥122,37 kg/m^2	
	Zone 4	163,15 kg/m^2	
	Zone 5, Altitude 0,93exp(0.00134 A)	≥203,94 kg/m^2	
Weight density of snow γ (kN/m^3)			It increases with the duration of the snow cover and depends on the site location, climate and altitude
	• Fresh • Settled (several hours or days after its fall) • Old (several weeks or months after its fall) • Wet	• 1,0 • 2,0 • 2,5 - 3,5 • 4,0	

The Eurocode EN 1991-1-3 refers to the structural design of buildings and civil engineering works for sites at altitudes under 1500 m. In the case of altitudes above 1500 m, advice may be found in the appropriate National Annex. The thresholds contained in the Eurocode document are applicable to the CI sectors energy (control rooms and buildings), transport (public transport stations, gasoline stations, road bridges, rescue coordination centres, fire dispatch centres, lighthouses, bridges) and public (base stations, call centre, dispatch centre, military personnel buildings, police station, detention rooms, jails, public buildings, hospitals).

EN 1991-1-3 does not give guidance on the following specialist aspects:

- "impact loads" due to snow sliding off or falling from a higher roof,
- additional wind loads resulting from changes in shape or size of the roof profile due to presence of snow or to the accretion of ice,
- loads in areas where snow is present all the year,
- loads due to ice,
- lateral loading due to snow (e.g. lateral loads due to drifts) and
- snow loads on bridges.

The characteristic snow load on the ground with probability of exceedence of 0.02, and mean recurrence interval of 50 years is referred according to European snow load maps, altitude and zone number for different climatic regions. The snow layers on a roof depend on the characteristics of the roof: shape, thermal properties, roughness of its surface, the amount of heat generated under the roof, the proximity of nearby buildings, the surrounding terrain, the local meteorological climate, in particular its windiness, temperature variations, and likelihood of precipitation (either as rain or as snow). In absence of wind or with very low wind velocities (< 2 m/s), snow deposits on the roof in a balanced way and generally forms a uniform cover. For wind velocities above 4 - 5 m/s, snow particles can be picked up from the snow cover and re-deposited on the lee side, on lower roofs in the lee side or behind obstructions on the roof.

4.5 Extreme Temperature

Water scarcity and drought mainly affect pumping stations, transportation and distribution pipes and treatment plants. Decreased water volumes cause sedimentation and depressurisation that lead to service loss, pipe failures and even decreased water quality. Furthermore, the imbalance between water supply and demand affects the groundwater pumping infrastructure because of the increased groundwater resources usage. Another direct impact to the water infrastructure, its operators and managing bodies is the requirement for new infrastructure in order to increase the available water volume by either transporting water from other river basin districts or constructing new reservoirs[137]. Additionally, there are other indirect impacts mainly due to the decreased volume of available water. Such impacts are service disruptions and the inability to meet the requested demand (esp. during peak hours). Efforts should be made to manage the system pressures in order to prevent failures. Further, policy makers and water utilities may chose to impose restrictions on certain water uses, such as outside use of water for washing cars and watering gardens[138]. Beyond the water sector, the electricity sector is highly dependent on water availability (esp. the energy production infrastructures are highly dependent on water for cooling). Nearly all thermal power plants—coal, natural gas, nuclear, biomass, geothermal, and solar thermal plants— require water for condensing the steam that drives the turbines. The availability of cooling water is the most limiting factor for the efficiency of thermal power plants. Therefore, the parameters air temperature, precipitation and combined events have the biggest influence. Table 21 lists functional and structural thresholds for assets of different CI sectors.

Table 21: Drought critical functional and structural thresholds

Electricity		
Asset	**Impacts on asset**	**Design threshold**
Power plant	Electricity generation requires ≈ 100 litres of freshwater/kWh [1] (cooling)[139] Severe streamflow droughts are major threats for hydropower and thermoelectric power[140]. Increased ambient air temperature reduces thermal efficiency of fossil-fuelled power plants[141].	Functional threshold[142]: 100 days of streamflow drought 100 days and high water temperature for more than 50 days Ambient temperature = 30°C

[137] EEA, 2010, Water resources: Quantity and flows, The European Environment: State and outlook 2010, SOER 2010 report, European Environment Agency, SOER 2010 website: www.eea.europa.eu/soer.

[138] EEA, 2010, Water resources: Quantity and flows, The European Environment: State and outlook 2010, SOER 2010 report, European Environment Agency, SOER 2010 website: www.eea.europa.eu/soer.
[139] DOE, "Climate Change and the Electricity Sector Guide for Climate Change Resilience Planning," Sep. 2016.
[140] Asian Development Bank, "Climate risk and adaptation in the electric power sector," Mandaluyong City, Philippines, 2012
[141] S. Espinoza, M. Panteli, P. Mancarella, and H. Rudnick, "Multi-phase assessment and adaptation of power systems resilience to natural hazards," Electr. Power Syst. Res., vol. 136, pp. 352–361, Jul. 2016
[142] Asian Development Bank, "Climate risk and adaptation in the electric power sector," Mandaluyong City, Philippines, 2012

Distribution lines EHV transmission lines Distribution substations	Surrounding trees suffer from drought stress and may fall[143] → lower height towers or poles, conductors vulnerable to damage by falling trees[144]. Expansion of material and resulting cable sag[145] High ambient air temperature and humidity resulting in humidity within substations[146] Increased resistance of aluminium and copper wires[147]	Functional thresholds: Ambient Temperature = 35°C Cable surface Temperature = 50°C For Distribution Substations: Ambient Temperature = 40°C
Distribution underground lines[148]	Dried soil around underground cables lowers conductivity and carrying capacity (cable rating can drop by up to 29 %)[149]	Functional threshold: Temperature > 55°C at cable surface Ambient air temperature > 35°C.
Step up/down substations	Higher deterioration rate of substation components High ambient temperature reduces peak load capacity of banks of transformers[150] Condensation may occur[151]	Functional threshold: Ambient air temperature > 40°C Ambient air temperature > 35° (24h)
Transformer	Reduced peak load capacity of the bank of transformers [152]	Functional & structural

[143] http://www.nhregister.com/environment-and-nature/20160829/drought-conditions-in-connecticut-raise-concerns-of-tree-damage-to-power-lines

[144] DOE, "U.S. energy sector vulnerabilities to climate change and extreme weather," U.S. Department of Energy, DOE/PI-0013., Jul. 2013

[145] Hazus - MH 2.1, "Multi-hazard Loss Estimation Methodology Flood Model Technical Manual," Department of Homeland Security Federal Emergency Management Agency Mitigation Division, Washington, D.C., 2011;
CSN EN 50341-2-22, "Overhead Electrical Lines Exceeding AC 45 KV. Set of National Normative Aspects," PN-EN 50341-1, 2005

[146] M. T. H. van Vliet, J. Sheffield, D. Wiberg, and E. F. Wood, "Impacts of recent drought and warm years on water resources and electricity supply worldwide," Environ. Res. Lett., vol. 11, no. 12, p. 124021, Dec. 2016.;

M. Hulme, H. Neufeldt, H. Colyer, and A. Ritchie, "Adaptation and mitigation strategies: supporting European climate policy," 2009.

[147] B. Ruszczak and M. Tomaszewski, "Extreme Value Analysis of Wet Snow Loads on Power Lines," IEEE Trans. Power Syst., vol. 30, no. 1, pp. 457–462, Jan. 2015

[148] DOE, "Climate Change and the U.S. Energy Sector: Regional Vulnerabilities and Resilience Solutions," US Department of Energy, 2015

[149] Ossama E. Gouda, Ghada M. Amer, Adel Z. El Dein, „Effect of dry zone formation around underground power cables on their ratings", CIRED 2009 - 20th International Conference and Exhibition on Electricity Distribution - Part 1, 8-11 June 2009

[150] EPRI, "Key Climate Variables Relevant to the Energy Sector and Electric Utilities. Climate Science Newsletter. Palo Alto (Cal., USA): 4.," 2009.

[151] M. Hulme, H. Neufeldt, H. Colyer, and A. Ritchie, "Adaptation and mitigation strategies: supporting European climate policy," 2009.

	Reduced operability, failures	threshold: Maximum Ambient temperature=40°C
Water		
DHS Underground thermal water pipes	Lack of water might result to waste of water, warm water system designed so that warm water reaches tap within ≈ 10 s	Functional threshold: Design water flow: 0,2 l/s
DHS Network	Issues in network functionality	Link to drinking water treatment plant sector.
DHS Substation	Forward temperature of water from production plants should be about 10°C higher than targeted supply temperature[153]	Functional threshold: Substation Temperature inlet = 65°C
Transport		
Bridges	Maximum temperature of concrete ≤ 75°C Thermal gradient from centre to surface ≤ 25°C If temperature is likely to exceed 75°C, designer shall submit proposal for controlling the concrete temperature	Loss of structural integrity, collapse
Tunnels	Fast to ultra fast growth rate to a heat release rate of 100 MW (sensitivity case of 120 MW)	Loss of structural integrity

As average global temperatures continue to rise, droughts and reduced water supplies are likely to become the norm in some regions. Since thermal power plants rely heavily on water for cooling, a changing climate is likely to put them at higher risk from drought[154]. Electricity assets are highly dependent on water for cooling. Nearly all thermal power plants (coal, natural gas, nuclear, biomass, geothermal, and solar thermal plants) require water for condensing the steam that drives the turbines. The availability of cooling water is the limiting factor for the efficiency of thermal power plants. Electricity generation with thermal power plants requires about 100 l/kWh for cooling purposes[155]. Therefore, the parameters air temperature and precipitation have the biggest influence[156].

[152] https://www.copper.org/environment/sustainable-energy/transformers/education/trans_efficiency.html
[153] Gregg Garfin, Angela Jardine, Robert Merideth, Mary Black, and Sarah LeRoy, Assessment of climate change in the southwest United States. A report prepared for the National CLimate Assessment, Island press. Washington, D.C., 2013
[154] T. J. Feeley et al., “Water: A critical resource in the thermoelectric power industry,” Energy, vol. 33, no. 1, pp. 1–11, Jan. 2008
[155] Hatt R, “Handling coal: Sticky when wet. PowerOnline. http://www.poweronline.com/doc/Handling- Coal-sticky-when-wet-

In an extended drought event, any trees surrounding the distribution network may suffer from drought stress and fall. Conductors are more vulnerable to damage by falling trees in lower height of towers or poles[157], while the cable rating of distribution underground lines can drop by up to 29 % if the soil around it dries out thoroughly. This starts when the surface temperature of the cable reaches around 55°C, depending on soil conditions. Ambient air temperature must rise above 30 - 35°C for this to happen[158].

Fluctuations in temperature affect the demand for heating and cooling, causing reductions in the efficiency power plants and changes in hydropower potential in some regions. According to Espinoza et al. (2016)[159], above 30 °C an increase in ambient air temperature of about 1 K would reduce thermal efficiency of fossil-fuelled power plants by 0.1 - 0.5% and may result in a capacity loss of 1.0 - 2.0 %. During hot days, overhead line problems also can occur due to an expansion of material and resulting cable sag. A temperature of 50 °C at conductor surface is enough to cause a sag of 4.5 cm per 1 K (for 35°C ambient temperature and span of 400 m)[160]. Furthermore, the resistance of aluminium and copper wires increases by 0.4 % per 1 K rising air temperatures between 0 °C and 100 °C, leading to - 0,5% to - 1% line load per 1 K rise[161]. On the contrary, ambient air with high humidity and high temperatures can result in the larger amount of water that air can hold within substations[162]. Higher ambient temperatures also reduce the peak load capacity of banks of transformers in substations[163]. The basic relationship of power capacity to temperature used in most studies is linear[164]. Therefore, any optional changes in temperature might affect their capacity (- 0.7 % for each degree above 30 °C[165]). According to Hule et al. (2009)[166], condensation may occur based on standards regarding the normal service conditions for

0001. Accessed 19 April 2013," 2001.

156 Hatt R, "Coal quality and combustion workshop. Coal Combustion, Inc. http://www.coalcombustion.com/PDF%20Files/webcqcclassoutline.pdf." 2004.

157 B. Azevedo de Almeida and A. Mostafavi, "Resilience of Infrastructure Systems to Sea-Level Rise in Coastal Areas: Impacts, Adaptation Measures, and Implementation Challenges," Sustainability, vol. 8, no. 11, p. 1115, Nov. 2016.

158 Hazus - MH 2.1, "Multi-hazard Loss Estimation Methodology Flood Model Technical Manual," Department of Homeland Security Federal Emergency Management Agency Mitigation Division, Washington, D.C., 2011

159 S. Espinoza, M. Panteli, P. Mancarella, and H. Rudnick, "Multi-phase assessment and adaptation of power systems resilience to natural hazards," Electr. Power Syst. Res., vol. 136, pp. 352–361, Jul. 2016.

160 Hazus - MH 2.1, "Multi-hazard Loss Estimation Methodology Flood Model Technical Manual," Department of Homeland Security Federal Emergency Management Agency Mitigation Division, Washington, D.C., 2011;

CSN EN 50341-2-22, "Overhead Electrical Lines Exceeding AC 45 KV. Set of National Normative Aspects," PN-EN 50341-1, 2005.

161 B. Ruszczak and M. Tomaszewski, "Extreme Value Analysis of Wet Snow Loads on Power Lines," IEEE Trans. Power Syst., vol. 30, no. 1, pp. 457–462, Jan. 2015.

162 M. T. H. van Vliet, J. Sheffield, D. Wiberg, and E. F. Wood, "Impacts of recent drought and warm years on water resources and electricity supply worldwide," Environ. Res. Lett., vol. 11, no. 12, p. 124021, Dec. 2016.; M. Hulme, H. Neufeldt, H. Colyer, and A. Ritchie, "Adaptation and mitigation strategies: supporting European climate policy," 2009

163 EPRI, "Key Climate Variables Relevant to the Energy Sector and Electric Utilities. Climate Science Newsletter. Palo Alto (Cal., USA): 4.," 2009

164 J. F. Feenstra, "Handbook on methods for climate change impact assessment and adaptation strategies," 1998; T. Brandt, A. Varma, R. Brent, S. Marcu, R. Connor, and K. Harries, "Effects of Fire Damage on the Structural Properties of Steel Bridge Elements. Final Report," 2011.

165 M. T. H. van Vliet, J. Sheffield, D. Wiberg, and E. F. Wood, "Impacts of recent drought and warm years on water resources and electricity supply worldwide," Environ. Res. Lett., vol. 11, no. 12, p. 124021, Dec. 2016.

166 M. Hulme, H. Neufeldt, H. Colyer, and A. Ritchie, "Adaptation and mitigation strategies: supporting European climate policy," 2009.

indoor switch gear and control gear. Higher ambient temperatures affect the hot spot conductor temperature (HST) within the transformer, which in turn reduces the peak load capacity of the bank of transformers[167]. Additionally, Feenstra (1998)[168] also reports the transformer load capacity as a function of ambient temperature, as heat waves can lead to distribution transformer failures of all ages, and not necessarily only old ones[169]. As a consequence at temperatures of the order of 40 ℃ ambient, accelerated ageing tests demonstrate that the useful life of the paper may only be a few days[170].

Table 22: Extreme cold temperature thresholds of the electricity sector

Extreme Temperature		
Asset	**Impacts on asset**	**Design threshold**
District Heating Underground Thermal Water pipes	If the extreme cold temperature occurs long enough and heat supply is not restored, there is a risk that water will freeze within these pipelines [32].	<u>Functional threshold:</u> Underground Pipes Temperature = 50°C
District Heating network	In DH networks, the magnitude of distribution heat losses generally increases in extreme low conditions [43].	<u>Functional threshold:</u> Ambient Temperature = - 20°C

Despite the fact that district heating assets are well protected under the earth, doesn't mean that they are not affected by extreme fluctuations in temperatures. During extreme cold temperatures there is high risk that water will freeze within these pipelines[171]. In district heating networks, the magnitude of distribution heat losses generally increases in extreme low conditions. Each substation is designed for a nominal load of 250 kWth that is assumed to occur when the outdoor ambient temperature reaches – 20 °C[172]. Alternatively district heating substations should maintain stable water temperatures and stable water temperature differences in the supply and the discharge of the pipes[173]. Regarding the district heating underground lines in case that the

[167] https://www.copper.org/environment/sustainable-energy/transformers/education/trans_efficiency.html
[168] J. F. Feenstra, "Handbook on methods for climate change impact assessment and adaptation strategies," 1998
[169] DOE, "Climate Change and the Electricity Sector: Guide for Assessing Vulnerabilities and Developing Resilience Solutions to Sea Level Rise," Jul. 2015; J. A. Sathaye et al., "Estimating impacts of warming temperatures on California's electricity system," Glob. Environ. Change, vol. 23, no. 2, pp. 499–511, Apr. 2013.; T. Byrne, "Humidity effects in substations," in Petroleum and Chemical Industry Conference Europe, 2014, 2014, pp. 1–10.

[170] J. A. Sathaye et al., "Estimating impacts of warming temperatures on California's electricity system," Glob. Environ. Change, vol. 23, no. 2, pp. 499–511, Apr. 2013.; T. Byrne, "Humidity effects in substations," in Petroleum and Chemical Industry Conference Europe, 2014, 2014, pp. 1–10.

[171] AECOM, "Torondo Hydro-Electric System Public Infrastructure Engineering Vulnerability Assessment Pilot Case study," 60263582, Sep. 2012.
[172] X. Li, R. W. Mazur, D. R. Allen, and D. R. Swatek, "Specifying Transformer Winter and Summer Peak-Load Limits," IEEE Trans. Power Deliv., vol. 20, no. 1, pp. 185–190, Jan. 2005.
[173] Gregg Garfin, Angela Jardine, Robert Merideth, Mary Black, and Sarah LeRoy, Assessment of climate change in the southwest United States. A report prepared for the National CLimate Assessment, Island press. Washington, D.C., 2013.

extreme cold temperature occurs long enough and heat supply is not restored, there is a risk that water will freeze within these pipelines. Thus, metal pipes can be torn apart by expansion of density when water crystalises[174]. Hence temperature should never get below 50 °C in any part of the telemetering system.

Thermal actions are imposed on a structure or a structural element as a result from the changes of temperature fields within a specified time interval. The magnitude of the thermal effects is dependent on local climatic conditions, together with the orientation of the structure, its overall mass, finishes (e.g. cladding in buildings), and in the case of building structures, heating and ventilation regimes and thermal insulation. EN 1991-1-5[175] gives design guidance for thermal actions arising from climatic and operational conditions on buildings and civil engineering works, including bridges, other structures with their structural elements, cladding and other appendages of buildings are also provided. Characteristic values of thermal actions are presented for use in the design of structures which are exposed to daily and seasonal climatic changes. Structures not so exposed may not need to be considered for thermal actions. Thermal actions are classified as variable and indirect actions.

The strains and any resulting stresses, are dependent on the geometry and boundary conditions of the considered element and on the physical properties of the material. When materials with different coefficients of linear expansion are used compositely the thermal effect should be taken into account. Most materials expand when they are heated, and contract when they are cooled. Temperature difference will cause concrete to deform, expand or contract. The size of the concrete structure whether it is a bridge, a highway, or a building is irrelevant to the effects of temperature. The expansion and contraction with changes in temperature occur regardless of the structure’s cross-sectional area. Concrete expands slightly as temperature rises and contracts as temperature falls. Temperature changes may be caused by environmental conditions or by cement hydration. Bridges expand and contract due to temperature change. This movement is accommodated by bearings and expansion joints or by deformation of the piers and abutments with integral construction. Bridge movements depend upon average bridge temperatures rather than air temperature. Bridge temperatures vary through the bridge cross section as a function of time. Temperature calculations are based on radiation, convection, and conduction heat flow, and these three mechanisms all contribute to the time dependent cross sectional variation.

[174] AECOM, “Torondo Hydro-Electric System Public Infrastructure Engineering Vulnerability Assessment Pilot Case study,” 60263582, Sep. 2012.
[175] EN 1991-1-5. Eurocode 1 - Actions on structures - Part 1-5: General actions – Thermal actions

Table 23: Critical climatic parameters and thresholds of buildings in Eurocodes

<table>
<tr><th>Assets</th><th></th><th></th></tr>
<tr><td rowspan="7">Control rooms
CI company buildings
Public transport stations
Gasoline stations
Rescue coordination centres
Fire dispatch centres
Lighthouses
Base stations
Call centres
Dispatch centres
Military buildings
Police stations
Detention rooms
Public buildings
Jails
Hospitals</td><td>Thermal differential between surface and interior of materials result in cracking, oversailing, buckling of walls, fracture of masonry units</td><td>Impacts</td></tr>
<tr><td>Initial Temperature T [^{o}C]

Common characteristic values of thermal actions: 50-year return values</td><td rowspan="6">Thresholds

(EN 1991-1-5)</td></tr>
<tr><td>Inner environment temperature T_{in} [^{o}C]

Summer: T_{in} = 20 °C

Winter: T_{in} = 25°C

(recommended)</td></tr>
<tr><td>Outer environment temperature T_{out} [°C]

Buildings above ground level:

<table>
<tr><th>Season</th><th colspan="2">Significant factor</th><th>T_{out} [^{o}C]</th></tr>
<tr><td rowspan="3">Summer</td><td rowspan="3">Relative absorptivity</td><td>bright light surface</td><td>$T_{max} + T_3$</td></tr>
<tr><td>light surface</td><td>$T_{max} + T_4$</td></tr>
<tr><td>dark surface</td><td>$T_{max} + T_5$</td></tr>
<tr><td colspan="3">Winter</td><td>T_{min}</td></tr>
<tr><td colspan="4">If no data available: for regions between latitudes 45°N and 55°N the values T_3=0°C, T_4=2°C and T_5=4°C, for North - East facing elements and T_3=18°C, T_4=30°C and T_5=42°C for South - West or horizontal elements.</td></tr>
</table>

Buildings below ground level:

<table>
<tr><th>Season</th><th>Level</th><th>T_{out} [^{o}C]</th><td rowspan="5">If no data available: for regions between latitudes 45°N and 55°N the values T_6=8°C, T_7=5°C and T_8=-5°C and T_9=-3°C</td></tr>
<tr><td rowspan="2">Summer</td><td>< 1 m</td><td>T_6</td></tr>
<tr><td>> 1 m</td><td>T_7</td></tr>
<tr><td rowspan="2">Winter</td><td>< 1 m</td><td>T_8</td></tr>
<tr><td>> 1 m</td><td>T_9</td></tr>
</table></td></tr>
<tr><td>Uniform temperature component ΔT_u [^{o}C]
$\Delta T_u = T - T_0$

difference between average temperature T of an element (climatic temperatures in winter or summer and operational temperatures) and its initial temperature T_0.</td></tr>
<tr><td>Linearly varying temperature component ΔT_M

difference between outer and inner surface temperatures of a cross section or individual layers</td></tr>
<tr><td>Temperature difference of different parts ΔT_p

difference of average temperatures of structure parts</td></tr>
</table>

Industrial chimneys Pipelines Silos Tanks Cooling towers	$15^{o}C$ concrete pipelines: stepped temperature component round the circumference (causing both overall and local thermal effects), one quadrant of its circumference has a mean temperature higher than that of the remainder of the circumference	

Table 24: Critical climatic parameters and thresholds of bridges in Eurocodes

Thresholds (EN 1991-1-5)

Uniform temperature component [°C]

depends on T_{min} and T_{max} of a bridge

a) Steel deck (steel box girder, steel truss or plate girder)

b) Composite deck

c) Concrete deck (concrete slab, concrete beam, concrete box girder)

Surfacing thickness [mm]	Temperature difference				
	Heating [°C]				Cooling [°C]
	ΔT_1	ΔT_2	ΔT_3	ΔT_4	ΔT_1
Unsurfaced	30	16	6	3	8
20	27	15	9	5	6
40	24	14	8	4	6

Initial bridge temperature T_o [°C]

thermal effects include spalled concrete around bearings at the supports, bent and pulled-out anchor bolts, locked expansion joints due to uneven gap opening across the bridge [176]

Minimum and maximum shade air temperature T_{min} [°C] and T_{max} [°C]

Characteristic values for the site location obtained e.g. from national maps of isotherms

T_{max} with an annual probability of being exceeded of 0,02 (≙ mean return period 50 years)

Minimum and maximum uniform bridge temperature components $T_{e,min}$ [°C] and $T_{e,max}$ [°C]

based on daily temperature ranges of 10 °C
steel truss and plate girders: $T_{e,max}$ may be reduced by 3 °C

Uniform bridge temperature component $\Delta T_{N,con} = T_0 - T_{e.min}$

Maximum expansion range of the uniform bridge temperature component $\Delta T_{N,exp}$
$\Delta T_{N,exp} = T_{e\,.max} - T_o$
recommended values: (ΔTN,exp + 20)°C and (ΔTN,con + 20)°C

if temperature at which the bearings and expansion joints are set is specified, recommended values are (ΔTN,exp + 10)°C and (ΔTN,con + 10)°C

Overall range of the uniform bridge temperature component $\Delta T_N = T_{e,max} - T_{e,min}$

[176] http://www.eng.auburn.edu/files/centers/hrc/IR-98-02.pdf

Vertical temperature differences $\Delta_{TM,heat}$ and $\Delta T_{M,cool}$ a) Vertical linear component b) Vertical temperature components with non-linear effects considered by using equivalent linear temperature difference component with $\Delta T_{M,heat}$ and $\Delta T_{M,cool}$, valuesapplied between top and bottom of the bridge deck
Horizontal components - linear temperature difference between the outer edges If no other information available: 5°C recommended (linear temperature difference between outer edges of the bridge, independent from width)
Temperature difference components within walls of concrete box girders recommended value for linear temperature difference is 15 °C
Differences in uniform temperature component between different structural elements Recommended values: – 15°C between main structural elements (e.g. tie and arch) – 10°C and 20°C for light and dark colour, between suspension/stay cables and deck or tower
Linear temperature differences between opposite outer faces 5 °C (concrete piers, hollow or solid) 15 °C (walls between inner and outer faces)

DIN 1072	Temperature difference in 20 °C [K]	Linear temperature difference [K]			
		Under construction	Final satge	Under construction	Final stage
Steel	± 35	15	10	5	5
Composite	± 35	8	10	7	7
Concrete	+ 20; - 30	10	7	3.5	3.5

4.6 Wind

Extreme winds pose a major threat to transmission line networks in many regions around the world. Almost all transmission structures failures in electricity infrastructure in the last 20 years can be attributed to extreme winds. Interruptions in the delivery of electric power associated with structural failures are a continuing problem and can have significant economic impacts on the local economy. Transmission lines in service today have been designed using a multitude of design approaches and structural loading criteria. The principal cause of structural failures is associated with weather events that produce loads that exceed the structural loading design criteria. In some cases, failures have been the result of inadequate design, construction and/or maintenance practices, airplane or vehicle accidents and criminal activities. Table 25 presents an overview of critical threshold values for wind on different CI assets.

Table 25: Wind - critical Functional & Structural thresholds of the electricity sector

Extreme winds		
Asset	**Impacts on asset**	**Design threshold**
Distribution lines	Under strong winds with speeds over 100 km/h or 30 m/s, electric wires and other electricity distribution components can easily collapse[177]	Functional threshold: Wind speed= 30 m/s
High voltage transmission lines	According to Hashmi et al. (2013) [178], structural failures will occur in EHV transmission lines and towers after 50 m/s and 150 m/s. However in most cases after 150 m/s lines failure towers also collapse.	Structural thresholds: Wind speed (lines) = 50 m/s Wind speed (towers) = 150 m/s
Distribution substations Step up_down substations Transformer	In case of an overhead distribution substation: Under strong winds with speeds over 100km/h or more, components collapse In case of substation placed in basement ground floor level: Substations collapse at 60-80 m/s[179].	Structural thresholds: Wind speed = 30 m/s Wind speed = 60 - 80 m/s
Electrical grid operation	Indirect impacts to distribution lines: Increasing wind speeds can also have a minor positive effect on overhead lines. Provided winds remain below damage levels, stronger winds help cool overhead lines by increasing heat convection[180].	Functional threshold: Wind speed < 30 m/s

[177] R. Contreras-Lisperguer and K. de Cuba, "The potential impact of climate change on the energy sector in the Caribbean region," Wash. DC Dep. Sustain. Dev. Organ. Am. States OAS, 2008.; S. Dunn, S. Wilkinson, C. Galasso, L. Manning, and D. Alderson, "Development of empirical vulnerability curves for electrical supply systems subjected to wind hazard," 2015.
[178] M. Hashmi, M. Lehtonen, and S. Hänninen, "Effect of Climate Change on Transformers Loading Conditions in the Future Smart Grid Environment," Open J. Appl. Sci., vol. 03, no. 02, pp. 24–29, 2013

[179] A. L. López, L. E. P. Rocha, D. L. Escobedo, and J. S. Sesma, "Reliability and vulnerability analysis of electrical substations and transmission towers for definition of wind and seismic damage maps for Mexico," in 11th Americas Conference on Wind Engineering-San Juan, Puerto Rico, 2009.
[180] Hazus - MH 2.1, "Multi-hazard Loss Estimation Methodology Flood Model Technical Manual," Department of Homeland Security Federal Emergency Management Agency Mitigation Division, Washington, D.C., 2011

Eurocodes documents are related to the structural design of construction works and products involving several climatic hazards that are imposed on structures in the form of loads[181]. In case of wind hazard, as building structures are designed for a certain design wind load they may fail when the actual wind exceed the design load. EN 1991-1-4[182] refers to natural wind actions for the structural design of building and civil engineering works. This includes the whole structure or parts of the structure or elements attached to the structure, e.g. components, cladding units and their fixings, safety and noise barriers. Wind vulnerability can seriously affect construction components which are installed on the roof or the façade (e.g. antenna, chimneys, solar panel, scaffolding). Buildings that are situated in a prominent position, high altitudes (hills, mountains), slopes and locations on lakes or in open areas, in wind corridor etc. are especially vulnerable to wind actions. Moreover, buildings that stand out from their environment (high warehouses), with irregular shapes (strongly texturer exterior wall or roof surfaces), with critical forms causing aerodynamic stresses or with critical operating conditions (open building gates) have also an increased risk on storm hazards.

The fundamental value of the basic wind velocity, $v_{b,0}$, is the characteristic 10 minutes mean wind velocity, irrespective of wind direction and time of year, at 10 m above ground level in open country terrain with low vegetation such as grass and isolated obstacles with separations of at least 20 obstacle heights. There are maps with the thresholds of basic wind velocities in Europe (see Figure 4). Most damage occurs because various building elements have limited wind resistance due to inadequate design, poor installation, or material deterioration. The magnitude and frequency of strong windstorms vary by locale. When wind interacts with a building, both positive and negative pressures occur simultaneously. Wind loads are transferred through the structure's envelope to the structural system, where in turn they must be transferred through the foundation into the ground. The characteristics of the terrain (i.e. ground roughness and surface irregularities of a building) influence the wind loading.

The effect of the wind on the structure (i.e. the response of the structure), depends on the size, shape and dynamic properties of the structure: quasi-static response (the majority of building structures). For structures when the lowest natural frequency is so high that wind actions in resonance with the structure are insignificant, the wind action is called quasi-static dynamic and aeroelastic response (lightweight structures e.g. steel chimneys). The dynamic response is significant for structures, if the turbulence (or gust effect) of the wind is in resonance with the structure's natural frequency whereas the aeroelastic response occurs if an interaction between the movement of a particular structure and the circumfluent wind flow exists[183].

In most Codes and Standards in Europe or worldwide (USA, Canada, New Zealand) the basic wind speed is determined for the design of wind loads. Abrupt changes in topography, such as isolated hills, ridges, and escarpments, increase the wind to speed. Therefore, a building located near a ridge would receive higher wind pressures than a building located on relatively flat land. Taller

---

[181] Leonardo da Vinci Pilot Project CZ/02/B/F/PP-134007 DEVELOPMENT OF SKILLS FACILITATING IMPLEMENTATION OF EUROCODES HANDBOOK 3 ACTION EFFECTS FOR BUILDINGS

[182] Eurocode 1: Actions on structures - Part 1-4: Wind actions
EN 1991-1-4:2005/A1:2010. Eurocode 1: Actions on structures - Part 1-4: General actions - Wind actions. Brussels: CEN/TC 250 - Structural Eurocodes, April 2010.
EN 1991-1-4:2005. Eurocode 1: Actions on structures - Part 1-4: General actions - Wind actions. Brussels: CEN/TC 250 - Structural Eurocodes, March 2005 (DAV)

[183] https://www.apsei.org.pt/media/recursos/documentos-de-outras-entidades/CFPA-guideline-riscos-naturais/cfpa_e_guideline_no_3_2013_n_1389624941.pdf.

buildings are exposed to higher wind speeds and greater wind pressures. The highest uplift pressures occur at roof corners because of building aerodynamics (i.e., the interaction between the wind and the building[184]). The response of structures should be calculated from the characteristic peak velocity pressure, q_p, at the reference height in the undisturbed wind field for the determination of the wind actions on structures and accounts for the mean wind and the turbulence component. EN 1991-1-4 indicates q_p as a function of: wind climate (through the basic wind velocity *v*b at a given site), local factors (e.g. terrain roughness [$c_r(z)$], orography [$c_0(z)$]), height above the terrain (z) and structural factor $c_s c_d$.

w_e : Wind pressure on external surfaces (see EN 1991-1-4).

$w_e = q_p (z_e)\, c_{pe}$

$q_p(z_e)$ is the peak velocity pressure

*z*e is the reference height for the external pressure

*c*pe is the pressure coefficient for the external pressure

w_i : Wind pressure on the internal surfaces of a structure.

$w_i = q_p (z_i)\; c_{pi}$

$q_p(z_i)$ is the peak velocity pressure

z_i is the reference height for the internal pressure

c_{pi} is the pressure coefficient for the internal pressure, depending on the size and distribution of the openings in the building envelope. When in at least two sides of the buildings (facades or roof) the total area of openings in each side is more than 30 % of the area of that side, the actions on the structure should not be calculated

When the area of the openings at the dominant face is twice the area of the openings in the remaining faces,

*c*pi = 0,75 *c*pe

When the area of the openings at the dominant face is at least 3 times the area of the openings in the remaining faces,

*c*pi = 0,90 *c*pe

*c*pe is the value for the external pressure coefficient at the openings in the dominant face.

Open silos and chimneys *c*pi = - 0,60

Vented tanks with small openings *c*pi = - 0,40

Wind forces

F_w : Wind force, acting on a structure or a structural element may be determined by vectorial summation of the forces $F_{w,e}$, $F_{w,i}$ and F_{fr} calculated from the external and internal pressures and the frictional forces.

$F_w = c_s c_d\; c_f\; q_p (z_e)\; A_{ref}$

[184] https://www.fema.gov/media-library-data/20130726-1557-20490-6102/fema543_chapter3.pdf

$F_w = c_s c_d \; c_f \; \sum_{elements} q_p(z_e) \; A_{ref}$

$c_s c_d$ is the structural factor

c_f is the force coefficient for the structure or structural element

$q_p(z_e)$ is the peak velocity pressure at reference height z_e

A_{ref} is the reference area of the structure or structural element

$c_s c_d$ is the structural factor

w_e is the external pressure on the individual surface at height z_e

w_i is the internal pressure on the individual surface at height z_i,

A_{ref} is the reference area of the individual surface

c_{fr} is the friction coefficient

A_{fr} is the area of external surface parallel to the wind

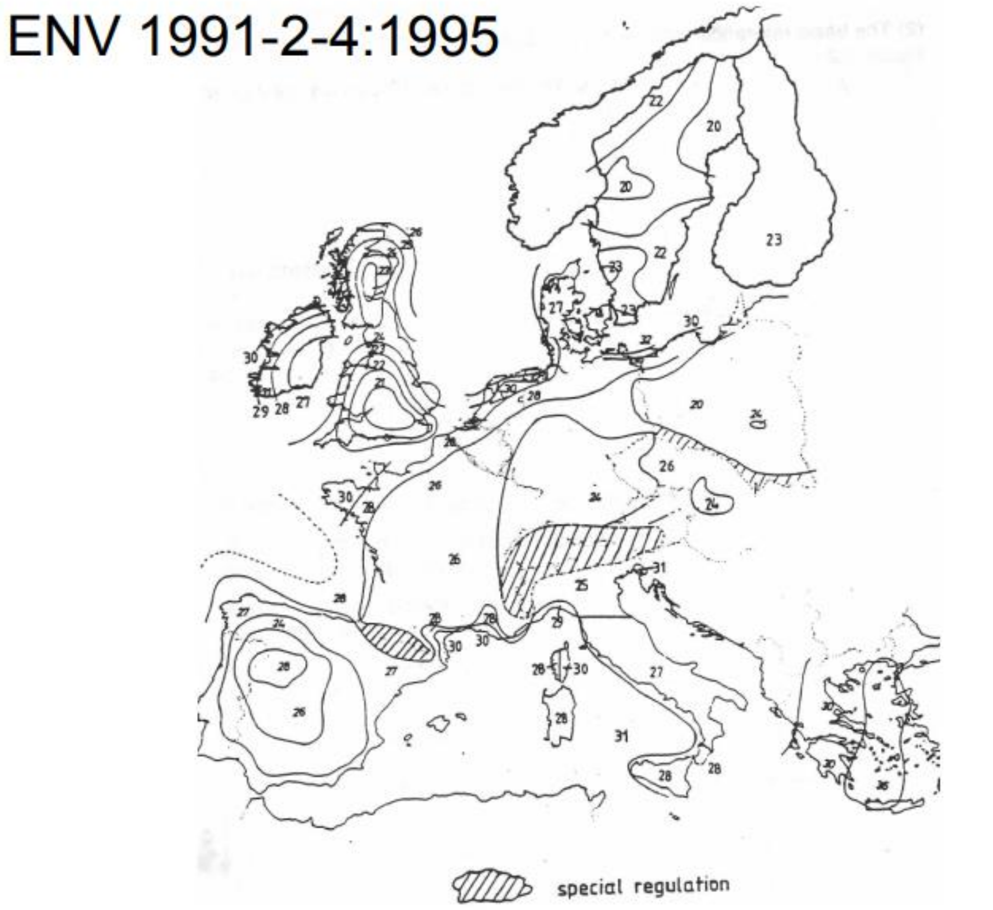

Figure 4: Map with the thresholds of basic wind velocities in Europe[185,186]

[185] http://eurocodes.jrc.ec.europa.eu/doc/WS2008/EN1991_4_Hansen.pdf
[186] https://www.eurocode.us/wind-actions/wind-maps-and-meteorological-information.html

Table 26: Critical climatic parameters and thresholds of wind for buildings

Assets	Thresholds EN 1991-1-4
Buildings, civil engineering works (maximum height 200 m) Bridges (maximum span 200 m)	*Fundamental basic wind velocity [m/s]* wind actions are characteristic values, determined from basic values of wind velocity or velocity pressure (values having annual probabilities of exceedence of 0.02 ≙ return period 50 years)
Control rooms CI company buildings Public transport stations Gasoline stations Rescue coordination centres Fire dispatch centres Lighthouses Base stations Call centres Dispatch centres Military buildings Police stations Detention rooms Public buildings Jails Hospitals	*Basic wind velocity [m/s]* = $c_{dir}\, c_{season}\, v_{b,0}$ $v_{b,}$ modified to account for wind direction function of wind direction and time of year at 10 m above ground of terrain category II
	Mean wind velocity at height z $v_m(z) = c_r(z)\, c_o(z)\, v_b$ v_b modified to account for effect of terrain roughness and orography $c_r(z)$ = roughness factor $c_o(z)$ = orography factor (1.0 unless otherwise specified)
	Wind pressure w [kN/m²] a) external wind pressure: $w_e = qp * cp_e$ b) internal wind pressure: $w_i = qp * cp_i$ qp = peak velocity pressure cp = pressure coefficient (external/ internal pressure)
	Peak velocity pressure q_p *and Reference mean velocity pressure* q_b $q_p(z) = [1+7I_v(z)](1/2)\rho v^2{}_m(z) = c_e(z) q_b$ *qb=(1/2)ρv2b* ρ = air density, depends on altitude, temperature, barometric pressure during wind storms (e.g. 1,25 kg/m³) $c_e(z)$ = exposure factor For flat terrain where $cO(z)$ = 1,0 q_p equal to q_b plus contribution from short-term pressure fluctuations Aeroelastic response considered for flexible structures (cables, masts, chimneys, bridges)
	Standard deviation of the turbulence σ_v turbulent component of wind velocity has a mean value of 0 and a standard deviation σ_v
	Turbulence factor k_I recommended value = 1.0
	Turbulence intensity $I_v(z)$

Table 27: Critical climatic parameters and thresholds of wind for bridges

Wind pressure [kn/m²]			
Height above ground [m]	**Bridge with traffic load**		**Bridge without traffic load**
	Without parapets	*With parapets*	*With/without parapets*
0 - 20	1.75	1.45	0.9
20 – 50	2.1	1.75	1.1
50 - 100	2.5	2.05	1.25

For the purposes of calculating the wind force, the structure should be divided into a series of sections, where a section comprises severalldentical or nearly identical panels. In determining the wind force under iced conditions, the projected areas of structural elements and ancillades should be increased to take due account of the thickness of ice as relevant. Towers and masts should be examined for gust induced vibrations (causing vibrations in the direction of the wind), vortex induced vibrations for towers or masts containing prismatic cylindrical or bluff elements or shrouds (causing vibrations perpendicular to the direction of the wind), galloping instability (causing vibrations of the guys) and rain-wind induced vibrations.

5 Probability of occurrence for extreme climate events

5.1 Probability estimation approaches

One methodology for climate output processing is to define and recognise risk parameters expressed in mean recurrence time or return periods, defining the probability of occurring extreme events and infrastructure operating states. They evaluate the intensity and frequency of rare events based on thresholds, related to the infrastructure design and engineering standards. The method for calculating return periods and the probability of exceeding a value is based on the Extreme Value Theory (EVT). The EVT complements the descriptive indices in order to evaluate the intensity and frequency of rare events that lie far in the tails of the probability distribution of climate variables. It assumes the reader is familiar with the concept of the cumulative probability distribution function and related statistics. The description is primarily based on Holmes (2001) [187]. The determination of the return periods of some variable (e.g. extreme wind speeds, extreme total precipitation's amounts) requires selection and definition of the underlying distribution function.

Two general methods can be used. One method is the "peaks-over-threshold" method, applicable under suitable conditions and using a high enough threshold. Extremes identified in this way follow a generalised Pareto distribution. The second, more generally used method based on an explicit extreme value theory is the so-called "block maximum" method. In this method the sample of extreme values is obtained by selecting the maximum (or in some cases the minimum) value observed in each block (usually during a year or season). The theoretical work by Jenkinson (1955)[188] generalised earlier contributions to this field, and introduced the Generalised Extreme Value (GEV) Distribution concept. Under certain conditions, this is the asymptotically correct model for block-maxima (usually annual maxima) values. This approach can be applied to both observed and simulated time-series. For the variable U (e.g. extreme wind speed), cumulative probability distribution function $F_U(U)$ is defined as:

$$F_U(U) = \exp\left[-\left(1 - k\frac{U-u}{a}\right)^{\frac{1}{k}}\right]$$

Where k is so called shape parameter, a is scale or dispersion parameter and u is location or mode parameter. Based on the sign and the value of the shape factor, following special cases are present:

1. When ***k*** tends to 0, GEV is known also as Type I Extreme Value Distribution (or Gumbel Distribution)
2. When ***k*** < 0, GEV is known also as Type II Extreme Value Distribution (or Frechet Distribution)
3. When ***k*** > 0, GEV is known also as Type III Extreme Value Distribution (or Weibull Distribution).

[187] Holmes, J. D. (2001) Wind loading of structures. Spon Press, 356 p

[188] Jenkinson A. F., "The frequency distribution of the annual maximum (or minimum) values of meteorological elements", Quarterly Journal of the Royal Meteorological Society, Q.J.R. Meteorol. Soc.,https://doi.org/10.1002/qj.49708134804, doi:10.1002/qj.49708134804, 1955

In practice, Types I and III are often used in the geophysical applications:

Type I because of the simplicity and existence of the graphical solution, while the use of the Type III is relevant because it predicts bounded values (in contrast to Type I and Type II which are unbounded and may lead to unphysical values). However, it should be noted that different notations can be found in the literature (e.g., Coles, 2001[189]) with the sign of the shape parameter ***k*** in (1) reversed, thus leading to the opposite definition of long- and short-tail distributions.

In practice, it is more convenient to express the extreme value distribution by the inverse (quantile) function of (1), U(F). In common terminology, the quintile function is the return level associated with the return period T=1/p, with p being probability defined by p=1-F_U(U) (Coles, 2001). E.g., regarding wind speed, if the return level associated with the return period T =150 years equals 30 m/s, there is a probability *p* = 1/150 that this level will be exceeded by any single event. The formal definition of T is:

$$T = \frac{1}{1 - F_U(U)} \qquad (2)$$

For possible extensions of F_U(U) and T related to the effects of (i) separation by storm type, (ii) composition of data from several stations to create a single time-series, (iii) wind direction effects (e.g. Palautikof et al.(1999)[190] and Holmes (2001)[191]).

There are various methods for estimating GEV parameters available from literature. For an example of graphical solution to Type I Extreme Value Distribution (Figure 5) estimation consider Octave[192] code.

After fitting data to distribution, for a given return period value as input, a critical value of the examined variable is provided. Respectively, given a critical hazard threshold as input, the probability of exceeding a critical value is calculated as output.

[189] Coles, S. (2001) An Introduction to Statistical Modeling of Extreme Values. Springer Verlag, Berlin. http://dx.doi.org/10.1007/978-1-4471-3675-0

[190] Palutikof J P, Brabson B B,Lister D H, Adcock S T. "A review of methods to calculate extreme wind speeds". Meteorological Applications,https://doi.org/10.1017/S1350482799001103, doi:10.1017/S1350482799001103, 1999

[191] Holmes, J. D. (2001) Wind loading of structures. Spon Press, 356 p

[192] https://www.gnu.org/software/octave/

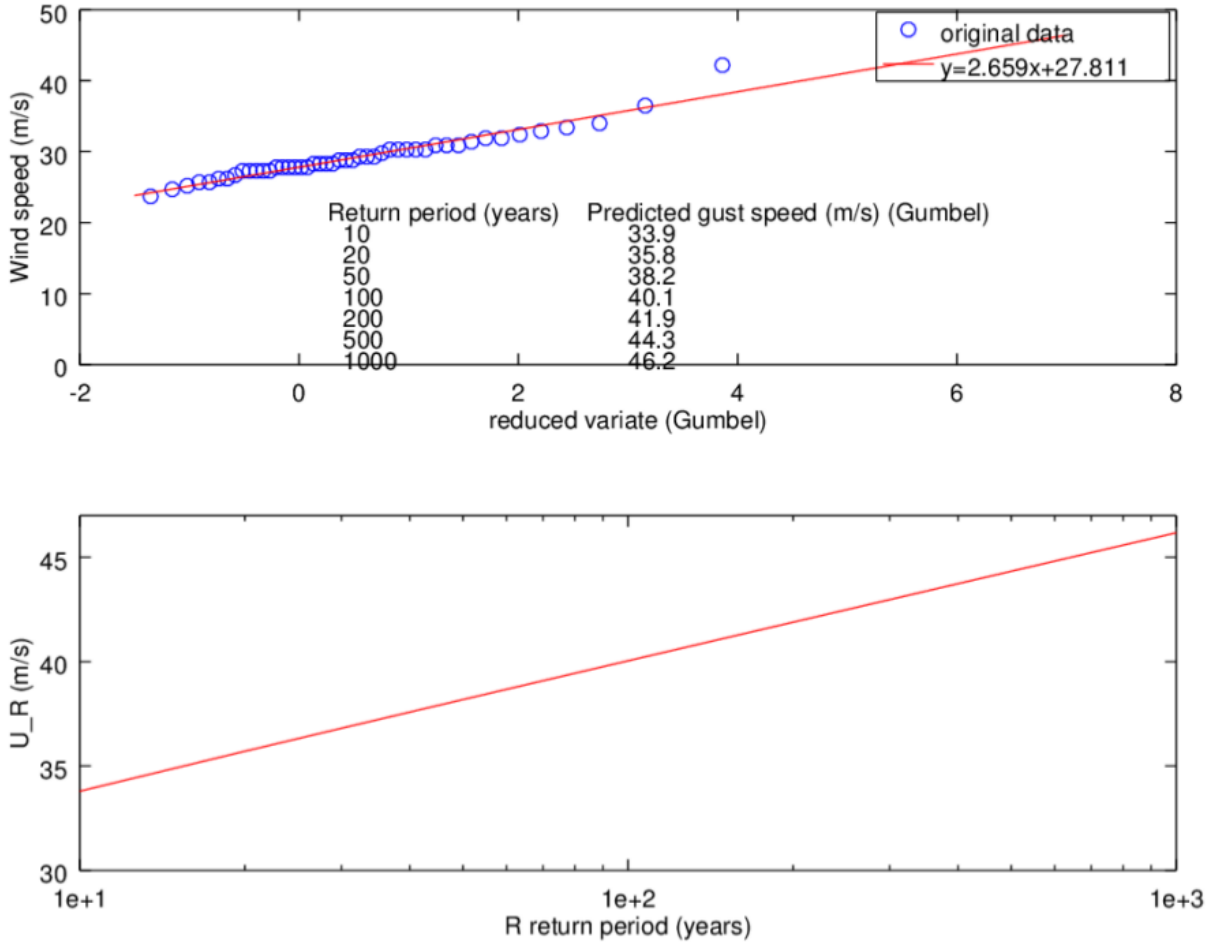

Figure 5: Estimation of the return periods for the case of Type I Extreme Value Distribution (or Gumbel Distribution).

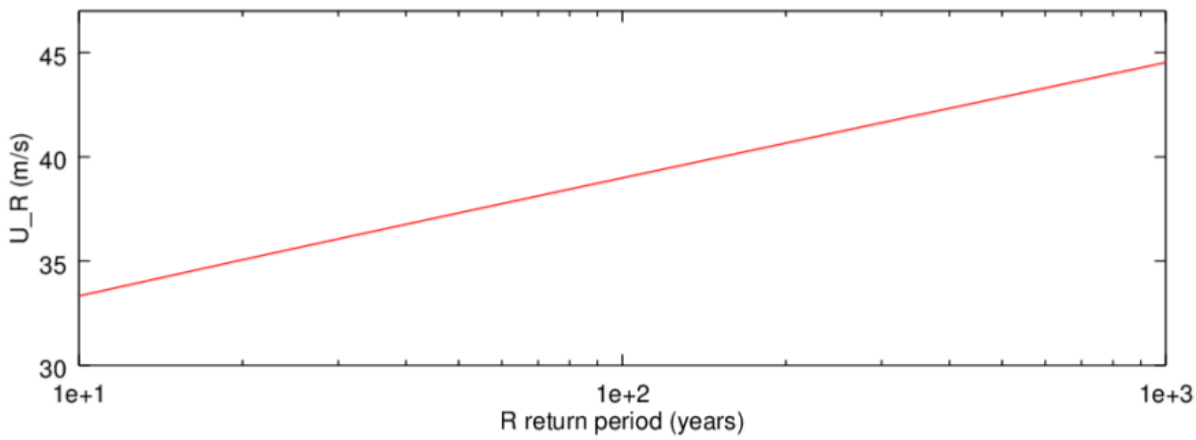

Figure 6 Estimation of the return periods based on the same input time-series as in Figure 5 but using Octave function gevfit.

5.2 Limitations and caveats

The use of the GEV analysis must be performed with following limitations considered:

1. All recorded time-series contain sampling errors which can be reduced by the proper site sitting and continuous insurance of the high data quality.

2. Since some of the extreme parameters are usually defined on an annual time scale (e.g., annual maximum daily precipitation amount, or annual maximum hourly wind speed), the length of the time-series should include several decades.

3. For some applications, data should be separated by the underlying mechanisms. For example, separate return periods of the extreme precipitation amounts can be estimated from the convective or large scale (e.g. fronts) extreme precipitation events.

4. GEV distribution is correct distribution for the largest quantities in an infinite population of an independent variable. For example, all wind speeds at 10-m at some location define the population, while annual maximum values define largest quantities. In practice, observations are finite in length and care must be taken to ensure the independence.

The method of Extreme Value Theory and the definition of return period of a risk are extensively analysed in D2.3 and D3.4 and developed through R programming tool[193] and Octave code[194]

[193] https://www.r-project.org/

[194] https://www.gnu.org/software/octave/

6 Exposure models for CI Hazards

The analyses of single and multi-hazard exposure have been performed for single, independed assets and for CI networks comprised of a number of assets. Two methods of analyses have been considered, the first based on return period estimation of the hazard(s) under consideration and the second based on hazard threshold analysis for each CI asset or CI network of assets. The spatial dimension of the hazards is represented by a grid of geographical points. The climatic data inputs of the analyses derive from the EU-CIRCLE climate databases and are created based on the estimation of temporal data series for each hazard grid-point, according to a selected climatic scenario. An important part of the procedure for all the analyses is the application of EVT on these data series, at the grid of geographical points which represent the area of interest for the analyses. The procedures of the various hazard exposure analyses are described in more detail in the sections below and are presented in the corresponding conceptual diagrams.

6.1 Single-hazard analyses

6.1.1 Asset exposure for selected return period (procedure 1a)

Analysis 1a estimates the exposure of a single asset to a single hazard based on the selection of return period of the hazard. The steps of this procedure are the following:

(1) The user inputs are the return period of the hazard and the minimum of the operational or structural climate thresholds of the asset.

(2) The procedure finds the hazard geographical point of interest (Hazard_POI) nearest to the asset and a time series of the hazard values for this point is extracted from the EU-CIRCLE climate database.

(3) The EVT is applied for the estimation of the corresponding extreme level value (EL_{haz}) for the asset.

(4) The asset is classified to vulnerable or non-vulnerable class according to the estimated EL_{haz}.

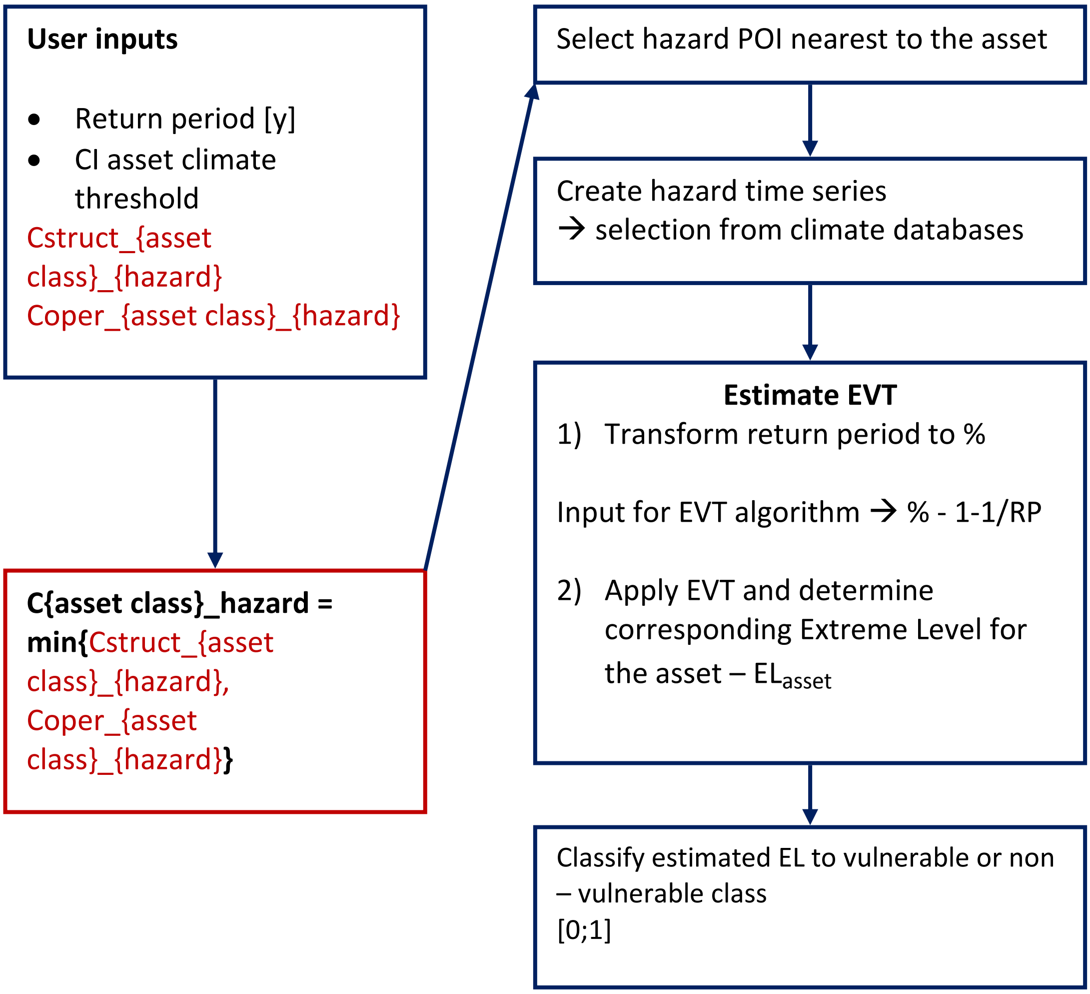

Figure 7: Procedure 1a - Single hazard exposure of single asset based on selection of return period

6.1.2 Asset exposure under selected climate hazard threshold (procedure 1b)

Analysis 1b estimates the exposure of a single asset to a single hazard based on the selection of the climate hazard threshold for the particular asset. The steps of this procedure are the following:

(1) The user inputs are the minimum of the operational or structural climate threshold of the asset in hazard units and the asset return period categories (five classes).

(2) The procedure finds the hazard geographical point of interest (Hazard_POI) nearest to the asset and a time series of the hazard values for this point is extracted from the EU-CIRCLE climate database.

(3) The EVT is applied for the determination of corresponding proportion [%] of the climate hazard for the asset and a transformation of the % to return period of the hazard (RP_h) is performed according to the formula RP = 1/(1 - %).

(4) The classification of RP_h is performed in any of the five period categories which have provided as input in the analysis. The defined class expresses the exposure of the asset in the particular hazard.

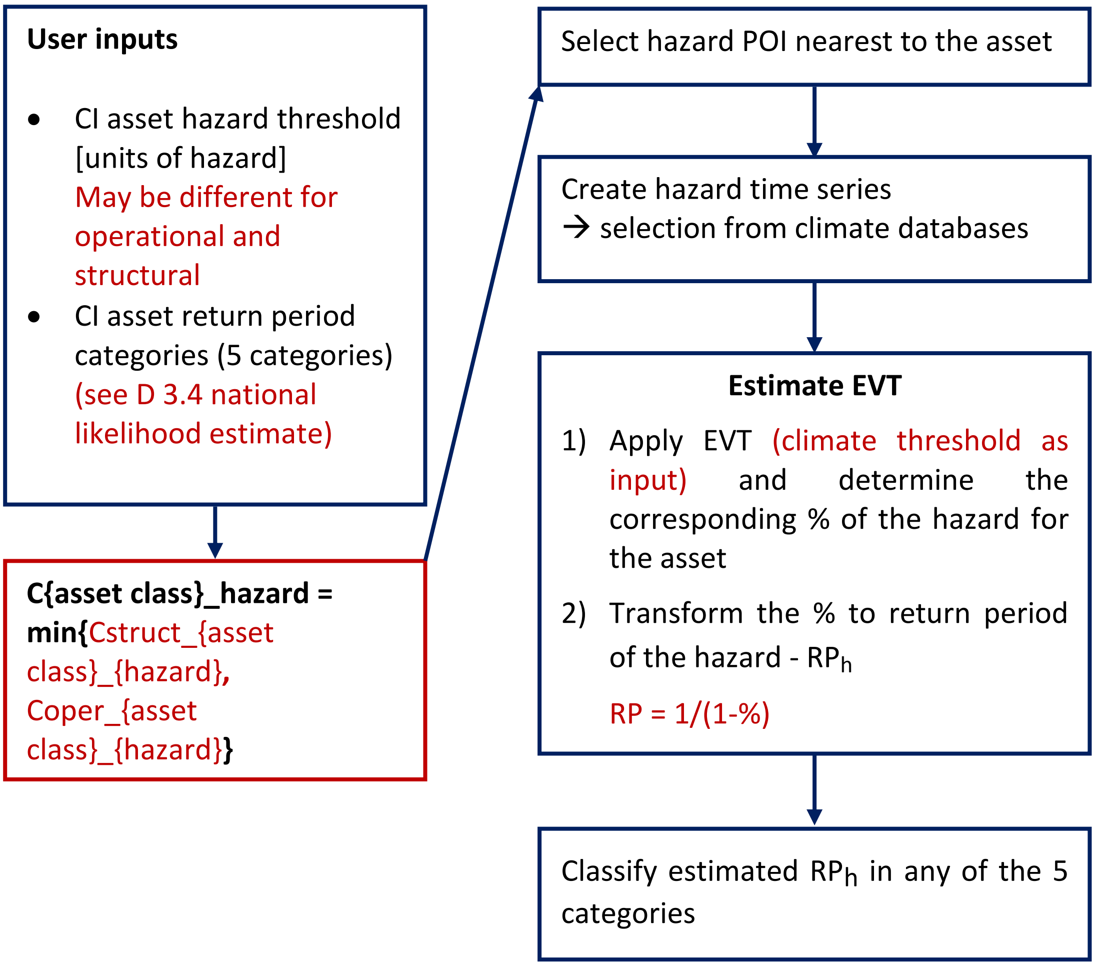

Figure 8: Procedure 1b - Single hazard exposure of single asset based on CI hazard threshold analysis

6.1.3 CI network exposure under selected return period (procedure 2a)

Analysis 2a estimates the exposure of a CI network of assets to a single hazard based on the selection of return period of the hazard. The steps of this procedure are the following

(1) The user inputs are the return period of a hazard and the minimum of the operational or structural climate thresholds of the CI.

(2) The procedure finds the hazard geographical points of interest (Hazard_POIs) nearest to the CI asset and time series of the hazard values for every point are created from the EU-CIRCLE climate database.

(3) The EVT is applied for the estimation of the Extreme Values for each Hazard POI.

(4) Attribution of the hazard values to the CI asset-points follows, using one of the two available methods:

   a. overlay spatial analysis based on the raster map of the hazard which has beed created from Hazard_POIs using natural interpolation methods

   b. spatial analysis based on the nearest hazard point in order to attribute the hazard value to each CI asset.

(5) The estimation of single hazard exposure of the CI is based on two methods:

   a. "Single CI asset exposed" where the CI is considered as exposed to the hazard if at least one single asset is exposed,

   b. "Percentage of CI assets exposed" where the whole CI is considered as exposed to the hazard if the exposed CI assets represent more than 30% of the total number of CI assets.

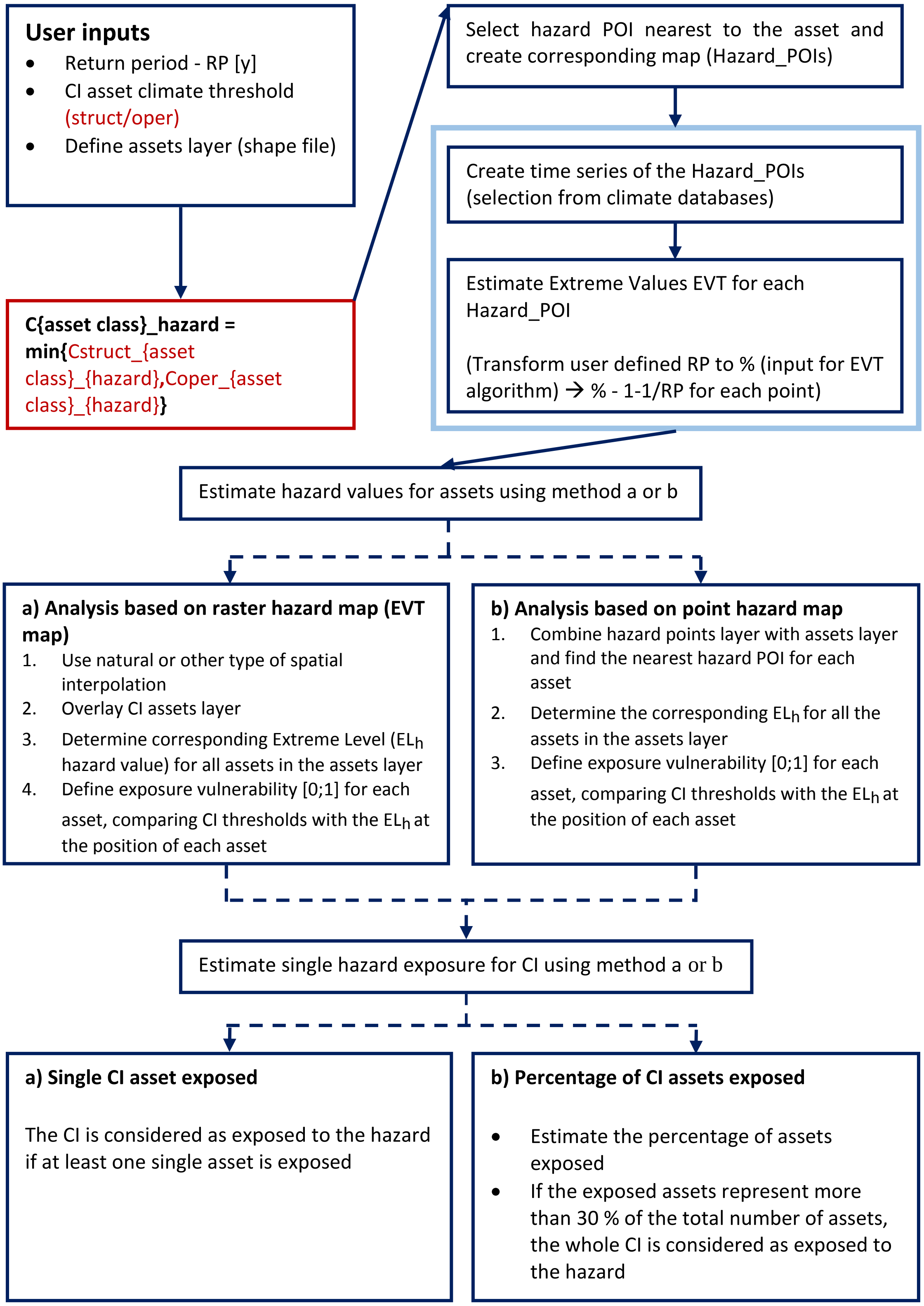

Figure 9: Procedure 2a - Single hazard exposure of CI (multiple assets and network) based on selection of return period

6.1.4 CI network exposure under selected climate hazard threshold (procedure 2b)

Analysis 2b estimates the exposure of a CI network of assets to a single hazard based on the selection of the climate hazard threshold for the CI. The steps of this procedure are the following:

(1) The user inputs are:

a. the minimum of the operational or structural climate threshold of the CI in hazard units,

b. the CI return period categories (five classes) and

c. a shape file of the CI points in which the capacity value of each asset of the CI is provided in the related field of the Attribute table of the shape file.

(2) The procedure finds the hazard points of interest (Hazard_POIs) and time series of the hazard values for every point are created from the EU-CIRCLE climate database.

(3) An overlay analysis follows, with the CI assets layer (CIAsset_POIs) in order to find the closest Hazard_POI for each asset.

(4) The EVT is applied for each CI asset for the determination of the corresponding proportion [%] of the climate hazard for the CI asset and a transformation of the proportion to the return period of the hazard (RP_h) is performed according to the formula RP=1/(1-%).

(5) A classification of each CI asset RP_h is performed in any of the five period categories which were provided as input in the analysis. The defined class expresses the exposure of the CI asset in the particular hazard.

(6) The estimation of single hazard exposure for the whole CI (CIAsset_POIs), is based on four indicators:

a. on the maximum value of CI assets exposure,

b. on the mean values of CI assets exposure,

c. on a weighted value according to the total capacity of CI assets,

d. on a weighted value according to the spatial frequency of CI assets).

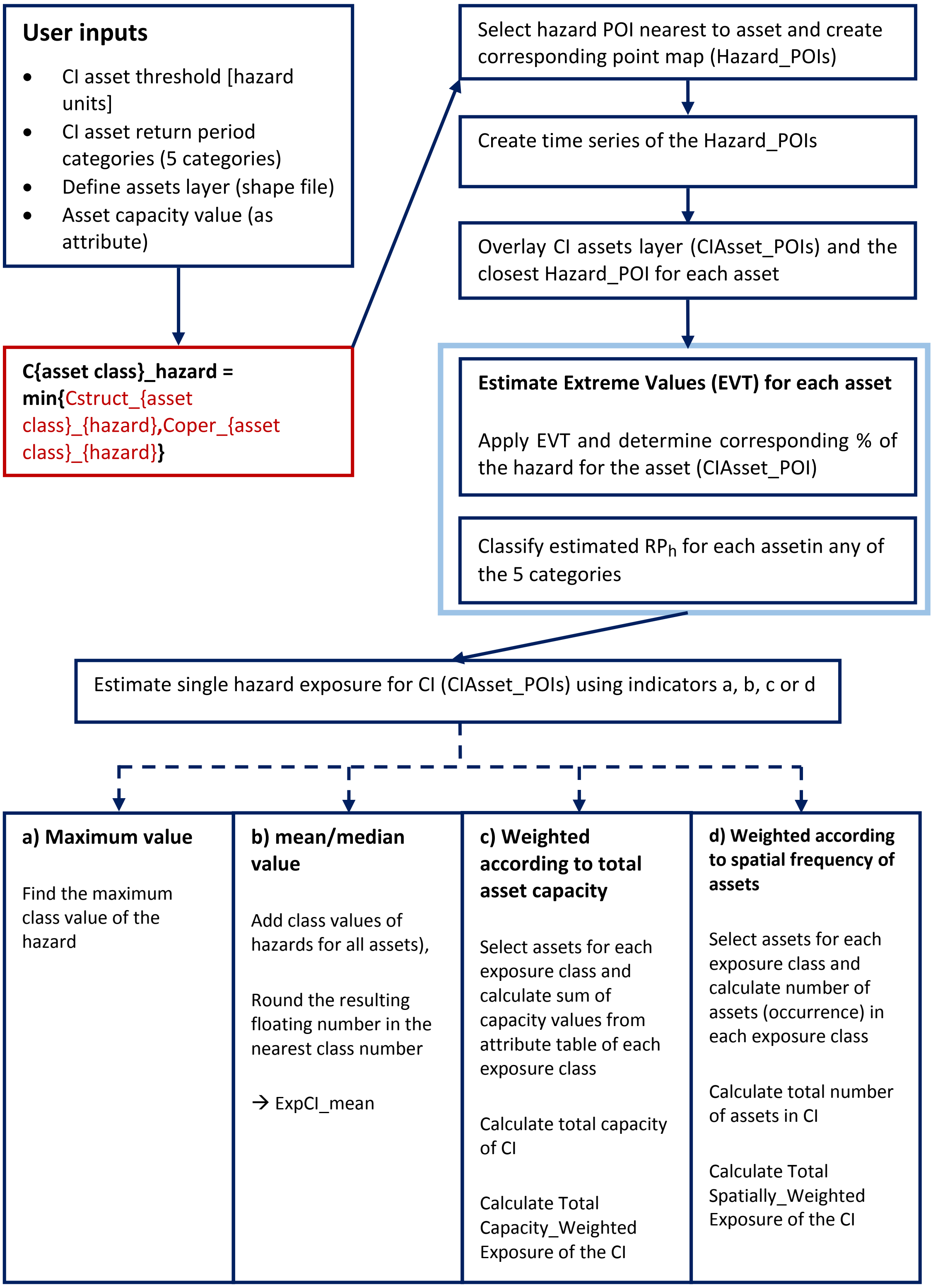

Figure 10: Procedure 2b – Single hazard exposure of CI (assets and network) based on CI hazard threshold analysis

6.2 Multi-hazard risk analyses

6.2.1 Asset multi-hazard exposure for selected return period (procedure 3a)

Analysis 3a estimates the exposure of a single asset to multiple hazards based on the selection of return period of the hazard.

(1) The inputs of this procedure are the same as in procedure 1a for each hazard under consideration.

(2) The single hazard exposure is estimated for each hazard using the steps of 1a procedure:

(3) The total exposure is expressed with the number of hazards that the asset is exposed compared to the total number of hazards examined.

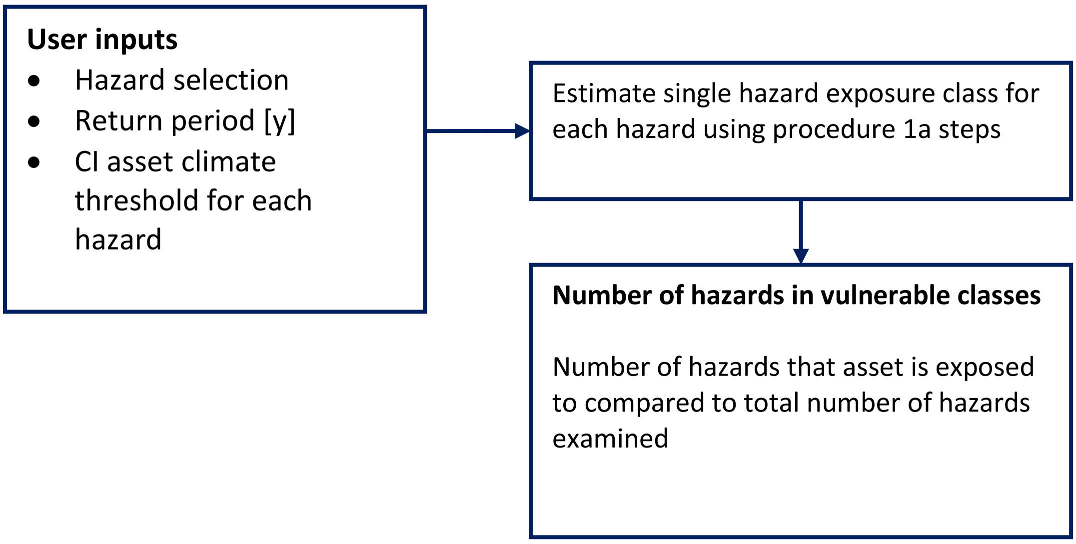

Figure 11: Procedure 3a – Multi-hazard exposure of single asset based on CI hazard threshold analysis

6.2.2 Asset multi-hazard exposure under selected climate hazards thresholds (procedure 3b)

Analysis 3b estimates the exposure of a single asset to multiple hazards based on the selection of climate hazards thresholds.

(1) The inputs of this procedure are the same as in procedure 1b for each hazard under consideration.

(2) The single hazard exposure is estimated for each hazard using the steps of 1b procedure.

(3) The creation of an associate table or list follows, with all the return period classes per hazard for the asset.

(4) The multi-hazard exposure is based on three alternative methods:

   a. The estimation of maximum hazard class,

   b. The estimation of mean hazard class,

   c. The calculation of the number of hazards in the two higher classes (i.e. hazard class >= 4)

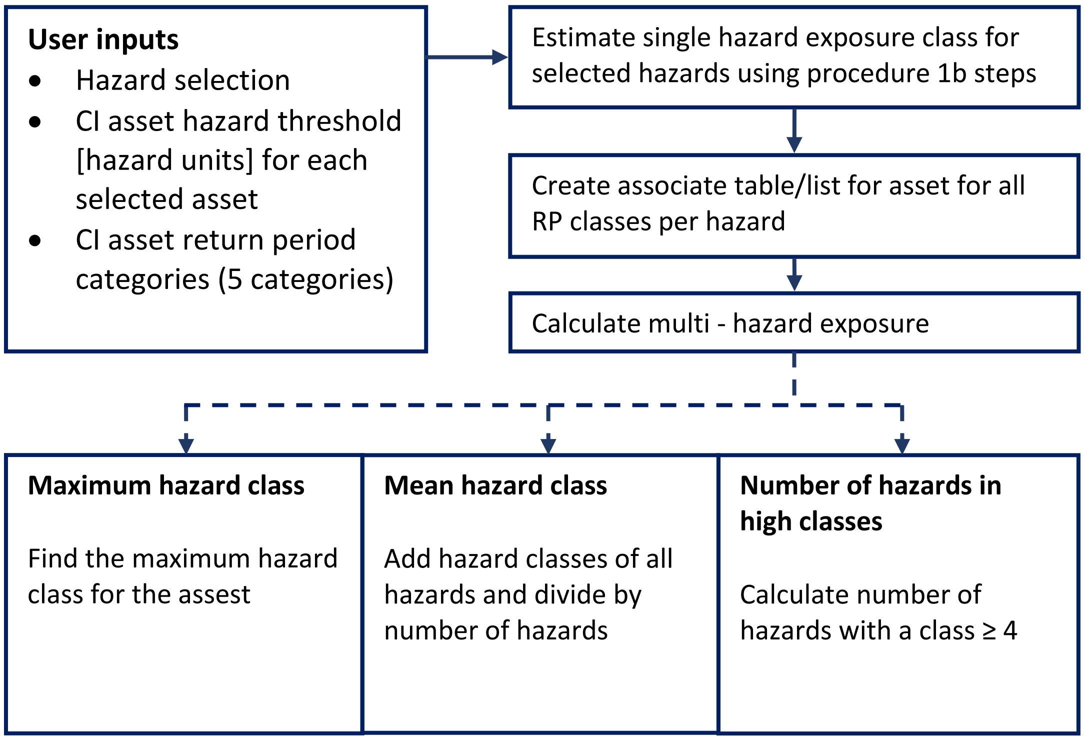

Figure 12: Procedure 3b – Multi hazard exposure of single asset based on CI hazard threshold analysis

6.2.3 CI network multi-hazard exposure under selected return period (procedure 4a)

Analysis 4a estimates the exposure of CI networks of assets to multiple hazards based on the selection of return period of the hazard.

(1) The inputs of this procedure are the same as in procedure 2a for each hazard under consideration.

(2) The single hazard exposure is estimated for the CI, for each hazard, using the steps of 2a procedure.

(3) The total exposure is expressed with the number of hazards that the CI is exposed to compared to the total number of hazards examined.

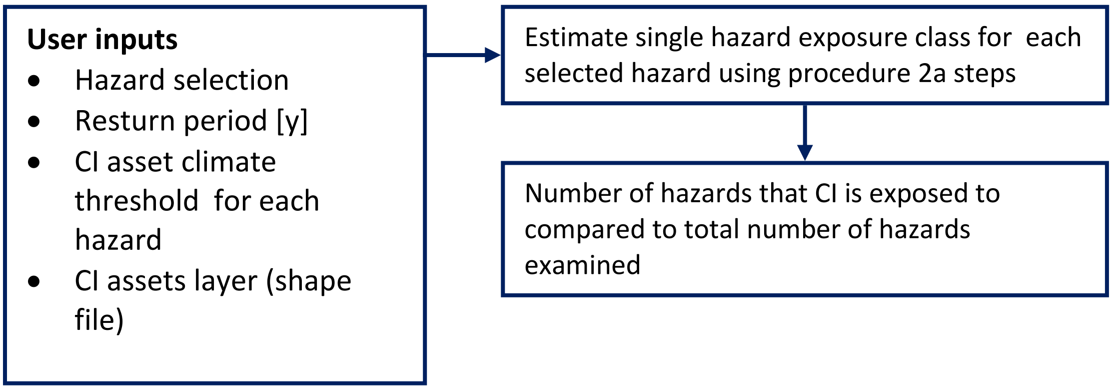

Figure 13: Procedure 4a - Multi hazard exposure of CI (multiple assets and network) based on selection of return period

6.2.4 CI network multi-hazard exposure under selected climate hazards thresholds (procedure 4b)

Analysis 4b estimates the exposure of CI networks of assets to multiple hazards based on the selection of climate hazards thresholds.

(1) The inputs of this procedure are the same as in procedure 2b for each hazard under consideration.

(2) The single hazard exposure is estimated for each hazard using the steps of the 2b procedure.

(3) The creation of an associate table or list follows, with all the return period classes per hazard for the CI.

(4) The multi-hazard exposure estimation is performed in four steps according to the corresponding single-hazard indicators. Each step is based on the previous estimation of the corresponding indicator for all the hazards under consideration. The analysis related to "indicator a" is based on the selection of the maximum return period class of the hazards calculated for the CI assets while the analyses related to indicators b, c and d are based on the mean return period classes of the hazards.

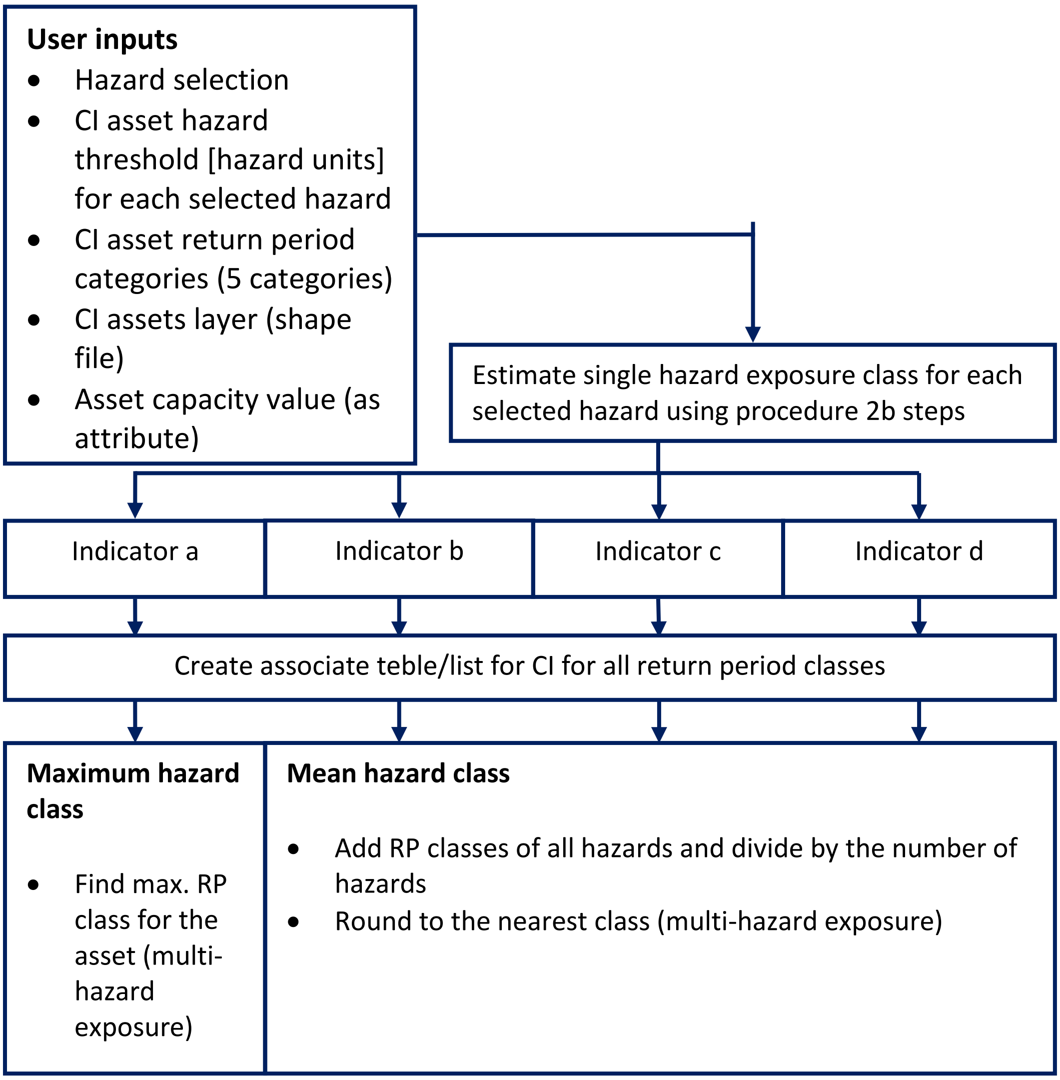

Figure 14: Procedure 4b – Multi hazard exposure for CI (assets and network) based on CI hazard threshold analysis

7 Conclusions

Various considered assets in the EU-CIRCLE project are subject to european or national regulations. The variety of regulations on national level exacerbates the comparibility between standards in different countries. The Eurocodes, published by the European Commission, introduce specific recommended methods and values regarding to discrete climate hazards imposed on a structure. Until now, there have been default values for the crucial parameters that characterise these climate hazards. These parameters assume stationary climate conditions using historic statistical values and observations. Although climate is variable, these variations are considered constant with time.

For climate hazard modelling, plenty of different modelling and simulation approaches exist. The choice of the method determines the modelling outcomes and the use of the ensemble of climate model simulations is advisable. The application of an appropriate method for the modelling of hazard exposure is determined according to the amount of regarded hazards, whether the modelling is conducted either at asset level or at network level and whether either selected return periods or hazard thresholds are under consideration. Hence, the modelling of hazard exposure can follow eight different analysis approaches.

The aim of this deliverable is to characterise the types of natural hazards using related critical event parameters for CI, pertaining to the duration, spatial scale, magnitude and evolution of the hazard. In the scope of the EU-CIRCLE project, the speed of the event, the intensity or magnitude and the affected area are regarded as parameters. The expression of these parameters in physical units allows the mapping of changing hazards within the modelling. However, the regarded parameters are subject to various restrictions, resulting from the need to quantify variables and the complexity of the modelling. The appropriate selection of parameters allows the understanding of the characteristics of natural hazardous events for CI operators and stakeholders. The derivation and inclusion of new values in climatic variables (thresholds, return periods, etc.) and advanced estimation methods can complement the existing methods, thus increasing the level of safety, reliability and societal protection.

8 Bibliography/References

Abi-Samra N., K. Forsten and R. Entriken, “Sample Effects of Extreme Weather on Power Systems and Components, Part I: Sample Effects on Distribution Systems,” 2010.

AECOM, “Torondo Hydro-Electric System Public Infrastructure Engineering Vulnerability Assessment Pilot Case study,” 60263582, Sep. 2012.

Alan H. Taylor, Carl N. Skinner: Fire history and landscape dynamics in a late-successional reserve, Klamath Mountains, California, USA, Forest Ecology and Management, Volume 111, Issues 2–3, 1998, Pages 285-301, ISSN 0378-1127, https://doi.org/10.1016/S0378-1127(98)00342-9.

Alexander ME (1994) Proposed revision of fire danger class criteria for forest and rural areas in New Zealand. NRFA / NZFRI, Circular 1994/2, Wellington

Alfieri L, Burek P, Dutra E, et al (2013) GloFAS - global ensemble streamflow forecasting and flood early warning. Hydrol Earth Syst Sci 17:1161–1175 . doi: 10.5194/hess-17-1161-2013

Andrews, Patricia L. BEHAVE: fire behavior prediction and fuel modeling system-BURN Subsystem, part 1. General Technical Report INT-194. Ogden, UT: U.S. Department of Agriculture, Forest Service, Intermountain Research Station; 1986

Andrews, Patricia L.; Chase, Carolyn H. 1989. BEHAVE: fire behavior prediction and fuel modeling system-BURN subsystem, Part 2. Gen. Tech. Rep. INT-260. Ogden, UT: U.S. Department of Agriculture, Forest Service, Intermountain Research Station.

ANSI/IEEE, “National Electrical Safety Code.” 2007

Aquaveo (2018) WMS 10.1 - The All-in-one Watershed Solution. https://www.aquaveo.com/software/wms-watershed-modeling-system-introduction. Accessed 20 Jul 2018

Asian Development Bank, “Climate risk and adaptation in the electric power sector,” Mandaluyong City, Philippines, 2012

Azevedo de Almeida and A. Mostafavi, “Resilience of Infrastructure Systems to Sea-Level Rise in Coastal Areas: Impacts, Adaptation Measures, and Implementation Challenges,” Sustainability, vol. 8, no. 11, p. 1115, Nov. 2016.

Bates PD, De Roo APJ (2000) A simple raster-based model for flood inundation simulation. J Hydrol 236:54–77 . doi: 10.1016/S0022-1694(00)00278-X

Brandt, A. Varma, R. Brent, S. Marcu, R. Connor, and K. Harries, “Effects of Fire Damage on the Structural Properties of Steel Bridge Elements. Final Report,” 2011.

Brunner GW (2016) HEC-RAS River Analysis System Users Manual Version 5.0. http://www.hec.usace.army.mil/software/hec-ras/documentation/HEC-RAS%205.0%20Users%20Manual.pdf. Accessed 20 Jul 2018

Brussels: CEN/TC 250 - Structural Eurocodes, March 2005 (DAV)

Burgan, Robert E.; Rothermel, Richard C. BEHAVE: fire behavior prediction and fuel modeling system--FUEL subsystem. General Technical Report I NT-167. Ogden, UT: U. S. Department of Agriculture, Forest Service, Intermountain Forest and Range Experiment Station; 1984. 126 p.

Byrne, “Humidity effects in substations,” in Petroleum and Chemical Industry Conference Europe, 2014, 2014, pp. 1–10

Camia A. and Bovio G, 2000, Description of the indices implemented in EUDIC software for the European meteorological forest fire risk mapping. Joint Research Centre, Institute for Environment and sustainability Land Management Unit.

Chakraborti SK, “American electric power’s coal pile management program,” in Bulk Solids Handling, vol. 15, 1995, pp. 421–428

Chen AS, Djordjević S, Leandro J, Savic D (2007) The urban inundation model with bidirectional flow interaction between 2D overland surface and 1D sewer networks. Lyon, France, pp 465–472

Chen A, Leandro J, Djordjevic S (2016) Modelling sewer discharge via displacement of manhole covers during flood events using 1D/2D SIPSON/P-DWave dual drainage simulations. Urban Water J 13:830–840 . doi: 10.1080/1573062X.2015.1041991

Coles, S. (2001) An Introduction to Statistical Modeling of Extreme Values. Springer Verlag, Berlin. http://dx.doi.org/10.1007/978-1-4471-3675-0

Cole S, Robson A, Moore B (2010) The Grid-to-Grid Model for nationwide flood forecasting and its use of weather radar

Contreras-Lisperguer and K. de Cuba, "The potential impact of climate change on the energy sector in the Caribbean region," Wash. DC Dep. Sustain. Dev. Organ. Am. States OAS, 2008.; S. Dunn, S. Wilkinson, C. Galasso, L. Manning, and D. Alderson, "Development of empirical vulnerability curves for electrical supply systems subjected to wind hazard," 2015CSN EN 50341-2-22, "Overhead Electrical Lines Exceeding AC 45 KV. Set of National Normative Aspects," PN-EN 50341-1, 2005

Davis and Clemmer, "How Climate Change Puts Our Electricity at Risk," Power Failure, 2014

De Roo APJ (1999) LISFLOOD: a rainfall-runoff model for large river basins to assess the influence of land use changes on flood risk. Ribamod River Basin Model Manag Flood Mitig Concert Action Eur Comm EUR 18287:349–357

DHI (2017) MIKE 11. A modelling system for rivers and channels, Reference Manual. DHI Water & Environment

Dimitrakopoulos AP, Bemmerzouk AM, Mitsopoulos ID (2011) Evaluation of the Canadian fire weather index system in an eastern Mediterranean environment. Meteorological Applications. 18, Issue 1, 83–93

Djordjević S, Prodanović D, Maksimović C (1999) An approach to stimulation of dual drainage. Wat Sci Tech 39:95–103

Djordjević S, Prodanović D, Maksimović Č, et al (2005) SIPSON–Simulation of Interaction between Pipe flow and Surface Overland flow in Networks. Water Sci Technol 52:275–283

DOE, "U.S. energy sector vulnerabilities to climate change and extreme weather," U.S. Department of Energy, DOE/PI-0013., Jul. 2013

DOE, "Effect of Sea Level Rise on Energy Infrastructure in Four Major Metropolitan Areas," Sep. 2014.

DOE, "Climate Change and the Electricity Sector: Guide for Assessing Vulnerabilities and Developing Resilience Solutions to Sea Level Rise," Jul. 2015

DOE, "Climate Change and the U.S. Energy Sector: Regional Vulnerabilities and Resilience Solutions," US Department of Energy, 2015.

DOE, "Climate Change and the Electricity Sector Guide for Climate Change Resilience Planning," Sep. 2016

Draxler, R.R. and G.D. Hess (1997), Description of the HYSPLIT_4 modeling system. NOAA Technical Memo ERL ARL-224, December, 24 p.

Draxler, R.R. and G.D. Hess (1998), An overview of the HYSPLIT_4 modelling system for trajectories, dispersion, and deposition. Aust. Meteor. Mag. 47, 295-308.

Ducloux and Nygaard, "50-year return-period wet-snow load estimation based on weather station data for overhead line design in France," Nat. Hazards Earth Syst. Sci., vol. 14, no. 11, pp. 3031–3041, Nov. 2014.

Duncan AP, Chen AS, Keedwell EC, et al (2012) Urban flood prediction in real-time from weather radar and rainfall data using artificial neural networks. Weather Radar Hydrol - IAHS Red Proc 351:568–573

EEA, 2010, Water resources: Quantity and flows, The European Environment: State and outlook 2010, SOER 2010 report, European Environment Agency, SOER 2010 website: www.eea.europa.eu/soer.

EIONET NFP of Malta (Malta Resources Authority, Regulation Unit) during the EEA Consultation of the WEI+ in August 2012, in Kossida et. al., 2012

EN 1991-1-3. Eurocode 1 - Actions on structures - Part 1-3: General actions - Snow loads

EN 1991-1-4:2005/A1:2010. Eurocode 1: Actions on structures - Part 1-4: General actions - Wind actions. Brussels: CEN/TC 250 - Structural Eurocodes, April 2010

EN 1991-1-5. Eurocode 1 - Actions on structures - Part 1-5: General actions – Thermal actions

EPRI, "Key Climate Variables Relevant to the Energy Sector and Electric Utilities. Climate Science Newsletter. Palo Alto (Cal., USA): 4.," 2009.

Espinoza, M. Panteli, P. Mancarella, and H. Rudnick, "Multi-phase assessment and adaptation of power systems resilience to natural hazards," Electr. Power Syst. Res., vol. 136, pp. 352–361, Jul. 2016

EU-CIRCLE consortium (2017): D2.1 Report on Typology of Climate Related Hazards, http://www.eu-circle.eu/research/deliverables/

EU-CIRCLE consortium (2017): D2.2 Report on Climate Related Hazards Information Collection Mechanisms, http://www.eu-circle.eu/research/deliverables/

Eurocode 1: Actions on structures - Part 1-4: Wind actions

Eurocode 3 - Design of steel structures - Part 3-1: Towers, masts and chimneys - Towers and masts

European Commission, "Energy in Europe 1999 - Annual Energy Review," Jan. 2000

European Commission: Addressing the challenge of water scarcity and droughts in the European Union, COMMUNICATION FROM THE COMMISSION TO THE EUROPEAN PARLIAMENT AND THE COUNCIL, COM(2007) 414 final, Brussels, 18.7.2007.

European Commission, "Investment needs for future adaptation measures in EU nuclear power plants and other electricity generation technologies due to effects of climate change. Final report.", 2011

Feeley et al., "Water: A critical resource in the thermoelectric power industry," Energy, vol. 33, no. 1, pp. 1–11, Jan. 2008

Feenstra, "Handbook on methods for climate change impact assessment and adaptation strategies," 1998

FEMA. Hazus - MH 2.1, "Multi-hazard Loss Estimation Methodology Flood Model Technical Manual," Department of Homeland Security Federal Emergency Management Agency Mitigation Division, Washington, D.C., 2011

FEMA. Risk Management Series Snow Load Safety Guide FEMA P-957 / January 2013

Feofilovs and F. Romagnoli, "Resilience of critical infrastructures: probabilistic case study of a district heating pipeline network in municipality of Latvia," Energy Procedia, vol. 128, pp. 17–23, Sep. 2017

Flores, B. Lacarrière, J. N. W. Chiu, and V. Martin, "Assessing the techno-economic impact of low-temperature subnets in conventional district heating networks," Energy Procedia, vol. 116, pp. 260–272, Jun. 2017.; EUROHEAT & POWER, "Guidelines for District Heating Substations," Oct. 2008.

Frandsen (1971): Fire spread through porous fuels from the conservation of energy, Combustion and Flame, Volume 16, Issue 1, 1971, https://doi.org/10.1016/S0010-2180(71)80005-6.

Garfin, Jardine, Merideth, Black and LeRoy, Assessment of climate change in the southwest United States. A report prepared for the National CLimate Assessment, Island press. Washington, D.C., 2013

Glenis V, McGough AS, Kutija V, et al (2013) Flood modelling for cities using Cloud computing. J Cloud Comput Adv Syst Appl 2:1

Guidolin M, Chen AS, Ghimire B, et al (2016) A weighted cellular automata 2D inundation model for rapid flood analysis. Environ Model Softw 84:378–394 . doi: 10.1016/j.envsoft.2016.07.008

Hashmi, M. Lehtonen, and S. Hänninen, "Effect of Climate Change on Transformers Loading Conditions in the Future Smart Grid Environment," Open J. Appl. Sci., vol. 03, no. 02, pp. 24–29, 2013.

Hatt R, "Handling coal: Sticky when wet. PowerOnline. http://www.poweronline.com/doc/Handling- Coal-sticky-when-wet-0001. Accessed 19 April 2013," 2001.

Hatt R, "Coal quality and combustion workshop. Coal Combustion, Inc. http://www.coalcombustion. com/PDF%20Files/webcqcclassoutline.pdf." 2004

Hirsch, K.G. 1996. Canadian forest Fire Behavior Prediction (FBP) System: user's guide. Nat. Resour. Can., Can. For. Serv., North. For. Cent., Edmonton, Alberta. Spec. Rep.7

Holmes, J. D. (2001) Wind loading of structures. Spon Press, 356 p

Holsten A, Dominic AR, Costa L, Kropp JP. (2013) Evaluation of the performance of meteorological forest fire indices for German federal states. Forest Ecology and Management. 2013;287:123-31

Hsu MH, Chen SH, Chang TJ (2000) Inundation simulation for urban drainage basin with storm sewer system. J Hydrol 234:21–37 . doi: 10.1016/S0022-1694(00)00237-7

Hsu MH, Chen SH (2002) Urban inundation model with dynamic interactions between overland and storm sewer flows. Chongli, Taiwan

Huesca M, Litago J, Palacios-Orueta A, Montes F, Sebastián-López A, Escribano P. (2009) Assessment of forest fire seasonality using MODIS fire potential: A time series approach. Agricultural and Forest Meteorology.;149:1946-55

Hulme, H. Neufeldt, H. Colyer, and A. Ritchie, "Adaptation and mitigation strategies: supporting European climate policy," 2009.

Jenkinson A. F., "The frequency distribution of the annual maximum (or minimum) values of meteorological elements", Quarterly Journal of the Royal Meteorological Society, Q.J.R. Meteorol. Soc.,https://doi.org/10.1002/qj.49708134804, doi:10.1002/qj.49708134804, 1955

Jurgemeyer and B. Miller, "NESC Wind and Ice load effects on wood distribution pole design," in Rural Electric Power Conference (REPC), 2012 IEEE, 2012, pp. B1–1Lamb R, Crossley M, Waller S (2009) A fast two-dimensional floodplain inundation model. Proc Inst Civ Eng-Water Manag 162:363–370 . doi: 10.1680/wama.2009.162.6.363

Katz, R.W., "Statistical methods for nonstationary extremes". Extremes in a changing climate, Springer Netherlands, 2013.

Leandro J, Chen AS, Schumann A (2014) A 2D parallel diffusive wave model for floodplain inundation with variable time step (P-DWave). J Hydrol 517:250–259 . doi: 10.1016/j.jhydrol.2014.05.020

Leandro J, Djordjević S, Chen AS, Savić DA (2009) Flood inundation maps using an improved 1D/1D model. Tokyo, Japan

Leonardo da Vinci Pilot Project CZ/02/B/F/PP-134007 DEVELOPMENT OF SKILLS FACILITATING IMPLEMENTATION OF EUROCODES HANDBOOK 3 ACTION EFFECTS FOR BUILDINGS

Li, R. W. Mazur, D. R. Allen, and D. R. Swatek, "Specifying Transformer Winter and Summer Peak-Load Limits," IEEE Trans. Power Deliv., vol. 20, no. 1, pp. 185–190, Jan. 2005.

Lin G-F, Chen G-R, Wu M-C, Chou Y-C (2009) Effective forecasting of hourly typhoon rainfall using support vector machines: EFFECTIVE FORECASTING OF HOURLY TYPHOON RAINFALL. Water Resour Res 45:n/a-n/a . doi: 10.1029/2009WR007911

López, L. E. P. Rocha, D. L. Escobedo, and J. S. Sesma, "Reliability and vulnerability analysis of electrical substations and transmission towers for definition of wind and seismic damage maps for Mexico," in 11th Americas Conference on Wind Engineering-San Juan, Puerto Rico, 2009.

Martins Ricardo Daniel Oliveira Mendes (2016) Development of a Fully Coupled 1D/2D Urban Flood Model. University of Coimbra

Maksimović C, Prodanović D, Boonya-Aroonnet S, et al (2009) Overland flow and pathway analysis for modelling of urban pluvial flooding. J Hydraul Res 47:512–523 . doi: 10.3826/jhr.2009.3361

McColl, T. Angelini, and R. Betts, "Climate Change Risk Assessment for the Energy Sector," Defra Project Code GA0204, Cimate change risk assessment UK, 2012

McKee et al., 1993, The relationship of drought frequency and duration to time scales, T.B. McKee, N.J. Doeskin, J. Kleist, Proceedings of the 8th Conference on Applied Climatology, American Meteorological Society, Boston, MA (1993), pp. 179-184

MEDITERRANEAN WATER SCARCITY & DROUGHT WORKING GROUP: Mediterranean Water Scarcity and Drought Report, Technical Report - 009 – 2007, MED WS&D WG, April 2007

Melillo, J. M., Richmond, Terese (T. C.), and Yohe, G. W., “Climate Change Impacts in the United States: The Third National Climate Assessment,” 2014.

Néelz S, Pender G (2013) Benchmarking 2D hydraulic models Summary. Environment Agency

New Mexico Department of Transportation 2007: Drainage Design Criteria – Revision of 06/07

O’Brien JS, Julien PY, Fullerton WT (1993) Two-Dimensional Water Flood and Mudflow Simulation. J Hydraul Eng 119:244–261 . doi: 10.1061/(ASCE)0733-9429(1993)119:2(244)

Ossama E. Gouda, Ghada M. Amer, Adel Z. El Dein, „Effect of dry zone formation around underground power cables on their ratings“, CIRED 2009 - 20th International Conference and Exhibition on Electricity Distribution - Part 1, 8-11 June 2009

Palheiro PM, Fernandes P, Cruz MG (2006) A fire behaviour-based fire danger classification for maritime pine stands: Comparison of two approaches. Forest Ecology and Management 234,S54.

Palutikof J P, Brabson B B,Lister D H, Adcock S T. "A review of methods to calculate extreme wind speeds". Meteorological Applications,https://doi.org/10.1017/S1350482799001103, doi:10.1017/S1350482799001103, 1999

Paysen, Timothy, R.J. Ansley, J. Brown, G. Gottfried, S. Haase, M. Harrington, M. Narog, S. Sackett, R. Wilson. 2000. Fire in Western Shrubland, Woodland, and Grassland Ecosystems. Chapter 6. USDA Forest Service Gen. Tech. Rep. RMRS-GTR-42-vol. 2.

Pender G (2006) Briefing: Introducing the flood risk management research consortium. Proc Inst Civ Eng Water Manag 159:3–8 . doi: 10.1680/wama.2006.159.1.3

Roger A and Pielke Sr, Climate Vulnerability, Understanding and Addressing Threats to Essential Resources, vol. 1. 2013

Rossman LA (2010) Storm Water Management Model User’s Manual Version 5.0. National Risk Management Research Laboratory, Office of Research and Development, U.S. Environmental Protection Agency

Rothermel, Richard C. (1980): How to Predict the Spread and Intensity of Forest and Range Fires. Gen. Tech. Rep. INT-143. Ogden, UT: U.S. Department of Agriculture, Forest Service, Intermountain Forest and Range Experiment Station; 1983. 1 61 p

Rothermel, Richard C. 1991. Predicting behavior and size of crown fires in the Northern Rocky Mountains. Res. Pap. INT-438. Ogden, UT: U.S. Department of Agriculture, Forest Service, Intermountain Research Station. 46 p.

Ruszczak and M. Tomaszewski, “Extreme Value Analysis of Wet Snow Loads on Power Lines,” IEEE Trans. Power Syst., vol. 30, no. 1, pp. 457–462, Jan. 2015

Sathaye et al., “Estimating risk to California energy infrastructure from projected climate change,” CEC-500-2012-057, Sacramento, CA, California Energy Commission., 2012.

Sathaye et al., “Estimating impacts of warming temperatures on California’s electricity system,” Glob. Environ. Change, vol. 23, no. 2, pp. 499–511, Apr. 2013.

Scharffenberg W (2016) HYdrologic Modeling System HEC-HMS User’s Manual, Version 4.2

Sieber née Schulz, “Adaptation Options and Decision-Support for Electricity Infrastructure Operators under Influence of Extreme Hydro-Meteorological Events,” Journal of Integrated Disaster Risk Management, Special IDRiM2010 Conference Paper, ISSN: 2185-8322, 2011a

Skamarock, W. C., J. B. Klemp, J. Dudhia, D. O. Gill, D. M. Barker, M. G. Duda, X.-Y. Huang, W. Wang, and J. G.Powers (2008), A description of the Advanced Research WRF version 3, NCAR Tech. Note, NCAR/TN- 475 +STR, 125pp., Natl. Cent. for Atmos. Res., Boulder

Smith, “The Performance of Distribution Utility Poles in Wildland Fire Hazard Areas. What We Know and Don’t Know.” 2014

Smith LS, Liang Q (2013) Towards a generalised GPU/CPU shallow-flow modelling tool. Comput Fluids 88:334–343 . doi: 10.1016/j.compfluid.2013.09.018

Spironi et al., 2015, The biggest drought events in Europe from 1950 to 2012, Jonathan Spironi, Gustavo Naumann, Jürgen V. Vogt, Paulo Barbosa, Journal of Hydrology: Regional Studies

State of Queensland (Department of Transport and Main Roads) 2015: Road Drainage Manual

State of Queensland (Department of Transport and Main Roads) 2018: Design Criteria for Bridges and Other Structures, http://creativecommons.org/licenses/by/3.0/au/

Stockholm Environmental Institute, Sweden – Raskin et al. 1997: Comprehensive assessment of the freshwater resources of the world (Document prepared for UN Commission for Sustainable Development 5th Session 1997)

Stohl, A., M. Hittenberger, and G. Wotawa (1998): Validation of the Lagrangian particle dispersion model FLEXPART against large scale tracer experiments. Atmos. Environ. 32, 4245-4264.

Stohl, A., and D. J. Thomson (1999): A density correction for Lagrangian particle dispersion models. Bound.-Layer Met. 90, 155-167.

Stohl, A., C. Forster, A. Frank, P. Seibert, and G. Wotawa (2005): Technical Note : The Lagrangian particle dispersion model FLEXPART version 6.2. Atmos. Chem. Phys. 5, 2461-2474.

Strosser et al., 2012, Gap Analysis of the Water Scarcity and Droughts Policy in the EU

Strosser, Dworak, Garzon Delvaux, Berglund, Schmidt, Mysiak, Kossida, IacovosIacovides, Ashton, European Commission, Tender ENV.D.1/SER/2010/0049

Sunrise Powerlink Project, “Attachment 1A: Effect of Wildfires on Transmission Line Reliability Collocation of Transmission Alternatives with the Southwest Powerlink,” Jan. 2008

Tebaldi, D. Adams-Smith, and N. Heller, “The heat is on: U.S. temperature trends,” Climate Central. Online at www.climatecentral.org/news/the-heat-is-on/, Princeton, NJ, 2012.

van Vliet, J. Sheffield, D. Wiberg, and E. F. Wood, “Impacts of recent drought and warm years on water resources and electricity supply worldwide,” Environ. Res. Lett., vol. 11, no. 12, p. 124021, Dec. 2016.; M. Hulme, H. Neufeldt, H. Colyer, and A. Ritchie, “Adaptation and mitigation strategies: supporting European climate policy,” 2009

van Vliet, J. Sheffield, D. Wiberg, and E. F. Wood, “Impacts of recent drought and warm years on water resources and electricity supply worldwide,” Environ. Res. Lett., vol. 11, no. 12, p. 124021, Dec. 2016.

Viegas DX, Reis RM, Cruz MG, Viegas MT (2004). Calibração do Sistema Canadiano de Perigo de Incêndio para Aplicação em Portugal. Silva Lusitana.;12:77-93

Ward, “The effect of weather on grid systems and the reliability of electricity supply,” Clim. Change, vol. 121, no. 1, pp. 103–113, Nov. 2013.

Water Scarcity Drafting Group: Waterscarcity management in the context of the WFD”, , MED Joint Process WFD /EUWI, June 2006.

Wilson, Ralph (1980): Reformulation of forest fire spread equations in SI units, USDA Forest Service, ttps://www.fs.fed.us/rm/pubs_int/int_rn292.pdf

WMO, 2012, Standardized Precipitation Index. User Guide, World Meteorological Organization, Geneva, Switzerland (2012)

WMO-No. 01090. ISBN 978-92-63-11091-6

Yu, T. Jamasb, and M. Pollitt, “Does weather explain cost and quality performance? An analysis of UK electricity distribution companies,” Energy Policy, vol. 37, no. 11, pp. 4177–4188, Nov. 2009.